Design and Control of Weak Grid-connected Converter for Distributed Power Generation

By

Tila Muhammad

Reg.No. 3-FET/PhDEE/F16

A dissertation submitted to I.I.U.I. in partial fulfillment of the requirements for the degree of

DOCTOR OF PHILOSOPHY

Department of Electrical and Computer Engineering
Faculty of Engineering and Technology
INTERNATIONAL ISLAMIC UNIVERSITY
ISLAMABAD
August, 2023

Artificial intelligence.
systems control
system design
Power generation

DEDICATED TO

MY FATHER, MOTHER, WIFE, BROTHERS, SISTERS AND

TEACHERS

CERTIFICATE OF APPROVAL

Title of Thesis: Design and Control of Weak Grid-connected Converter for Distributed Power Generation

Name of Student: Tila Muhammad

Registration No: 03-FET/PHDEE/F16

Accepted by the Department of Electrical and Computer Engineering, Faculty of Engineering and Technology, International Islamic University (IIU), Islamabad, in partial fulfillment of the requirements for the Doctor of Philosophy Degree in Electrical Engineering.

Viva voce committee:

Dr. Adnan Umar Khan (Supervisor)
Assistant Professor DECE, FET IIU Islamabad

Dr. Aqdas Naveed Malik (Internal)
Professor DECE, FET, IIU Islamabad

Dr. Muhammad Zia (External)
Professor, DEE, Quaid Azam University, Islamabad

Dr. Hammad Omer (External)
Associate Professor, DECE, Comsats University, Islamabad

Dr. Shahid Ikram (Chairman, DECE)
Assistant Professor DECE, FET, IIU Islamabad

Prof. Dr. Nadeem Ahmad Sheikh (Dean, FET)
Professor DME, FET, IIU Islamabad

ABSTRACT

Background: Grid-connected inverters play a vital and efficient role to integrate distributed renewable energy sources with micro or national grids.

Motivation: However, the connection between power inverters and the utility grid has been seen to be liable for several stability concerns in a weak grid. The insertion of power from distributed energy resources into the grid is a challenging task due to continuously varying grid impedance and frequency which affects the stability margins in response and the inverters become vulnerable to instability. Moreover, the grid impedance boosts the harmonics in the grid voltage which further degrades the performance of grid-connected inverters. These voltage harmonics penetrate into the Phase-Locked Loop (PLL) and reach the control unit of the inverter which in turn increases the total harmonics distortion in the current entering the grid from the inverter.

Method: The main objective of this research is to establish a novel strategy that decreases the influence of grid impedance and frequency variations on the performance and stability of a grid-connected inverter. This research contributes twofold: one is a new multilevel inverter topology along with an equal voltage source sharing algorithm and the other is its adaptive hybrid control unit. The advantages of the proposed grid-connected multilevel inverter are i) decreasing stress on switching transistors, ii) improving power handling capability iii) decreasing the rate of change of voltage (dV/dt), and iv) producing lesser harmonic distortion within the output current. Moreover, the multilevel inverter architecture is also more appropriate for photovoltaic power plants to connect it to the grid. The control unit of the proposed system further consists of two parts: one is the synchronous framed current controller, and the other is stationary framed adaptive harmonic compensators. The grid current controller ensures that regulated current is injected into the grid. It is not suitable to implement harmonic compensators in a synchronous reference frame due to tedious computation complexities. Therefore, the stationary reference frame is adapted for harmonic compensators. Due to the narrow bandwidth of stationary framed compen-

sators, they cannot handle the variations in grid frequency and this problem is resolved by designing adaptive harmonic compensators which adapt their parameters according to the instantaneous frequency of the grid voltage extracted by the phase lock loop circuit. The proposed design is evaluated with the help of case studies: first, a three-level weak grid-connected inverter is designed and tested to validate the working of the control technique proposed in this research, and then the control technique is validated for a nine-level reduced switch cascaded multilevel inverter connected with a weak grid.

Results: The proposed hybrid adaptive control enhances the performance by decreasing total harmonic distortion (THD) and improving the stability under the distorted voltage, variation in impedance, and variations in the frequency of the grid.

Impact and utility: The findings of the research show that the system becomes less sensitive to voltage distortions, changes of grid impedance, and frequency variations of the grid which makes the proposed technique very appropriate to the stability performance applications.

LIST OF PUBLICATIONS AND SUBMISSIONS

[1] **Muhammad, Tila**, Adnan Umar Khan, Yousra Abid, Hilal Khan, Nasim Ullah, Vojtech Blazek, Lukas Prokop, and Stanislav Misák. "Adaptive Hybrid Control of Reduced Switch Multilevel GCI for Weak Grid Applications" accepted in IEEE access.

[2] **Muhammad, Tila**, Adnan Umar Khan, Muhammad Tajammal Chughtai, Reyyan Ahmad Khan, Yousra Abid, Muhammad Islam, and Sheroz Khan. "An Adaptive Hybrid Control of Grid Tied Inverter for the Reduction of Total Harmonic Distortion and Improvement of Robustness against Grid Impedance Variation." Energies 15, no. 13 (2022): 4724.

[3] Batool, Dania, Qandeel Malik, **Tila Muhammad**, Adnan Umar Khan, and Jonghoon Kim. "Comparative study on minimization of conduction and switching losses in cascaded multilevel inverter via reduced switches and equal voltage source-sharing." Circuit World (2022).

[4] Abid, Yousra, Muhammad Adil Khan, and **Tila Muhammad**. "Design and analysis of hybrid power generation system for rural electrification. a case study." 2019 3rd International Conference on Energy Conservation and Efficiency (ICECE). IEEE, 2019.

[5] **Muhammad, Tila**, Adnan Umar Khan, Jan Hanif, Muhammad Yasir Usman, Junaid Javed, and Arsalan Aslam. "Cascaded symmetric multilevel inverter with reduced number of controlled switches." International Journal of Power Electronics and Drive Systems 8, no. 2 (2017): 795.

Declaration: The research work presented in this dissertation is based on publications 1 and 2. The author declares that the thesis is their own work and it is not been plagiarized or used as someone else's work without appropriate acknowledgment. At some points, in this thesis, if the author has used any published work, ideas, or data from others, it is declared by giving proper credit and citing the sources accurately. Moreover, the author states that the research conducted in the thesis complies with ethical standards and guidelines.

ACKNOWLEDGEMENTS

In the name of Allah (SubhanahuWaTa'ala), who is the kindest and generous. I am grateful to ALLAH (SWT) for granting me strength, stamina, and direction throughout this work and for thoughts, which originated in my mind to complete this research work. Indeed, there is nothing that can happen without His will.

I am really thankful to my advisor Dr. Adnan Umar Khan who guided me throughout my Ph.D. journey and supported me in all possible ways, without his support, guidance, and motivation the accomplishment of this research was not possible. I would also like to thank Engr. Reyyan Ahmed currently working as a research engineer in South Korea for his technical help. I am also thankful to all my teachers who taught me the skills which enabled me to complete this work.

I am very thankful to all my family members specifically my mother, father, brothers, and sisters, without their support and prayers it was impossible to complete this research. I strongly believe that what I am today is due to the efforts they put into me throughout my entire life. I have no words to write few lines which can describe their sincerity and love for me. I am also thankful to my mother and father-in-law for their prayers. I would like to specifically mention the support, prayers, and help of my wife during the entire duration of this research work and pay special thanks to her.

I am thankful to my friend Bahrullah who is not less than a brother to me. He supported me throughout this research and prayed a lot for my success. I am also thankful to my all other friends, who supported me during my research work.

In the end, I am acknowledging all my students who assisted me during my research work. Above all, I am thankful to International Islamic University which provided me all the required facilities and opportunities to grow my skills and achieve my targets.

Tila Muhammad

August, 2023

TABLE OF ABBREVIATIONS

Abbreviations and their description.

Symbols	Description
C_f	Fiter Capicitor
DER	Distributed Energy Resource
f_g	Grid frequency
f_n	Low pass filter natural frequency
GCI	Grid-connected Inverter
G_f	Proportional voltage feed-forward
i_g	Current entering into the grid from inverter
k_c	Gain of active damping loop
K_i	Integral time constant
k_o	SOGI filter damping factor
k_{or}	Compensator damping factor
k_{on}	Notch filter damping factor
k_p	Proportional gain
k_{pwm}	Modulation index
k_{ppll}	Proportional gain PLL
K_r	Compensator gain
L_1	Inverter side inductor
L_2	Grid side inductor
MLI	Multilevel Inverter
P	Rated Power
PCC	Point of Common Coupling
PLL	Phase Lock Loop
RE	Renewable Energy
THD	Total Harmonic Distortion
Ti_{pll}	Integral time constant PLL
T_L	Low pass filter time constant
V_{DC}	DC voltage sources (V_{DC_1}, V_{DC_2}, V_{DC_3} and V_{DC_4})
V_s	Grid Source Voltage (RMS)
v_g	Grid voltage at the PCC
Z_g	Grid impedance

TABLE OF CONTENTS

LIST OF FIGURES

LIST OF TABLES

CHAPTER 1

INTRODUCTION

The demand for electricity is continuously increasing worldwide due to a variety of factors like economic development, population growth, and an increase in the use of electronic devices. In order to meet this growing demand, more electricity must be generated, transmitted, and distributed. This can be done through a variety of means, including the construction of new power plants and the expansion of existing ones. However, meeting the increasing demand for electricity can also pose challenges, such as the need for new infrastructure and the potential environmental impacts of electricity generation.

Conventional methods of electricity generation are based on fossil fuels like oil, coal, and natural gas are largely used around the world. These methods can be relatively inexpensive, but they also have serious environmental and sustainability impacts. The combustion of fossil fuels releases dangerous greenhouse gases, like methane and carbon dioxide, into the atmosphere, which are factors behind climate change and are producing many adverse effects. The extraction and transportation of fossil fuels can also have negative impacts on the environment, including air and water pollution and habitat destruction. In addition, fossil fuels are non-renewable energy resources which means that they will eventually deplete. As a result, they are not a sustainable long-term solution for electricity generation.

Nuclear energy is another form of conventional electricity generation. While it does not produce greenhouse gases when generating electricity, it does have other environmental and safety concerns. The disposal of nuclear waste, for example, can be a major challenge, and there is the potential for accidents at nuclear power plants. In addition, the construction and decommissioning of such power plants are expensive and time-consuming.

Overall, while conventional methods of electricity generation can be cost-effective in the short term, they have significant impacts on the environment and may not be feasible

and sustainable in the long run. Therefore, recently interest has grown in using RERs as an alternative to conventional energy resources.

The use of renewable energy (RE) resources can also have economic benefits. While the initial costs of setting up RE systems may be higher than those for conventional energy sources, RE often has lower long-term costs due to the fact that it does not require the continuous purchase of fuel. In addition, RE can help to reduce the need of fossil fuels, which are subject to price fluctuations and may become more expensive over time. Overall, RE is a sustainable and cost-effective source of electricity that can help to reduce the environmental impact of energy generation and support a transition to a low-carbon economy.

RE resources harvest energy from natural sources, such as sunlight, wind, water, and geothermal heat. It is a distributive energy resource because it can be generated and used locally, rather than being centrally produced and distributed over long distances. This makes it an attractive option for communities and individuals who want to reduce their reliance on fossil fuels and increase their energy independence. RE techniques, like photovoltaic panels and wind turbines, can be installed on a small scale, making it possible for individuals and communities to generate their own electricity. Additionally, RE sources are sustainable and have a low impact on the environment, making them a more attractive option.

One of the main challenges of relying on RE resources is that they are often intermittent. For example, solar panels only produce electricity when it is daytime and the sun is available, and wind turbines only harvest energy when the wind is blowing. The continuity of energy can be obtained by adding energy storage systems where excess energy can be stored. So that it can be used when the RE resource is not producing enough power.

Storing electrical energy from RE sources can be done using various technologies. One common method is through the use of battery storage systems, which can store excess energy generated by renewable sources and release it back when needed. Another option is through the use of pumped hydroelectric storage, which involves pumping water uphill to a reservoir when excess energy is available and releasing it back down through a turbine to

generate electricity when demand is high. Other methods of storing RE on the grid include compressed air energy storage and flywheel energy storage. The choice of technology depends on the specific needs and resources of the location where the energy is being stored.

Another very low-cost method of storing excess energy from RE sources is storing energy on an alternating current (AC) grid using grid-connected inverters. The grid-connected inverters are used to convert direct current (DC) electricity, which is the type of electricity produced by RE sources such as solar panels, into AC electricity, which is the type of electricity used on the grid. The AC electricity is then fed into the grid at the point nearer to the energy sources. The advantage of using inverters to store energy on the grid is the efficient use of excess energy produced by renewable sources, as it can be stored on the grid and used when demand is high.

It is important to note that in the legacy grid, there is no direct storage in the power grid but indirect storage can be used for this purpose. For example in our country, most of the electricity is generated through hydropower plants where the water can be stored in the dam as the reservoir of energy and the water can be released as per the requirement of the load. During the daytime when solar panels are generating power and the grid-connected inverter (GCI) injects that power into the grid. Then the water remains in the reservoir, and it can be released at nighttime. Thus, the surplus energy of solar panels can be injected into the grid and the users can get the energy again at night. The energy entering the grid can share the load on the hydropower plant in the daytime. The crux of the point is that solar energy shall be utilized merely in the daytime which will have an energy saving for the dam while hydropower will be dealing with the load in the nighttime when solar energy will not be available. Similarly, in the case of thermal power plants connected to the grid reserve fossil fuels during the daytime when energy enters from solar panels, and at night the thermal power plant runs by using the fuels reserved in the daytime. The theme looks like the energy is stored in the grid indirectly during the daytime and used at night.

Thus, this type of storage method is cost-effective. The inverters used for this purpose are called GCIs. Due to the important role of GCIs used for the integration of RE sources with utility grids, a lot of recent developments have been made in the area of the design and control of GCIs. Most of the work is focused on increasing the efficiency, cost, quality output, and stability of GCIs. The efficiency and stability of GCIs highly depend on the nature/strength of the grid available at the point where the inverter is connected with the grid. The inverters that are stable where the grid is strong but are not guaranteed to be stable if connected at places where grid characteristics of the grid are weak unless they have wide bandwidths. The stability issues can further rise when there are parallel inverters connected nearer to each other.

The strength of a grid can be described in two ways, grid impedance (Z_g), and short circuit ratio (SCR). The SCR can be defined as the ratio of the short circuit power at the point of common coupling (PCC) and the rated power of the inverter. The grid is considered as weak if the SCR is less than 10 while the grid is strong if SCR is above 20. Therefore, the increase of the rated inverter power or the transmission impedance will reduce the SCR which as a result makes the grid weaker. The PCC voltage can vary easily when a large amount of active power is injected into a weak grid. Moreover, the strength of a weak grid also depends on Z_g. A strong grid has near to zero Z_g and a weak grid has a large Z_g. The inverter should be robust enough that can be connected at either condition.

In this research, a hybrid adaptive control technique is proposed to make the GCIs robust against Z_g and frequency variations. Moreover, it produces less total harmonic distortion (THD) in the current injected into the grid. The proposed solution can also work effectively when there is a variation in grid frequency. Moreover, a new multilevel inverter (MLI) topology with equal sharing of voltage source sharing is proposed which further improves its performance.

1.1 Background

Due to the increasing electricity demand, more power plants are needed to be connected to the existing grid, it would require an increase in the capacity of the existing grid to accommodate more power plants. One solution to increase the capacity without increasing grid infrastructure is to add power through distributed energy resources (DERs). Therefore, DERs can help to increase the capacity of the electrical grid in a number of ways. First, DER systems can generate electricity locally, reducing the need to transmit power over long distances and potentially reducing the risk of transmission losses. This can help to increase the overall capacity of the grid by making more electricity available to consumers. Additionally, DER systems can help to reduce the peak demand for electricity. For example, the use of solar panels can reduce the demand for electricity from the grid during the middle of the day when solar radiation is highest. Finally, DER systems can provide additional capacity to the grid during times of high demand or when there are disruptions to the traditional power supply. For example, energy storage systems such as batteries can release stored electricity back into the grid during times of high demand or when there is an outage. These DERs can be connected with an AC grid with the help of GCIs. Therefore, GCIs not only supply surplus energy to the grid to save it but also enhance the capacity of the existing grid and reduce transmission losses.

A GCI is a type of power electronic device that converts direct current (DC) electric power generated by RE sources into alternating current (AC) synchronized with the voltage of the electric grid. This allows households and businesses that generate their own electricity to feed excess power back into the grid.

The development of GCIs can be traced back to the early days of solar power generation. In the early 20^{th} century, solar power systems were primarily used in isolated applications such as the lighting in remote locations. As technology advanced, researchers began experimenting with ways to connect these systems to the electric grid.

The first GCI used in solar power systems were relatively simple devices that primarily served to match the voltage of the solar system to that of the grid. But as technology continued to advance, inverters became more sophisticated, incorporating features such as maximum power point tracking (MPPT) to optimize the energy generated by solar panels, and communication protocols to allow for monitoring and control.

The development of GCIs also influenced the growth of small-scale RE development. The ability to connect RE system to the grid allows for a more distributed way of generating energy, it also increased the penetration rate of RE within the grid and help to reduce greenhouse gas emissions. A GCI plays a crucial role in the integration of RE sources with the electric grid, whether it is the legacy grid or the smart grid.

The legacy power system architecture is given in Figure 1.1 where the power is generated at the central stations and utilized at far-distanced utilities. The power is transported through transmission and distribution lines.

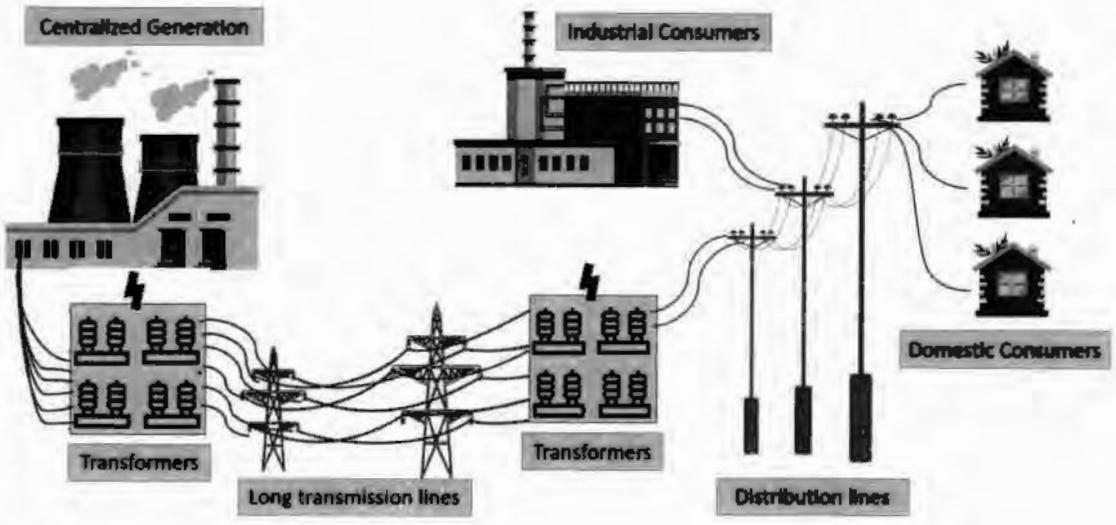

Figure 1.1: The legacy power grid structure [1].

In the legacy grid, a GCI acts as an intermediary between the RE source and the electric grid, converting the DC electricity generated by the source into AC electricity that can be fed back into the grid. However, the legacy grid is not designed to accommodate the

integration of large amounts of DERs such as RE systems. This can lead to challenges such as voltage fluctuations and power quality issues.

The smart grid, on the other hand, is a modernized electric grid that incorporates advanced technologies such as two-way communication, automation, and advanced metering to improve the integration of DERs as shown in Figure 1.2. GCIs in a smart grid can use these technologies to optimize the integration of RE sources with the electric grid by communicating with the grid to ensure that the voltage and frequency of the power generated by the renewable source match that of the grid. Additionally, smart GCIs can also help to improve the overall performance of the grid by providing additional services like frequency regulation and voltage support.

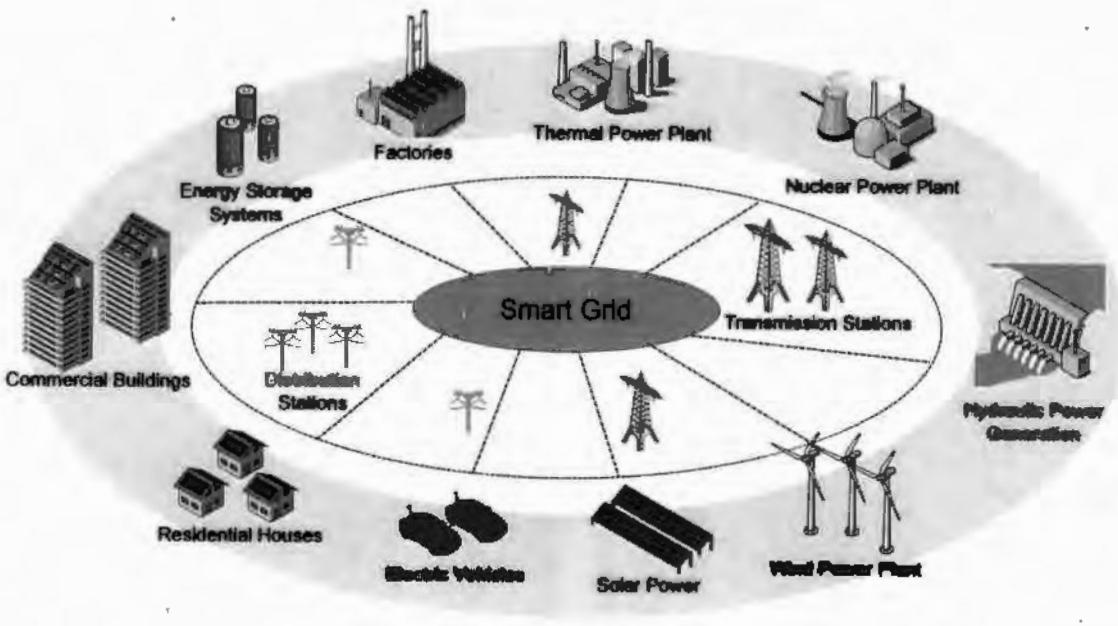

Figure 1.2: The smart grid conceptual architecture [2].

In short, grid-connected converters are the core components within the distributed grid-connected power generation system. A lot of research and development work has been done in the past and is concentrated on the topological improvement of inverter designs like multilevel inverters(MLIs), matrix converters, and Z-source inverters. The recent de-

velopment is focused on developing robust control techniques capable of reducing total harmonic distortion and increasing the power transfer efficiency [3]. For that purpose, control techniques were developed to regulate the voltage, frequency, and phase of the converter waveform while they are connected to the grid or even in islanding mode. A comprehensive literature on converters is found in [4].

In grid-connected applications, most of the inverters used are current-controlled which uses the concept of pulse width modulation (PWM). The PWM modulation index can be controlled with different techniques from the control theory to transfer the desired power to the grid. The configuration of control and modulation scheme used in power electronic converters is shown in Figure 1.3.

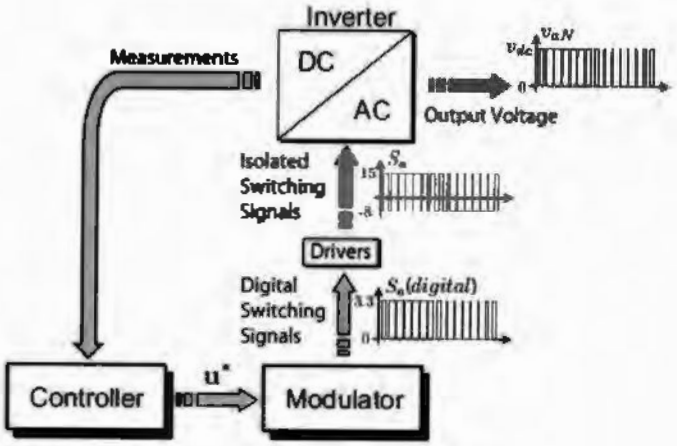

Figure 1.3: The Configuration of modulation and control scheme of voltage source inverters [5].

Most of the control techniques developed are based on the assumption that the grid is static, but in reality, grids have time-varying parameters. Thus, the control techniques designed based on static parameters may result in an unstable system if the designed converter is placed at different locations where the grid changes from strong to weak. Therefore, robust and adaptive control is needed in GCI, which can handle distortions, disturbances, and variations in the grid like Z_g and frequency.

A grid can be categorized as a stiff grid (strong grid) or a weak grid on the bases of its parameters. The stiff grid has a high short-circuit current due to low impedance and is capable of keeping the regulated voltage regardless of load variation. The impedance of a stiff grid is considered negligible. Therefore, the inverter with a smaller output impedance can remain stable. On the other hand, the short circuit current of a weak grid is small due to relatively high impedance, it has poor voltage regulations and it can result in unstable GCI if not properly controlled [6].

The grid-connected converters need to be plug-and-play irrespective of the properties of the grid. Therefore, again a robust and adaptive controller is required for grid-connected applications. In addition, the controllers of grid-connected converters must be robust enough to handle grid parameter variations. The distributed generators are usually located at utilities which are located at the far end of the distribution network. The far-end distribution lines are of low voltages and are connected through transformers with the transmission line which results in an increase in the Z_g. In Figure 1.4, a scheme of the PV home connected to the grid is shown. The resistive part of Z_g does not affect the stability of GCIs but the inductive part of the Z_g can variate the stability margins of the GCIs.

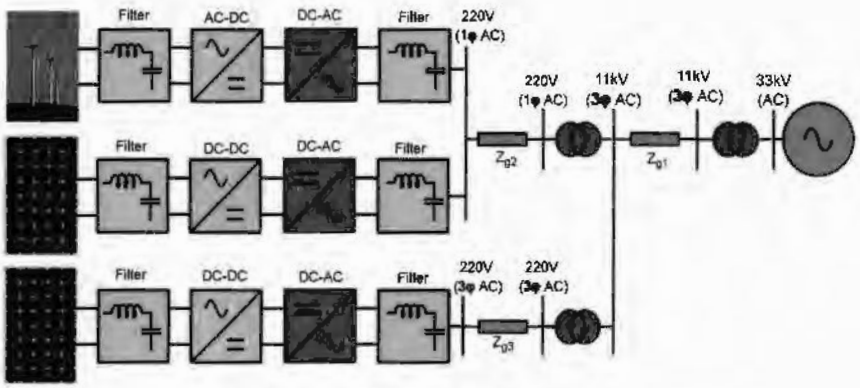

Figure 1.4: The network combines the high voltage (HV) distribution system with the utilities.

In order to develop robust and adaptive control strategies for a GCI, an accurate math-

ematical model of the system is needed. An average switched model of the GCI is used in this research [7].

Researchers have come up with a variety of controllers designed especially for grid-connected applications using the average switch model as a foundation. These controllers have undergone extensive testing, which has resulted in substantial gains in their general performance. Numerous articles that are appropriately referenced contain thorough explanations of these novel inverters [8, 9, 10].

The grid-connected inverters face more stability challenges when they are connected to weak grids. The operational environment becomes more difficult in these situations because the grid impedance, grid frequency, and grid voltage exhibit variations. In the cited papers [8, 9, 10], it is concluded that they emphasized how important it is to address these issues of grid impedance and frequency variation to guarantee the steady and reliable operation of grid-connected inverters. Thus, the importance of controllers increases particularly in scenarios with changeable grid conditions. More detail is given in Chapter 2.

In this research, a hybrid control technique is proposed for the GCI which works in synchronous and stationary frames simultaneously. The current regulator is a classical proportional integral controller which is capable to handle small variation in grid frequency and the harmonic compensators are proportional resonance controller which has a narrow bandwidth and is not able to handle the grid frequency variation. Therefore, adaptive resonance harmonic compensators are proposed to handle the frequency variations. Moreover, the control strategy proposed in this research consists of multiple control loops. Figure 1.5 depicts the block diagram of the method used for the control of GCI.

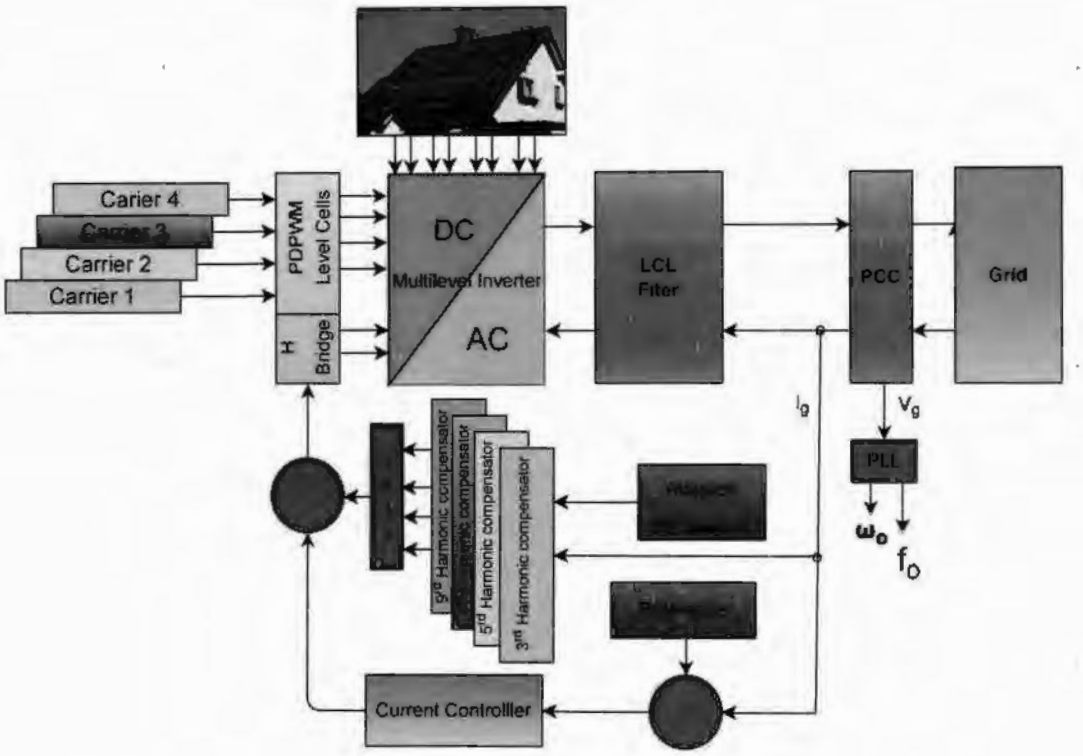

Figure 1.5: Block diagram of proposed system.

1.2 Problem Statement

The rapid adaptation of RE systems results in power electronic-based power systems (PEPS). These PEPS have lower mechanical and electrical inertia but more capacitive and inductive components, which make the PEPS network more likely to have resonance and oscillations. Consequently, unpredictable system dynamics may be observed. Due to these factors, the potential for stability and power quality issues have become a challenging task. Previously, the inverters were designed and stabilized by considering static grids, but recently it has been found that the variation of Z_g can destabilize the inverters. It is also found that the Z_g affects the performance of GCIs and can affect the THD of current injected into the grid. Moreover, this effect becomes more severe when there are parallel inverters near to each other. The parallel operation significantly enhances the overall network resonance and

stability problem. In the presence of Z_g, the grid frequency variation brings even more instability to the system. Therefore, the aim of this research is to design a robust and adaptive control technique for GCIs to make the system more stable and efficient.

1.3 Objectives of the Research

The objectives of this research are:

1. To design an inverter that injects fewer harmonics into the grid and can handle more power.

2. To propose a control law for a GCI that works under the variation of Z_g and is stable even when a large number of inverters are connected close to each other in a parallel configuration.

3. To design adaptive harmonic compensators to handle grid frequency variations.

1.4 Significance of the Research

Renewable distributed power generation is expected to play a key role in the future to enhance the capacity of electrical grids. Distributed power generation along with its efficient and reliable integration into the accessible grid can provide the possibilities to overcome energy shortages which is a common problem in developing countries. Moreover, RE utilization can decrease carbon emissions and play a significant role to produce green energy.

The important feature of the proposed system is that it makes the GCIs compatible with weak grids. Also, the designed adaptive harmonic compensators are suitable for PEPS where grid frequency has the possibility to vary due to lower inertia. Hence, as the proposed system has robustness against Z_g variation and has adaptive harmonic compensators, therefore, the proposed GCI is an appropriate inverter for a wide area network where the impedance of the grid can variate.

1.5 Contributions of the Research

The author contributed to the control and topology of GCI in this research. The contributions are listed as:

1. Designed a hybrid adaptive controller for 3-level GCI to regulate current and suppress harmonics. The current regulator is a fixed value controller working in the synchronous reference frame and harmonics compensators are adaptive working in stationary reference frames. The proposed solution is robust and has promising results under distorted grid voltages, Z_g variation, and grid frequency variation. This work is published in [11].

2. Designed and implemented cascaded symmetric multilevel inverter with a reduced number of controlled switches having equal sharing of voltage sources. This work is published in [12]

3. Did the comparative study on minimization of conduction and switching losses in cascaded multilevel inverter via reduced switches and equal voltage source-sharing. This work is published in [13]

4. Designed a hybrid adaptive controller for reduced switched cascaded MLI for grid-connected applications having the feature of equal source utilization. It is found that it has more promising results than the 3-level inverter and is more robust against Z_g and frequency variations. This work is submitted for publication to IEEE Access.

1.6 Thesis Layout

The research is related to the integration of DERs with a weak grid. The research procedure is divided into different phases to achieve the goal in a systematic manner. The following are the sequential phases of the research methodology:

1.6.1 Review of Literature

During this phase of research, a comprehensive study of converters' topologies is conducted. The recent trends in power converters and their control are studied. Moreover, the recent development in grid-connected converters is comprehensively studied. The study conducted for the literature survey is presented in *chapter 2* of this thesis. Where the discussion starts with inverters in general and then the discussion is narrowed down to a voltage source single-phase GCI. Later, in the same chapter, the discussion is limited to the current control of GCIs. Finally, a cascaded symmetric MLI is found suitable to enhance it further. It is found that GCI in weak grids faces challenges of stability which is considered as the research gap.

1.6.2 GCIs Modeling and Analysis

In this phase, a mathematical model of GCI is derived by using an average switch control technique and analyzed with the help of simulations which is presented in *chapter 3*. Moreover in this chapter, the grid voltage feed-forward is also discussed, and through analysis of the existing technology used for GCIs, the second-order generalized integrator (SOGI) based voltage feed-forward technique is opted for the proposed GCI. The impedance-based stability analysis is also discussed in this chapter.

1.6.3 Design and Control of 3-Level GCI

In this phase of research, the proposed hybrid adaptive control of the inverter is designed. To check the validity of the proposed design it is tested for 3-level GCI. In *chapter 4*, the model of GCI based on the proposed control technique is represented. The average switch control model is also derived. A detailed study of synchronization, the current controller, and the adaptive harmonic compensator is conducted. The stability of the proposed system is tested, and the performance is evaluated by using computer simulation. The results are evaluated by using different cases. In *case study 1*, the stability and total harmonic distortion of the inverter are tested by changing the Z_g. In *case study 2*, the results are extracted

and evaluated by changing the grid frequency. Moreover in this chapter, the results are also compared with the existing technique to show its effectiveness.

1.6.4 Design and Control of Reduced Switch Grid Connected MLI

In this phase, the hybrid control of GCI is implemented for the reduced switch MLI topology proposed by the author where an additional feature of equal voltage sharing is implemented through PWM by using a pseudo-code which is explained in *chapter 5*. In chapter 5, the control design proposed in Chapter 4 for the 3-Level inverter is applied to the reduced switch MLI. The new designed GCI is tested and evaluated through computer simulation and promising results were found. The results are categorized in three different cases. In *case study 1*, the multilevel GCI is tested for three different Z_g and the total harmonic distortion in the current entering the grid is observed. In *case study 2*, the frequency adaptiveness has been tested. In *case study 3*, the power handling capability of the design is tested. On the bases of better performance in all three cases, it is concluded that the results are promising.

1.6.5 Conclusion and Future Work

In the last chapter of the thesis, the conclusions of the research are presented and the directions for future work are given.

CHAPTER 2

LITERATURE REVIEW

Grid-connected inverters(GCIs) work as the core component in the integration of distributed energy resources with an existing AC grid. Due to the importance of GCI, a lot of research and development has been done in this area. The literature on GCIs reveals that there are two main areas of research in GCIs, to which the researchers are contributing. Some of them are focused on the topologies of GCIs and the focus is on power handling capability, efficiency and decreasing the size and cost. While the others are focused on control techniques. Both of these domains have their own significance and importance in different applications. In this chapter, a detailed study of GCIs is conducted. Which covers the topologies used for GCIs including 3-Level and MLIs along with its control consisting of synchronization, current controller and harmonic compensator. Moreover, stability analysis techniques used for GCIs are also covered in this chapter.

2.1 Grid-connected Inverters

The GCIs can be classified into single, three, and multi-phase inverters. Single-phase GCIs are used to convert DC electricity from RE sources, such as solar panels, into AC electricity that can be fed into the electrical grid. They are typically used for small-scale power generation, such as in residential homes. Three-phase GCIs are used for larger-scale power generation which is often used in commercial and industrial settings. These inverters convert DC electricity into three-phase AC electricity, which is more efficient for larger loads and long-distance transmission. They also synchronize the generated AC voltage and frequency with the grid voltage and frequency, so that the generated power can be fed into the grid. Multi-phase GCIs are an extension of three-phase inverters. They are used to gen-

erate more than three-phase AC power and feed it into the grid. They are mostly used in high-power applications such as power plants and wind turbines. They are used to generate more complex and efficient power systems. It's important to note that GCIs must comply with safety and power quality standards set by regulatory bodies in order to ensure stable and safe operation of the power grid.

Any one of these inverters can be selected as per the requirements of the application. Here, a single-phase inverter is designed, therefore single-phase inverter is discussed in this chapter. DERs are abundantly available in rural areas where the grids behave like weak grids due to the long distance of distribution lines. Therefore, the research is focused on inverters designed for weak grid applications. In Pakistan, the utilities in rural areas mostly have single-phase connections. Therefore, the proposed design is also a suitable solution that can be implemented in Pakistan.

In RE systems different types of voltage, current and Z- source inverters are used to inject power into a grid [14, 15, 16, 17]. Each [14],[15], [16] of these inverters has its own advantages and disadvantages but due to more applications of voltage source inverters, these inverters are commonly available. Therefore, this specific type of GCIs is focused in this research to improve its stability and efficiency.

RE resources can be connected to the grid by using two types of controlling techniques that are single-stage control and two-stage control. In the single-stage strategy, there is a single control unit connected to GCI, that is responsible for maximum power point tracking (MPPT) as well as injecting synchronized and stable power to the grid. While in the two-stage strategy, MPPT is achieved via first stage controller, connected to some converter (buck or boost) and synchronized power is injected into the grid via second stage controller which is connected to GCI [15, 18]. A detailed study on comparison of these single and two-stage GCIs is conducted in [19]. As the prime aim of this research is the inverter performance and stability, therefore the contributions of the author are to the second stage which is the inverter and its control unit. Therefore, in this research, the two-stage control

strategy is adopted and the discussion is limited to the second part. Hence, the RE source and the maximum power point tracking circuit are replaced with a fixed DC voltage source.

The GCIs can also be classified on the basis of the nature of power or current injection to the grid. There are two types of GCIs one is injecting a reactive power to the grid while the other is injecting real power to the grid [20, 21, 22]. In this research, the active power transfer is adapted, where the grid voltage is synchronized with the inverter current by using Phase Lock Loop(PLL) technique. The active power injecting GCIs can be divided into further two types, one is transformer-based GCIs while the other is transformer-less GCIs [4]. In this research, transformer-less GCI is designed and its control is presented.

One of the classifications of GCIs is based on the inverter's output waveform before passing it through the LCL filter. Thus GCIs can be classified into three types: Bipolar (2-level inverter), Unipolar (3-level inverter) and MLI(n-level inverter where 'n' can be any integer as per the requirement and constraint of the design). The 3-level and MLI are considered important due to their power-handling capability. Therefore, these two types of GCIs are discussed further in detail.

2.1.1 3-level Grid-connected Inverters

An inverter is a core element used within grid-connected DERs. Therefore, the selection of its topology for a specific grid-connected application is very important to meet certain requirements.

A "3-level" inverter utilizes a three-level topology, which means that it uses three voltage levels to generate the AC output waveform. This allows for a higher power density and increased efficiency compared to traditional 2-level inverters. It is a commonly used inverter for grid-connected medium power applications. A full bridge inverter can be used as a 3-level inverter. The bridge generates the PWM AC output by using the controlled switch patterns applied to its gate using the control technique. The low pass filter is used to generate a smooth AC signal from the PWM signal generated by the full bridge inverter.

Therefore a low pass filter also plays an important role in GCI.

The *L*, *LC* and *LCL* are the commonly used filters in the grid-connected application. Among these filters, *LCL* is the suitable candidate for GCIs application. But, the capacitor in the *LCL* filter is the source of resonance. To dampen these resonances, two types of damping methods are usually used i.e. passive and active damping. In passive damping, a passive element resistor is used in series with a filter capacitor [23, 24, 25]. But passive damping introduces energy losses across the damping resistor. Therefore, it is recommended to use active damping. In active damping, the current passing through the filter capacitor is extracted with the help of a current sensor and that current is fed back by using a dedicated feedback loop [26, 27, 28] having a damping factor. The loop can dampen the resonance produced by the capacitor of the *LCL* filter and also save the energy that dissipates in the damping resistor in case of passive damping. In this research, an active damping method is used for the damping of resonance and will be discussed in detail in the next chapter.

Furthermore, the 3-level inverter can be classified on the basis of the control technique used in it. Here, the 3-level inverters are divided into two types on the basis of control technique: one is the control of GCI without any harmonic compensator while the other is control of a 3-level inverter with an additional control part that is harmonic compensator. A detailed discussion on control techniques is given in Section 2.2. The classification discussed in this section is depicted in Figure 2.1.

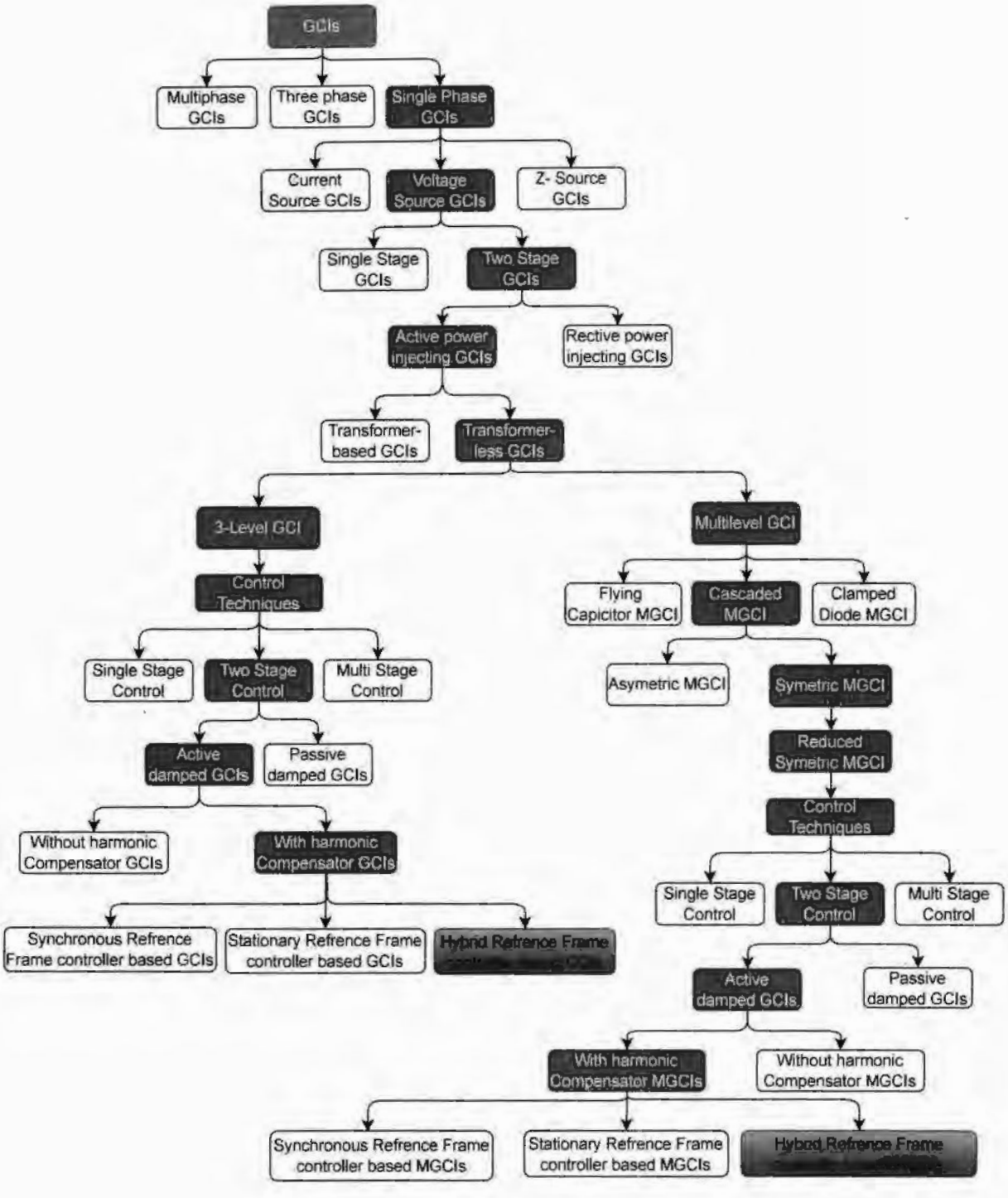

Figure 2.1: Taxonomy tree of GCIs.

2.1.2 Multilevel Grid-connected Inverters

MLIs have brought a revolutionary change in the emerging technology of GCIs. It is a suitable technology for low, medium and high power applications due to its high resolution of output and varying flexible structure.

MLIs have stair output waveform which is responsible for high stability and enhanced performance. The limitations of this inverter are its cost, size, weight and circuit complexity. But, in some applications, these limitations become advantages like in string converters, where several DC sources are available in form of a string of solar panels. These inverters can be used to cascade them and form a transformer-less GCI [29, 30, 31]. Like other applications, MLIs are also one of the favorite topologies for GCIs application [32].

Multilevel GCIs can further be classified into three classical categories i.e. clamped diode, flying capacitor and cascaded topologies[12]. The cascaded topologies of the GCI have many advantages as compared to others due to their simple modulation, easy control, and high output resolution [33, 34, 35]. Therefore, on the basis of these advantages, the cascaded topology is considered for grid-connected applications in this research.

Cascaded Multilevel GCIs (MGCIs) can be further classified as symmetric and asymmetric MGCIs. The Symmetric MGCIs are those types of inverters, which generate a positive and a negative level with one DC source at a time, while in asymmetric MGCIs more than two levels can be produced at the output with one DC source by adding and subtracting the voltage sources using different configurations. In the asymmetric MGCIs the stress does not remain the same on all switches and its PWM technique is also difficult. Therefore, in this research, the symmetric MLI is used for grid-connected application[36] due to its advantages. Therefore, further discussion is restricted to symmetric cascaded MLIs only.

Cascaded MLIs have some limitations of the large number of switches that are used for generating levels at the output. These switches increase the cost, size, and in-system losses

in symmetric MLIs. To minimize these limitations, reduced switch MLIs are used. In this research, a reduced switch MLI is used which has an additional feature of equal source sharing given in [13]. More detail about this inverter is given in Chapter 5.

A low pass filter is also used in MGCIs similar to the 3-level inverter and *LCL* is the suitable choice for the filter, hence again a damping technique is required to handle the resonance created by the capacitor of the filter. Therefore MGCIs can also be classified into active damping and passive damping GCIs and again active damping method has been opted for this part of the research. The further classification of MGCIs on the basis of control technique is similar to 3-level GCIs.

The above-discussed classification of MLIs used in the grid-connected applications is given in Figure 2.1.

2.2 Control of Grid-connected Inverters

To inject the desired power into the grid and keep the inverter stable, a feedback control system is required. Hence, the controller plays an important role in the performance and stability of an inverter. The control of a GCI needs an additional feature of synchronization which synchronizes the inverter current with the grid voltage. The control section of GCIs can be divided further into three subsections i.e. synchronization, current controller and harmonic compensators, which are discussed here in detail.

2.2.1 Synchronization of Grid-connected Inverters

The injection of power from RE sources into an existing AC grid needs a high degree of synchronization to avoid the mismatch of phase and frequency. Therefore, different techniques are used to accomplish this synchronization. There are two types of power injection techniques used in GCIs one is reactive power transfer while the other is active power transfer. In this research, the active power transfer technique is used. Where the grid

voltage at the point of common coupling (V_{PCC} or V_g) can be sensed to extract its phase and frequency. Then the current injected into the grid i_g can be synchronized with the voltage of the grid by using different types of control techniques and thus the active power can be transferred from RE sources to the grid.

The common technique used for the extraction of phase and frequency of the grid voltage is PLL. There are different types of PLL with a variety of implementation methods. The PLL used in this research is using the proportional-integral (PI) controller which is a synchronous frame controller. Therefore, the grid voltage signal can be converted into DC representation by using direct-quadrature-zero (DQZ) transformation.

In three-phase inverters, any two phases of voltage can be used for DQZ transformation. But in a single-phase inverter, there is no other phase available. Therefore, an orthogonal signal generator is required. The orthogonal signals can be generated by using different techniques. The use of first-order delay filters and second-order generalized integrator (SOGI) filters are the two common methods for the generation of orthogonal signals. The PLL also provides immunity to the inverter from disturbances and unwanted signals to reach the control part of the GCIs. Therefore, SOGI filters based PLL has more advantages to be used in GCIs. In this research SOGI based PLL technique is used.

For the case of weak grids, the estimated phase is distorted due to the presence of voltage harmonics. The harmonics propagate through PLL circuits and reach the control unit of the inverter [37]. These harmonics propagate further through the control unit and are added to the low-order harmonics present in the current feeding to the grid. An optimally designed PLL can be used with filters to prevent harmonics from entering the control unit, but still some low-order harmonics lie in the bandwidth of the PLL and make it to the control unit. SOGI filters play a characteristic role in such cases [38].

2.2.2 Current Controller of Grid-connected Inverters

The current control unit of GCIs is used to deliver the desired power to the grid. Over the past few years, the current controllers for GCIs have gained the attention of many researchers, resulting in plenty of research outcomes [39, 40]. The literature on current controllers covers a variety of control theories from the conventional controller to highly specialized controllers.

The commonly used current controllers are proportional resonance (PR) and proportional integrator (PI) which are stationary and synchronous frame controllers respectively [7]. The PR controller has good performance but due to its narrow bandwidth, it cannot handle frequency variations[41, 42] and are complex to be implemented using digital processors. In contrast to the PR controller, the PI controller can handle some variations in frequency and can easily be implemented on digital processors. The PI controllers can not work on AC, therefore the AC signals need to be converted from stationary frame to synchronous frame (DC signals) by using DQZ transformation. This conversion and its implementation make the power processing tedious but offer the advantage of robustness to frequency variation due to its high bandwidth. Therefore, it has the capability to handle a slight variation in the grid frequency[43]. The comparison of PR and PI controllers for GCIs is presented in [44].

In short, both PI and PR controllers have their own advantages and disadvantages and the choice between them depends on the specific application and system requirements. For example, PI controllers are less complex and less sensitive to parameter variations, but PR controllers can provide improved performance in certain types of systems. In grid-connected applications, PI controller is widely used due to its simplicity and robustness. But PR controllers are also used in some cases where better performance is required.

There are many other control techniques that are used to control GCIs. The model predictive control is also a commonly used controller for grid-connected applications. In

[45] the model predictive control for GCIs is proposed for a PV system. It is found that the proposed model predictive control has a good performance in the steady and transient states. With the help of a model predictive controller, the reduction in switching frequency and flexible power regulation is achieved which also reduces in-system power losses. For the model predictive controller, the system model and cost function are usually required. Similarly, in [46] the comparison between PR and model predictive controller is conducted. When PR controller has a narrow bandwidth, it works slower and takes time to track the reference. If it is designed with high bandwidth then the overshoot increases. So, this limitation of PR controller is overcome with the help of model predictive controller [46, 47, 48].

The repetitive controller is also an appropriate controller for GCIs. The repetitive controller has a good tracking capability and keeps the THD low of current injected into the grid. However, in repetitive control, the ratio between the sampling frequency to the fundamental frequency of the power grid cannot result always in an integer that deviates the resonant frequencies of the repetitive control from the fundamental of the grid and the frequencies of the harmonics present in the grid, which is a limitation of repetitive control. This issue is addressed in [49] and also a solution for its improvement is presented. It is also noted that the conventional repetitive controller has the auxiliary function for stabilization of steady-state tracking error and total harmonic distortion of the GCIs.

Researchers have also used fuzzy logic control for GCIs. The fuzzy logic controllers have the capability of approximation. Therefore, they are effective in nonlinear and uncertain systems. These types of controllers are sometimes suitable where the mathematical model is not known. Keeping in view the considerably uncertain and nonlinear characteristics of photovoltaic (PV) and PWM methods, it can be observed that a fuzzy logic controller can be a suitable candidate for grid-connected applications. In [50, 51], fuzzy logic controllers are used for improving the performance and stability of GCIs.

There are some other control techniques given in [39, 52, 10] which can also be used

for GCIs. The well-known techniques from them are dead beet controller [53, 54], LQG controllers [55, 56, 57], H-infinity controller[58, 59], neural network controller[60, 61], hysteresis controller[62], sliding mode controller[63, 64] and autonomous controller [65] etc. The selection of all these controllers depends on many parameters for example the model of the system is known or not, whether the system is linear (or linearized) or non-linear, the processing speed and the available digital controller etc. These controllers are the backbone of the stability and current regulation of GCIs.

2.2.3 Harmonic Compensators of Grid-connected Inverters

Although SOGI filters for PLL remove harmonics or tend to reduce voltage harmonics from grid signals and extract the phase of grid voltage with very little content of low-order harmonics, it is still not possible to estimate the phase of grid voltage free of harmonic. Furthermore, inverter switching also generates low-order harmonics. Therefore, it becomes necessary to add controllers for harmonic compensation. These controllers are called harmonic compensators. These compensators reduce total harmonic distortion in the current feeding into the grid and ultimately improve the performance characteristics and stability of the system.

There are different techniques used for designing of harmonic compensators. Some of these are working in a synchronous reference frame while others are in a stationary reference frame [66, 67, 68, 69, 70]. In some cases the current controllers work in different reference frame from the reference frame of harmonic compensators which is called as a hybrid frame like the case where the current regulators are synchronous, and the compensators are in a stationary reference frame. The selection of the appropriate compensators needs special attention.

In [71], the author introduced a new concept in power electronics from instrumentation which is known as a lock-in amplifier. This technique is quite useful in the extraction of low-order harmonics and their compensation, but it does not work if there is any variation

in the fundamental frequency. Although, the large-scale grids have higher inertia still the line frequency can vary by 2 percent of its rated value. Thus, a compensator designed based on the fixed values fails to reduce harmonics under these conditions.

An *LCL* filter is usually used to generate a pure sine wave, but the capacitor in an *LCL* filter generates resonance. Two methods are used to dampen this resonance [72], one is the active technique and the other is the passive based using resistors [24]. The resistor-based damping results in losses, therefore the active damping technique is preferable [73]. In this research, the resonance was reduced by using the active damping technique.

2.3 Stability of Grid-connected Inverters

GCIs are commonly used in distributed generation by bringing RE resources onboard with the existing grid networks as an additional power with the advantage of generating electricity near, where it is being used. A lot of work has been done on the design of inverters for injecting power into the grid. The nature of the grid is not always the same everywhere; in some regions, it is strong while in others it becomes weak. Hence, the inverters designed under strong grid assumptions may become unstable if it is tied at the point where the grid is weak. Now, it is a challenge to know whether a specific design will be stable or not. In the literature, there are many techniques used to know the stability of GCI with the help of software tools.

In recent studies, it has been found that the stability of GCIs depends on the ratio of the Z_g to the output impedance of an inverter and that this ratio must satisfy the Nyquist criteria of stability [74, 75]. The weak grids have a varying impedance which further complicates the system [76, 77, 78]. Under these conditions, the voltage harmonics of the grid also fluctuate with the flow of load current. The harmonics amplify with the increase of load current and vice versa. If these harmonics are not compensated within the inverters it can result in further amplification at the point of common coupling (PCC) and can make the system unstable. Therefore, the varying characteristics of the grids require inverters

designed with larger stability margins, enabling the inverters for stable dynamics under varying grid conditions. In the case of weak grids, the impedance of the grid depends on some parameters such as line frequency transformers, length of distribution and transmission lines. The number of GCIs also changes Z_g. If GCIs are connected nearer to each other and the impedance between them is ignored, then these inverters become parallel to each other. Such GCIs are modeled for the analysis of harmonics and the resulting stability of the distributed power generation systems [38]. This configuration varies impedance in two ways: the output impedance of the inverter decreases because it is in parallel with others or the Z_g is increased by a factor of N when N identical inverters are connected at the PCC, though the admittance of a single inverter cannot be directly summed to obtain the admittance of multiple parallel GTIs [79, 80]. Thus, the harmonics in grid current increase and stability margins decrease.

2.4 Research Gap

It is concluded by contemporary studies that in most cases the changes in grid characteristics like frequency (f) and grid impedance (Z_g) have frequently been overlooked, which has resulted in an inadequate understanding of the dynamics. Therefore, it is essential to design and develop a Grid-Connected Inverter (GCI) model that takes these factors into consideration. Harmonics, frequency, and impedance of the grid have been determined to vary both geographically and temporally. Inverters connected to these grids may perform poorly as a result of these variations, which could cause instability problems. Therefore, the topology and control methods of GCIs are of utmost significance in reducing these challenges.

Robust systems that may efficiently handle fluctuations in grid conditions have been proposed by numerous researchers. These systems still have certain drawbacks, thus more work needs to be done to increase the stability, robustness, and overall effectiveness of GCIs. In response to this challenge, the author of the research has proposed a novel hybrid adaptive controller as a solution to this issue, with the goal to enhance GCI performance as

a whole and under weak grid conditions specifically. In order to further boost the performance of the GCI system, this proposed control technique is further extended to a reduced switch multilevel inverter, also introduced by the author, which incorporates equal voltage source sharing to further improve the functionality of the GCI system.

More precisely, this research intends to advance current developments in grid-connected inverter technology by introducing this novel hybrid adaptive controller and integrating it with the reduced switch multilevel inverter. The proposed solution seeks to overcome the limitations observed in existing approaches, providing a more stable, robust, and efficient GCI system that can adapt effectively to varying grid parameters and ensure reliable power conversion in challenging grid environments.

2.5 Summary

The GCI is a core component to inject power from DERs into the grid. Therefore the literature is rich in the topologies and techniques used for it. In this chapter, recent topologies and control techniques used for GCIs are discussed briefly. Moreover, it is concluded that a weak grid does not increase the total harmonic distortion of connected inverters up to a certain limit but after that, the total harmonic distortion changes tremendously which can make the system highly unstable. Therefore, it is found that there is still capacity for improvement. Moreover, it is also concluded that the total harmonics distortion remains in the case of the weak grid but after a limit, once Z_g crosses that the total harmonic distortion increases tremendously which makes the system unstable. Therefore, the system stability can be improved by improving the performance of harmonic compensators.

CHAPTER 3

MODELING AND ANALYSIS OF GRID CONNECTED INVERTER

The grid-connected inverter is a nonlinear system here it is linearized by using the small signal model to implement the linear control technique in order to control its output current. In this chapter a standard average switch control model is considered and a mathematical model in the form of open-loop gain and output impedance is formulated. In addition to the control feedback loop, two other loops one for active damping and the other for grid voltage feed-forward are also used in modeling. Moreover, the stability of the system is analyzed at the end of this chapter.

3.1 System Modeling

Keeping the dynamic nature of the grid along with its non-linear nature, the modeling of grid-connected converters always remained a challenging task. In [81, 82], a small signal-modeled voltage source converter is proposed and also investigated. The Jacobian transfer matrix is used to represent the small signal model. By reviewing the literature, it is concluded that in most cases, the grid parameters variation in the form of frequency and Z_g are ignored. Therefore, a GCI model is needed to incorporate these aspects too.

Recent work shows that parallel weak GCIs can result in an unstable system even if all the individual inverters are stable. The reason is Z_g and inverter output impedance ratio can vary a lot when there are multiple GCIs working nearby each other. The parallel operation significantly aggravates the overall network resonance and stability problems, which hinder closely deployed distributed renewable plants. The work done in [79] investigates the mutual interaction and stability issues of multiple grid interfacing inverters in electronics-based power systems under varying grid conditions. The investigation reveals that such

interactions between power inverters and the grid may excite multiple resonances at various frequencies under certain grid conditions.

Typical GCIs consist of five main parts: 1. a DC power source, 2. power consists, 3. filter, 4. AC grid and 5. control unit. The general block diagram of the system consisting of these parts is given in Figure 3.1.

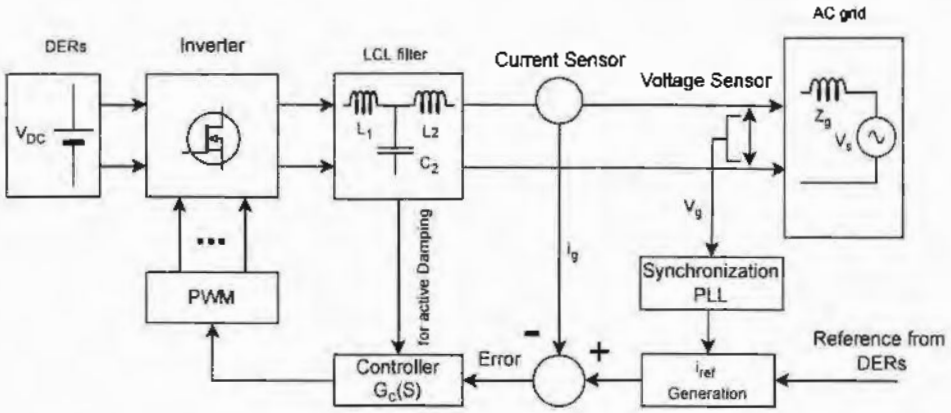

Figure 3.1: The block diagram of a closed loop GCI.

Here, for ease of analysis, the DC source is assumed as an ideal ripple-free DC power source with an output voltage V_{DC}. The full H-bridge configuration is used for power switches taking DC voltage V_{DC} and four PWM signals as input to gates and converting the input DC power into PWM-based alternating output voltage V_{inv} and current I_{inv}. The LCL filter converts PWM V_{inv} and I_{inv} into a smooth V_g and i_g waveform respectively. The LCL filter consists of inverter side inductor L_1, grid side inductor L_2, and Capacitor C_f along with parasitic resistors R_1, R_2, and R_c, respectively. The parasitic resistances do not devalue the stability of the system, therefore these are ignored in further analysis. The AC grid impedance is modeled as Z_g and voltage source V_s and is connected to an LCL filter at PCC where it has a voltage V_g. The resistive part of the Z_g is ignored and it is considered inductive only.

The grid voltage has a fundamental frequency of 50 Hz with possible variations of 4% (from 48Hz to 52Hz) and low-order odd voltage harmonics. The grid source voltage is V_s. The grid is represented by an equivalent Thevenin circuit. The control part consists of

a current controller, synchronization, reference generation and modulation. The values of parameters used in the GCI in this research are tabulated in Table 3.1.

Table 3.1: The system parameters with description and values

Symbols	Description	Values
P	Rated power	5 kW
V_{DC}	DC-link voltage	400 V
V_g	Grid voltage (RMS) at PCC	220 V
f_o	Grid frequency(fundamental)	50 Hz
L_1	Inverter side inductance	0.75 mH
L_2	Grid side Inductance	0.45 mH
C_f	Filter capacitor	6.01 uF
k_c	Active damping constant	10.6/400
Z_g	Grid impedance	0–15 mH
k_o	SOGI filter damping factor	0.5
k_{or}	Compensator damping factor	0.001
k_{on}	Notch filter damping factor	7
K_r	Compensator gain	250
K_p	Proportional gain	50
k_{pwm}	Modulation index	0.7
T_i	Integral time constant	741s
f_n	Low pass filter natural frequency	150 Hz
T_L	Low pass filter time constant	3.18×10^{-3}s
K_{pPLL}	Proportional gain PLL	10
T_{iPLL}	Integral time constant PLL	20×10^{-6}s

To simplify analysis instead of RE sources, an ideal DC source is considered here in this research. Therefore, only the second stage of control which is grid current control is considered here as discussed in Section 2.2.

3.2 Control Model

The block diagram of the average switch control model of the grid-tied inverter is given in Figure 3.2. An LCL filter is used in the model to reduce harmonic distortion caused by the inverter's switching operation. The filter helps to eliminate the common-mode noise and improve the power quality of the grid-connected system.

The resonance of an LCL filter occurs at the frequency where the reactance of the inductor and capacitor are equal, known as the resonant frequency. At this frequency, the filter will have the highest impedance, which helps to reduce the harmonic currents on the AC power line. However, if the system is not designed properly, the resonance of the LCL filter can cause instability and lead to a phenomenon known as sub-synchronous resonance (SSR). To prevent SSR, an active damping technique can be used. Active damping uses a control algorithm that adjusts the inverter's output voltage or current to dampen the resonance and stabilize the system.

The capacitor of the LCL filter generates a resonance which makes the system unstable. The feedback loop having gain k_c is used for active damping. The mathematical representation form of Figure 3.2 is given in (3.1).

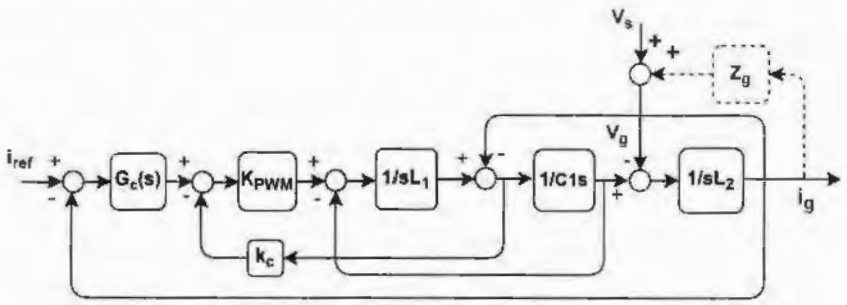

Figure 3.2: The average switch control model of GCI.

$$[(i_{ref} - i_g)\, G_c\,(s) - i_{c1} kc]\, k_{pwm} = i_{L1} L_1 s + i_g L_2 s + V_g \tag{3.1}$$

where
$$V_g = V_s + Z_g i_g \tag{3.2}$$

and
$$G_c(s) = k_p(1 + \frac{1}{T_i s}). \tag{3.3}$$

Moreover, k_p and T_i are the loop gain and time constant of the PI current controller respectively and k_{pwm} is the modulation index.

The GCIs have a very slow transient response. Therefore, an additional loop of grid voltage feedforward is used to decrease the response time. The voltage feed-forward starts from PCC voltage which is V_g and ends at the node between the current regulator and modulator. The feedforwarding of the grid voltage plays an important role in making the system response faster in addition to decreasing the burden on the current controller. A stability-enhancing voltage feed-forward inverter control method is proposed in [83, 84] to reduce the effect of PLL and grid-impedance. Similar feed-forward techniques for a GCI with an LCL filter are discussed in [85], while relatively extensive analysis of feed-forward strategies on the robustness in terms of harmonic suppression is discussed in [86]. Therefore, in the literature, there exist different strategies that demonstrate the importance of voltage feed-forwarding in grid-tied inverters.

In addition to the transient response, the voltage feed-forward improves steady-state performance in the form of a better power factor and produces less harmonic distortion in the current feeding to the grid. Usually, two voltage feed forwarding techniques are used. One is proportional voltage feed-forward; we refer to it as *Strategy A*, and the other is a SOGI-based feed-forward technique, which we refer to as *Strategy B*. There is another voltage feed-forward based on an adaptive algorithm which is mentioned as *Strategy C*. A detailed discussion of these three strategies is given below.

3.2.1 Voltage Feedforward *Strategy A*

The feed-forward in Figure 3.3a is the proportional feed-forward method which is considered here as strategy A. This method of voltage feed-forwarding is useful in reducing total harmonic distortion.

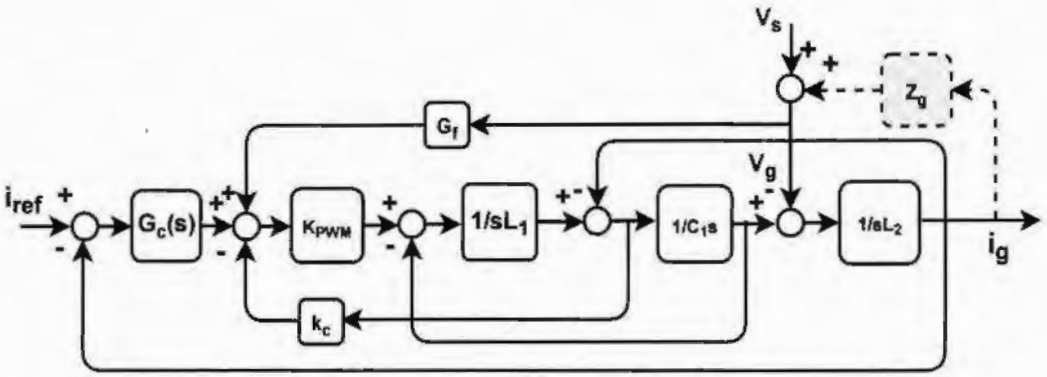

(a)

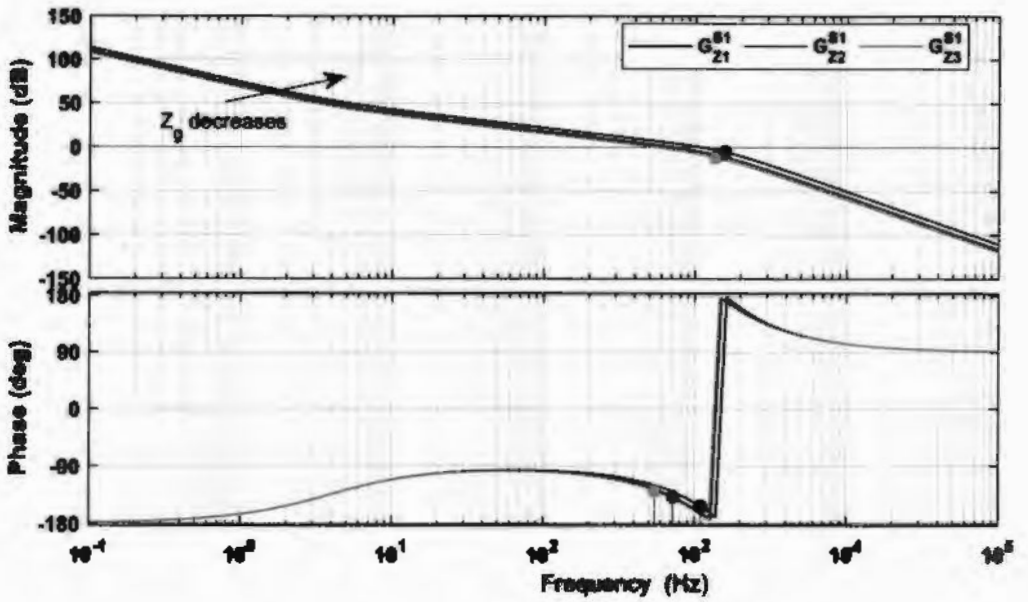

(b)

Figure 3.3: Strategy A: Proportional based grid voltage feedforward (**a**) Average switch control model. (**b**) Open loop system response.

There is also a limitation of this technique that it reduces the phase margin of the system. Therefore, it is effective in a strong grid or where Z_g is low. In weak grid application, it can destabilize. The mathematical representation of this system is expressed in (3.4).

$$\left[(i_{ref} - i_g).G_c(s) - i_{c1}.kc + V_g G_f(s)\right].k_{pwm} = i_{L1}L_1 s + i_g L_2 s + V_g \qquad (3.4)$$

where, V_g and $G_c(s)$ are as given in (3.2) and (3.3) respectively and G_f is

$$G_f(s) = \frac{1}{k_{pwm}} \tag{3.5}$$

There are two inputs i_{ref} and V_g and one output i_g. Therefore, the open loop gain of the system given in Figure 3.3a is calculated as the ratio between grid current i_g and reference current i_{ref} by ignoring grid voltage V_g. The extracted open loop gain is given in (3.6).

$$G^{S1}_{i_{ref}-i_g}(s) = \frac{k_{pwm}G_c(s)}{[L_1C_1L_2s^3 + (L_1C_1Z_g(s) + L_2C_1k_ck_{pwm})s^2 + (C_1Z_g(s)k_ck_{pwm} + L_1 + L_2)s + Z_g(s) - Z_g(s)k_{pwm}G_f(s)]} \tag{3.6}$$

In order to find its stability margin, the response of the open loop gain $G^{S1}_{i_{ref}-i_g}(s)$ is plotted with the help of a Bode plot. The simulated response by using values of Table 3.1 is given in Figure 3.3b which shows that the stability margin is highly dependent on the Z_g.

3.2.2 Voltage Feedforward *Strategy B*

The proportional feed-forward of Figure 3.3a with an additional SOGI filter is given in Figure 3.4a and is called the SOGI-based voltage feed-forwarding method which is mentioned here as strategy B.

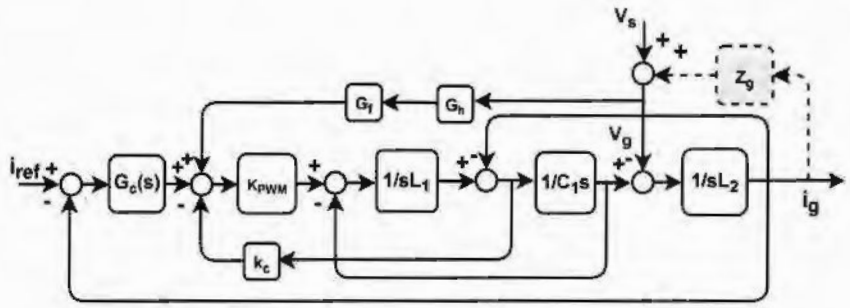

(a)

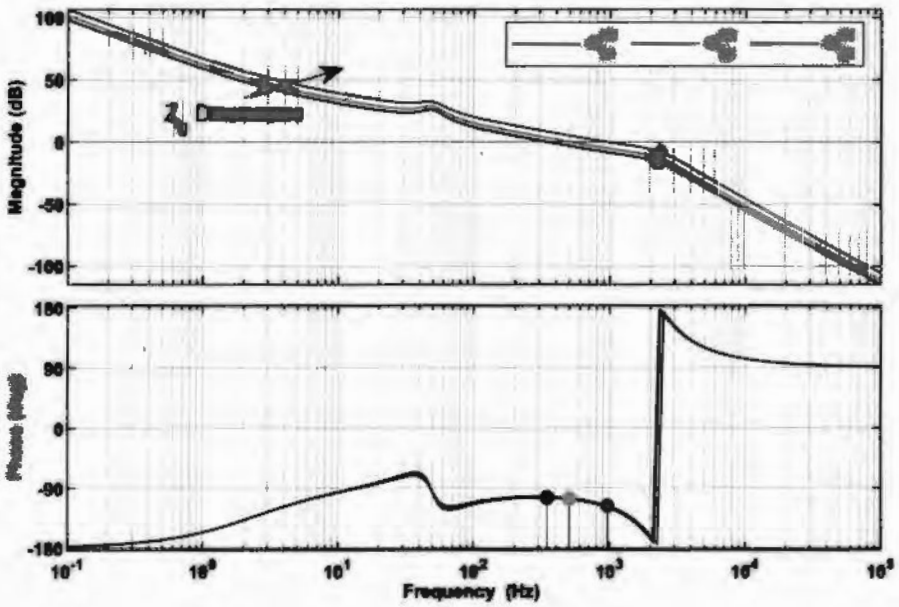

(b)

Figure 3.4: Strategy B: SOGI based grid voltage feedforward (a) Average switch control model. (b) Open loop system response.

It improves the phase margin and makes the system robust specifically in the case of weak grid applications where the Z_g varies from place to place but due to a SOGI-based voltage feed-forward, the system has a slow response and is less effective in reducing the harmonic distortion as compared to strategy A.

The mathematical expression of this system is given in (3.7).

$$\left[\left(i_{ref}-i_g\right)G_c\left(s\right)-i_{c1}kc+V_gG_f(s)G_h(s)\right]k_{pwm}=i_{L1}L_1s+i_gL_2s+V_g \tag{3.7}$$

where,
$$G_h(s)=\frac{k_o\omega_o s}{s^2+k_o\omega_o s+\omega_o^2} \tag{3.8}$$

k_o is proportional factor and ω_0 is $2\pi f_o$ where f_o is grid frequency.

The open loop gain $G^{S2}_{i_g-i_{ref}}(s)$ of the system is derived from Figure 3.4 using block reduction method and presented in (3.9).

$$G^{S2}_{i_g-i_{ref}}(s)=\frac{k_{pwm}G_c(s)}{[L_1C_1L_2s^3+(L_1C_1Z_g(s)+L_2C_1k_ck_{pwm})s^2+}$$
$$(C_1Z_g(s)k_ck_{pwm}+L_1+L_2)s+Z_g(s)-Z_g(s)k_{pwm}G_f(s)G_h(s)] \tag{3.9}$$

In order to find the stability margin of the system, the response of open loop gain of strategy B is plotted in Figure 3.4b with the help of a Bode plot. The Bode plot shows that the phase margin of the system changes with the change of Z_g, but the system remains stable for the larger values of Z_g as compared to contemporary works and shows robustness against Z_g variation. By comparing the phase margin of both Figures 3.3 and 3.4, it can be concluded that SOGI-based feed-forward is a better option for robust grid-tied inverters.

3.2.3 Voltage Feedforward *Strategy C*

In addition to strategies A and B mentioned in sectection 3.2.1 and 3.2.2 respectively, another voltage feedforward topology is introduced in [87]. We refer to it as strategy C, shown in Figure 3.5a. In this technique, multiple band-pass filters are used in the path of voltage feed-forward. These filters allow some low-order harmonics to reach the node between the current regulator and modulator while blocking the critical ones that reduce the phase margin by using an adaptive algorithm. The mathematical form of this system is shown in (3.10). The open loop gain of this system $G^{S3}_{i_g-i_{ref}}(s)$ is given in (3.13). The Bode plot of the open loop gain of strategy C is plotted to find its stability margins which is given in Figure 3.5b.

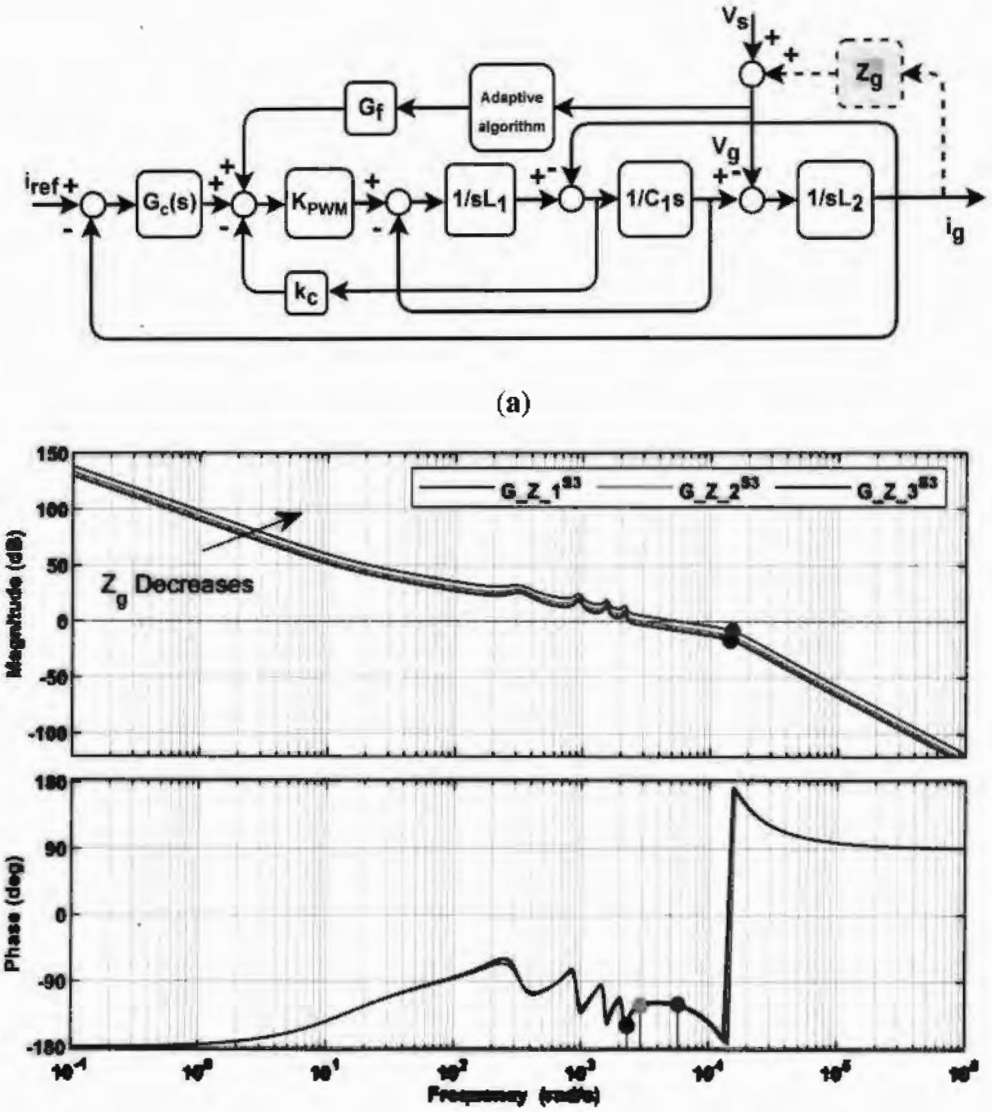

Figure 3.5: Strategy C: Adaptive grid voltage feedforward (**a**) Average switch control model. (**b**) Open loop system response.

$$\left[\left(i_{ref}-i_g\right)G_c\left(s\right)-i_{c1}kc+V_gG_f(s)G_{adap}(s)\right]k_{pwm}=i_{L1}L_1s+i_gL_2s+V_g \tag{3.10}$$

$$G_{adap}(s)=\left[x_1G_{h1}\left(s\right)+\ldots+x_7G_{hi}\left(s\right)\right] \tag{3.11}$$

where,

$$G_{hi}(s)=\frac{\omega_cs}{s^2+\omega_cs+\left(i.\omega_o\right)^2} \tag{3.12}$$

Where ω_c is the bandwidth of the filter and i is any odd number starting from 1 and ending at the number up to which the harmonics are desired to pass.

The open loop gain $G^{S3}_{i_g - i_{ref}}(s)$ of the system is derived from Figure 3.5(a) using block reduction method and presented in (3.13).

$$G^{S3}_{i_g - i_{ref}}(s) = \frac{k_{pwm} G_c(s)}{[L_1 C_1 L_2 s^3 + (L_1 C_1 Z_g(s) + L_2 C_1 k_c k_{pwm}) s^2 + (C_1 Z_g(s) k_c k_{pwm} + L_1 + L_2) s + Z_g(s) + Z_g(s) k_{pwm} G_f(s) G_{adap}(s)]}. \quad (3.13)$$

The main feature of this technique is to reduce the harmonic distortion and keep the stability margins in between the proportional and SOGI-based voltage feed-forward. In all the equations, the transfer function G_c is as given in (3.3) is the PI controller implemented in the synchronous reference frame and works as a current regulator. Moreover, all parameters used in these equations are listed in Table 3.1. The PI is used here, to provide a wider control bandwidth and simple implementation as compared to the PR controller.

3.3 Comparison of Voltage Feedforward Strategies and Research Gap

The analysis of Strategies A, B and C with the help of their respective Bode plots shows that the Z_g has a strong impact on its stability margins. It can also be observed that strategy B has larger phase margins as compared to other strategies but it has less capability to reduce the total harmonic distortion. Strategies other than Strategy B provide good immunity against total harmonic distortion but are less robust against the increase of Z_g and other variations. Therefore, strategy B is the best option for the system to be robust, hence SOGI-based voltage feed-forward is chosen for further improvements in this research. In the proposed system, the problem of total harmonic distortion is solved with the help of adaptive harmonic compensators. Hence, the system becomes robust and shows considerably reduced total harmonic distortion.

3.4 Impedance Based Stability

Impedance-based stability is an easy way to find the stability of GCIs, which is derived from the reduced average switch model of GCIs presented in the Norton and Thevenin form of the circuit in Figure 3.6.

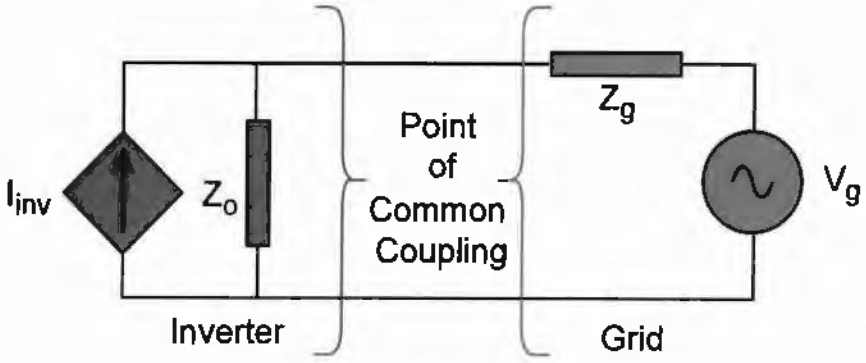

Figure 3.6: Norton and Thevenin models of inverter and grid in the grid-connected application.

By using the network-solving technique it can be transferred to the form of conventional control techniques used for finding the stability for a specific system. Although this idea is older in other power electronic converters, for a GCI the benchmark is given in [74]. The circuit in Figure 3.6 consists of two parts; one is the Norton circuit containing the feature of the GCI in the form of a dependent current source I_{inv} and inverter output impedance Z_o while the other part is the Thevenin circuit consisting of Z_g along with grid voltage V_s. By using superposition theorem on Figure 3.6, we get:

$$i_g = \frac{I_{inv}(s)Z_o(s)}{Z_o(s)+Z_g} - \frac{V_s(s)}{Z_o(s)+Z_g} \tag{3.14}$$

$$i_g = \left[I_{inv}(s) - \frac{V_s(s)}{Z_o(s)}\right] \frac{1}{1+Z_g(s)/Z_o(s)}. \tag{3.15}$$

where the impedance ratio Z_g/Z_o can be used for impedance-based stability analysis to meet the Nyquist criteria of stability. Now, the stability of the three strategies can be an-

alyzed by using the impedance-based stability test. The inverter output impedance can be derived from Figures 3.3–3.5 for Strategies A, B and C respectively by ignoring Z_g, shown by a dotted path in each figure. From the average model, the output impedance of the three strategies A, B and C are given in (3.16), (3.18) and (3.20) respectively.

Admittance of strategy A is

$$Y_o^{S1}(s) = \frac{-L_1C_1s^2 - C_1k_ck_{pwm}s - 1 + k_{pwm}(s)G_f(s)}{L_1C_1L_2s^3 + L_2C_1k_ck_{pwm}s^2 + (L_1 + L_2)s + k_{pwm}G_c(s)} \tag{3.16}$$

and impedance is

$$Z_o^{S1}(s) = \frac{1}{Y_o^{S1}(s)} \tag{3.17}$$

Admittance of strategy B is

$$Y_o^{S2}(s) = \frac{-L_1C_1s^2 - C_1k_ck_{pwm}s - 1 + k_{pwm}(s)G_f(s)G_h(s)}{L_1L_2C_1s^3 + L_2C_1k_ck_{pwm}s^2 + (L_1 + L_2)s + k_{pwm}G_c(s)} \tag{3.18}$$

and impedance is

$$Z_o^{S2}(s) = \frac{1}{Y_o^{S2}(s)}. \tag{3.19}$$

Admittance of strategy C is

$$Y_o^{S3}(s) = \frac{-L_1C_1s^2 - k_ck_{pwm}C_1s - 1 + k_{pwm}(s)\,G_f(s)\,G_h(s)\,G_{adap}(s)}{L_1C_1L_2s^3 + L_2C_1k_ck_{pwm}s^2 + (L_1 + L_2)s + k_{pwm}G_c(s)} \tag{3.20}$$

and impedance is

$$Z_o^{S3}(s) = \frac{1}{Y_o^{S3}(s)}, \tag{3.21}$$

where $Y_o^{Sn}(s)$ and $Z_o^{sn}(s)$ denotes admittance and impedance of nth strategy. The impedance-based stability can be checked by using the ratio of Z_g to inverter output impedance. There are two plots that can be used for this purpose one is the Bode plot and the other is the Nyquist plot. The combined Bode plots of impedance ratios strategies A, B and C are given in Figure 3.7.

In the regions of Bode plots where the gain of Z_g is less than Z_o^{sn} (n = 1, 2 and 3), the system is stable but in other regions where the inverter output impedance crossing the impedance of the grid the phase difference defines the stability. Therefore, inverter output impedance is important. If there is a certain phase difference between both impedance, the system remains stable otherwise it becomes unstable. The more comprehensive detail of

the conditions of the stability is mentioned in [74, 75, 88]. On the basis of these conditions, the Bode plot given in Figure 3.7 shows that the systems are stable for the given Z_g.

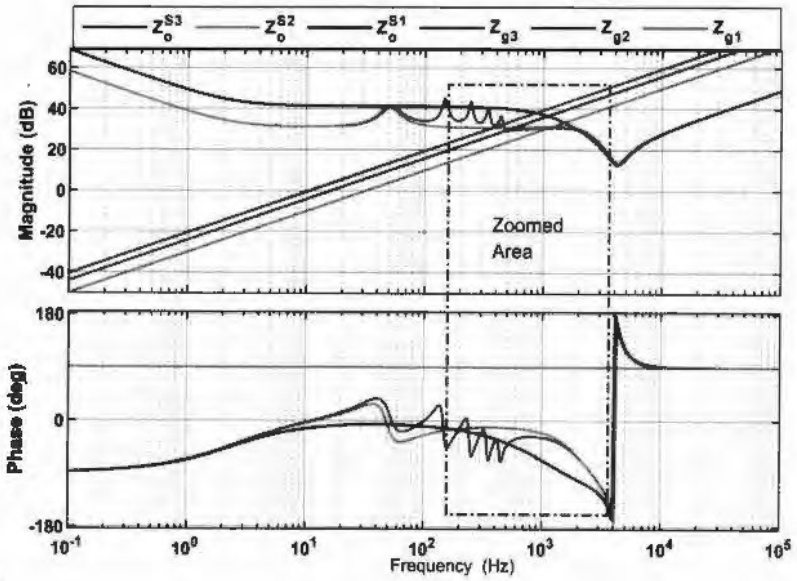

(a)

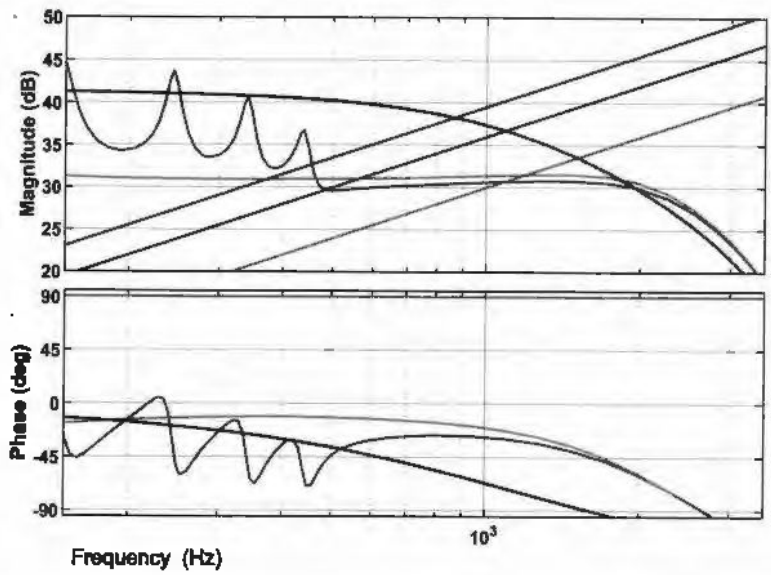

(b)

Figure 3.7: Impedance base stability analysis of GCI using Bode plot. (a) (b)

The Nyquist plot for the ratio of $Z_g/Z_o^{S(1,\,2\ and\ 3)}$ when Z_g is 5mH is given in Figure 3.8a. To check the encirclement of point (-1,0) for determining the stability, the figure

is zoomed in and the result is given in Figure 3.8b. The figures show that there is no clock-wise encirclement of point (-1,0). Hence the system is stable.

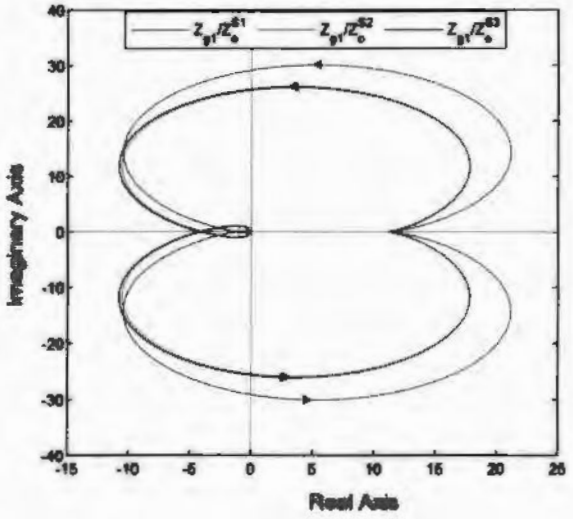

(a)

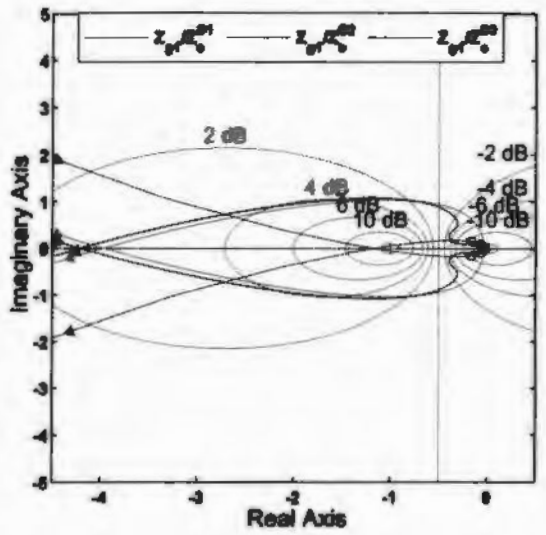

(b)

Figure 3.8: Impedance base stability analysis of GCI by using Nyquist plot for Z_{g1}/Z_o^{Sn} (a) Nyquist Plot (b) Zoomed in at point(-1,0).

The Nyquist plot for the ratio of $Z_g/Z_o^{S(1,\ 2\ and\ 3)}$ when Z_g is 10mH is given in Figure 3.9a. To check the encirclement of point (-1,0) the figure is zoomed in at (-1,0) and

the result is given in Figure 3.9b. Again the figures show that there is no clockwise encirclement of point (-1,0). Hence the system is stable

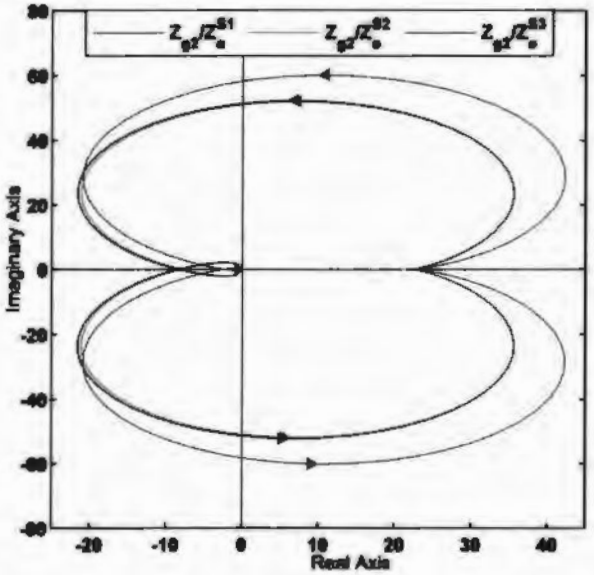

(a)

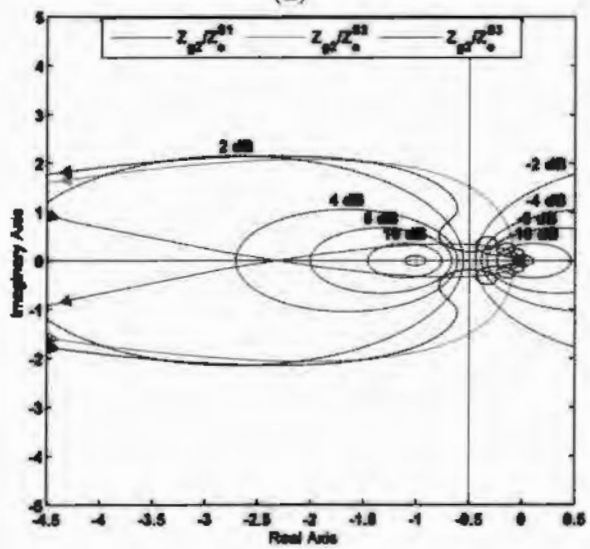

(b)

Figure 3.9: Impedance base stability analysis of GCI by using Nyquist plot for Z_{g2}/Z_o^{Sn} (a) Nyquist Plot (b) Zoomed in at point(-1,0).

The Nyquist plot for the ratio of $Z_g/Z_o^{S(1,\ 2\ and\ 3)}$ when Z_g is 15mH is given in Figure 3.10a. The figure is zoomed in at (-1,0) and the result is presented in Figure 3.10b.

Again the figures show that there is no clockwise encirclement of point (-1,0) and hence the systems are stable.

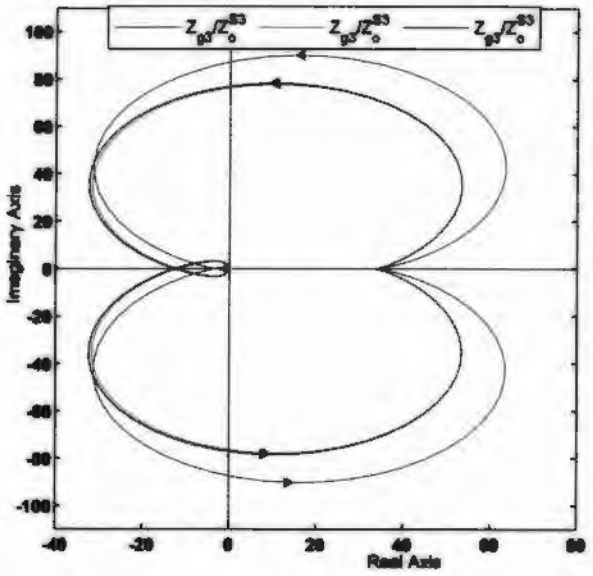

(a)

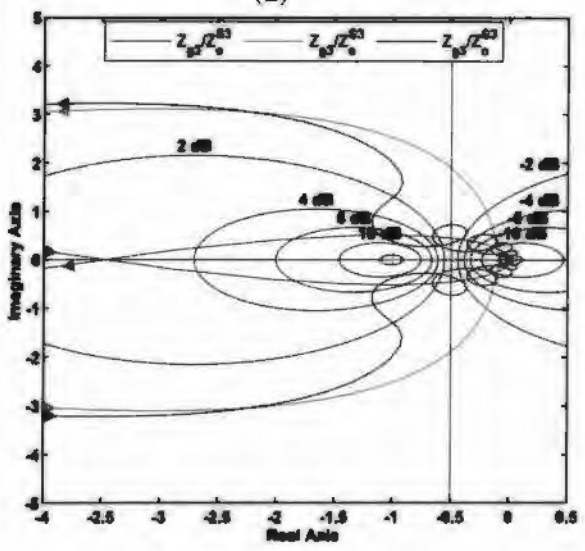

(b)

Figure 3.10: Impedance base stability analysis of GCI by using Nyquist plot for Z_{g3}/Z_o^{Sn} (a) Nyquist Plot (b) Zoomed in at point(-1,0) .

The Bode and Nyquist plots show that although all the systems are stable for the tested

parameters, but each system has different phase and gain margins. Therefore, the level of robustness of each system is different.

3.5 Summary

In this chapter, the generalized mathematical model of GCI is derived based on the average switch model and presented as a block diagram. Three strategies of voltage feed-forwarding techniques are also presented. The open loop gain of GCI is derived from the average switch control model which is further used in finding the stability margins and tuning of the controller. Moreover, the output impedance of GCI is also derived to analyze the stability of the GCI by using the Bode plot and Nyquist technique. It is also concluded that the SOGI-based voltage feed-forward technique is suitable for the proposed systems which are discussed in Chapters 4 and 5 in detail.

CHAPTER 4

DESIGN AND CONTROL OF 3-LEVEL GRID-CONNECTED INVERTER

In this chapter, the control law for GCI is proposed for the enhancement of stability and robustness against grid impedance variation. The proposed solution is a hybrid adaptive control technique for a 3-level full bridge inverter GCI. In this chapter, the average switch model, open loop gain, stability analysis, current controller, and adaptive harmonic compensators are presented. The proposed system is tested with the help of computer simulations and the results are analyzed. Moreover, the performance of the proposed solution is evaluated by comparing the generated results with the results of existing techniques. This chapter is based on the author's publication given in [11].

4.1 Limitations of Existing 3-Level Grid-connected Inverter

GCIs play a key role in the integration of DERs with utility grids. However, the connection between power inverters and the grid has been seen to be responsible for various stability issues. In the weak grid, and under weak grid conditions the injection of power to the grid becomes a challenging task due to continuously varying Z_g and grid frequency affecting the stability margins. Moreover, the Z_g related issues boost the voltage harmonics which further devalues its performance. These grid voltage harmonics propagate enter into the PLL and reach the control unit of the inverter which further amplifies the low-order harmonics of the inverter.

4.2 Proposed Controller Design

The objective of this research is to introduce a novel control strategy that decreases the effect of Z_g and frequency variations on the performance and stability of an inverter. Hence,

an adaptive hybrid control technique consisting of two parts is proposed. Part one consists of a PI current controller implemented in a synchronous reference frame designed with predefined fixed values of its parameters. The second part of the controller consists of adaptive PR controllers implemented in a stationary reference frame and its design is based on the adaptive notch and resonant filters. On the basis that the current controller is fixed values and the harmonics compensators are adaptive, we call our control law as hybrid control.

The adaptive harmonic compensators can effectively work under conditions where frequency varies whereas the fixed value-based harmonic compensator fails. It is found in this research that the adaptive harmonic compensators improved the performance by reducing THD even if there is a change of 1% in grid frequency, thus it improves the stability under the conditions when the grid has harmonic polluted voltage and variation in grid frequency. Under weak grid conditions, the impedance of the grid varies which further results in an increase in THD, and all of these factors can result in possibly an unstable GCI. The proposed control technique effectively reduces the THD and as a result, enhances the stability. The results show that the system becomes less sensitive to Z_g and frequency variations which justifies the proposed technique relevant to the stability performance applications. In this chapter, the proposed technique is discussed in detail and the generated results are compared with the existing techniques.

4.3 Functional Model of 3-Level Grid-connected Inverter

The functional block diagram of the proposed GCI is given in Figure 4.1 consisting of five main parts: i). *DC Source*, ii). *Power Switches*, iii). *Filter*, iv). *AC grid* and v). *Control unit*. Here, for simplicity, the DC source is assumed as a ripple-free ideal voltage source with an output voltage V_{DC}. The full H-Bridge configuration is used for power switches taking DC voltage V_{DC} and four PWM signals as input to gates and converting the input DC power into PWM-based alternating V_{inv} and I_{inv} output. The LCL filter converts V_{inv} and I_{inv} into a smooth V_g and i_g waveform. The LCL filter components are Capacitor C_f,

inverter side inductor L_1, and grid side inductor L_2 along with parasitic resistors R_c, R_1 and R_2 respectively. The parasitic resistances do not destabilize the system and therefore can be ignored. The AC grid is modeled by its equivalent Thavenin as an impedance $Z_g(s)$ and voltage source V_s connected to an LCL filter at PCC where its voltage is assumed to be V_g. The grid voltage frequency is considered as 50 Hz along with 1% variations. The low-order odd voltage harmonics are also added to model the characteristics of a weak grid. The hybrid control part consists of a current regulator and adaptive harmonic compensators. The current regulator is implemented in the synchronous reference frame while the harmonic compensators are implemented in the stationary reference frame which are discussed in detail in the coming sections. The values of system parameters used are listed in Table 4.1.

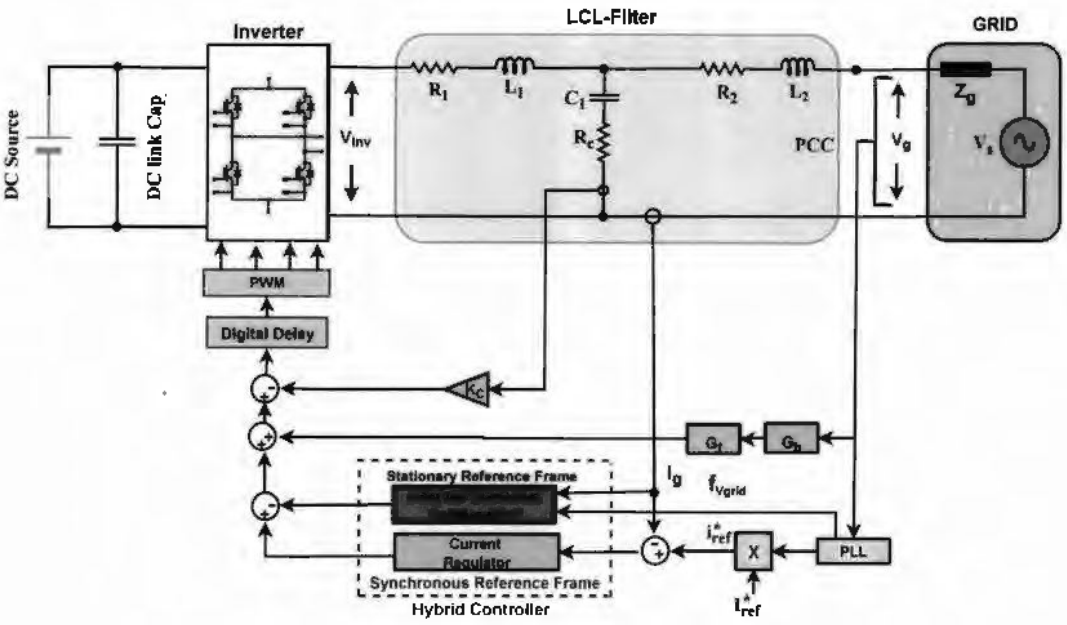

Figure 4.1: The functional block diagram of proposed GCI.

4.4 Proposed Hybrid Adaptive Control

The average switch control model of the proposed inverter is given in Figure 4.2. Based on the functionality, the system blocks are divided into two parts as: Area A consists of a grid, inverter, LCL filter, modulator, active damping loop, voltage feedforward loop and

Table 4.1: Symbols, description and values of system parameters

Symbols	Description	Values
P	Rated power	5 kW
V_{DC}	DC-link voltage	400 V
V_g	Grid voltage (RMS) at PCC	220 V
f_o	Grid frequency(fundamental)	50 Hz
L_1	Inverter side inductance	0.75 mH
L_2	Grid side Inductance	0.45 mH
C_f	Filter capacitor	6.01 uF
k_c	Active damping constant	10.6/400
$Z_g(s)$	Grid impedance	0–15 mH
k_o	SOGI filter damping factor	0.5
k_{or}	Compensator damping factor	0.001
k_{on}	Notch filter damping factor	7
K_r	Compensator gain	250
k_p	Proportional gain	50
T_i	Integral time constant	741s
f_n	Low pass filter natural frequency	150 Hz
T_L	Low pass filter time constant	3.18×10^3s
k_{pPLL}	Proportional gain PLL	10
T_{iPLL}	Integral time constant PLL	20×10^{-6}s

feedback current controller designed in a synchronous frame of reference and Area B represents the adaptive harmonic compensators that are working in the stationary reference frame. The harmonic compensators further consist of the adaptive resonant filters, adaptive notch filters and gain.

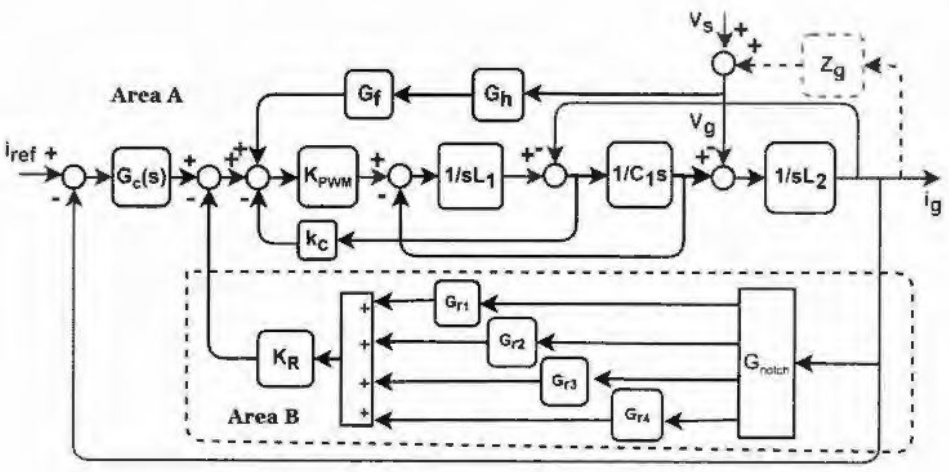

Figure 4.2: The proposed design of GCI with an adaptive hybrid control technique.

The important parts of the proposed hybrid control are elaborated in the next subsections.

4.4.1 Synchronization

The inverter output current i_g must be synchronized with grid voltage V_g for injecting active power within the grid. Here, PLL is used to estimate the phase and frequency of the grid voltage V_g.

The PLL used is based on a stationary frame controller, which needs DQZ transformation of AC signal but DQZ transformation of a single-phase system cannot be implemented directly like in a three-phase system. In a single-phase system, orthogonal signals are required for DQZ transformation which is generated by the SOGI-based orthogonal signal generation method. The α and β transfer functions of SOGI filters used are given in (4.1) and (4.2) respectively. The filter G_{pll_α} given in (4.1) removes high order harmonics and noise signals from V_g and generates V_α as an output and the filter G_{pll_β} given in (4.2) removes high order harmonic and also produces a delay of 90^o in its output signal V_β to make it orthogonal to V_α. The orthogonal signals generated are then converted from stationary reference frame to synchronous reference frame by using DQZ transformation which produces V_d and V_q as given in Figure 4.3. The PLL technique is used to extract instantaneous grid parameters f_g, i_{ref} and ω_{pll} as shown in Figure 4.3. The ω_{pll} used in (4.1) and (4.2) are previously estimated values from PLL.

$$G_{pll\alpha} = \frac{k_{pll}\omega_{pll}s}{s^2 + k_{pll}w_{pll}s + (\omega_{pll})^2}. \tag{4.1}$$

$$G_{pll\beta} = \frac{k_{pll}\omega_{pll}^2}{s^2 + k_{pll}w_{pll}s + (\omega_{pll})^2}. \tag{4.2}$$

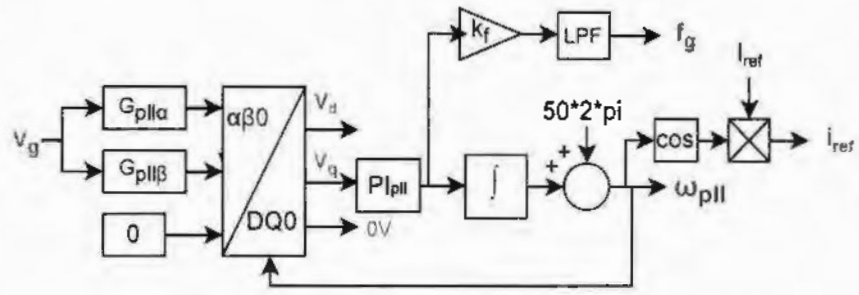

Figure 4.3: PLL block diagram for extraction of phase and frequency of V_g along with SOGI-based orthogonal signal generator

4.4.2 Current Controller

The current controller is used to inject desired power into the grid and to keep the system stable. The controller used for this purpose is the PI controller, and its transfer function is given in (4.3).

$$G_c(s) = k_p(1 + \frac{1}{T_i s}) \tag{4.3}$$

The injected current within the grid is AC. Therefore, if the PI controller is implemented to control AC waveform its bandwidth reduces and can easily become unstable. This issue can be overcome by converting the AC signal from a stationary reference frame to its corresponding synchronous reference frame as discussed in subsection 4.4.1. Where, the AC signal is converted into its corresponding DC, for this purpose a DQZ transformation is used. Therefore, again the orthogonal signal generators are required to convert a single-phase current signal into two orthogonal signals but the technique used in section 4.4.1 cannot be used here, because it will filter the information which is needed for the controller to work on it. Therefore, the grid current i_g is considered as i_α as given in (4.4) and the other signal i_β is produced by passing the grid current i_g through two low pass filters with a phase lag of 45^o per filter as given in (4.5).

$$i_\alpha(s) = i_g(s) \tag{4.4}$$

$$i_\beta(s) = i_g(s)\frac{1}{(1+T_L s)} \tag{4.5}$$

Where the T_L is the time constant of the low pass filter.

Then, with the help of Park transformation, the orthogonal signals are converted into their corresponding DC form I_d and I_q which is given (4.6).

$$\begin{bmatrix} I_d \\ I_q \end{bmatrix} = \begin{bmatrix} cosw_o t & sinw_o t \\ -sinw_o t & cosw_o t \end{bmatrix} \begin{bmatrix} i_\alpha \\ i_\beta \end{bmatrix} \tag{4.6}$$

The I_d and I_q are subtracted from their respective reference signals and the error signals are generated. The error signals of the d-axis and q-axis are passed through the PI controllers which are expressed in (4.7) and (4.8) respectively.

$$V_{cd}(s) = (I_d^* - I_d)G_c(s) \tag{4.7}$$

$$V_{cq}(s) = (I_q^* - I_q)G_c(s) \tag{4.8}$$

$$V_{inv\_d} = V_{cd}(s) - I_q(\omega_0(L_1 + L_2)) + V_{gd} \tag{4.9}$$

$$V_{inv\_q} = V_{cq}(s) - I_d(\omega_0(L_1 + L_2)) + V_{gq} \tag{4.10}$$

Where V_{inv_d} and V_{inv_q} are the controlled signals in d and q-axis respectively. The inverse Park transform is used to convert the controlled signals to their respective orthogonal signals in (4.11).

$$\begin{bmatrix} V_{inv\_\alpha} \\ V_{inv\_\beta} \end{bmatrix} = \begin{bmatrix} coswt & -sinwt \\ sinwt & coswt \end{bmatrix} \begin{bmatrix} V_{inv\_d} \\ V_{inv\_q} \end{bmatrix} \tag{4.11}$$

Where, the V_{inv_α} and V_{inv_β} are the controlled orthogonal AC signals. The voltage signal V_{inv_α} is used as a reference signal for PWM to generate the switching signals for the gate drive of the full bridge inverter. The whole process of the current controller is described in a simplified form in Figure 4.4.

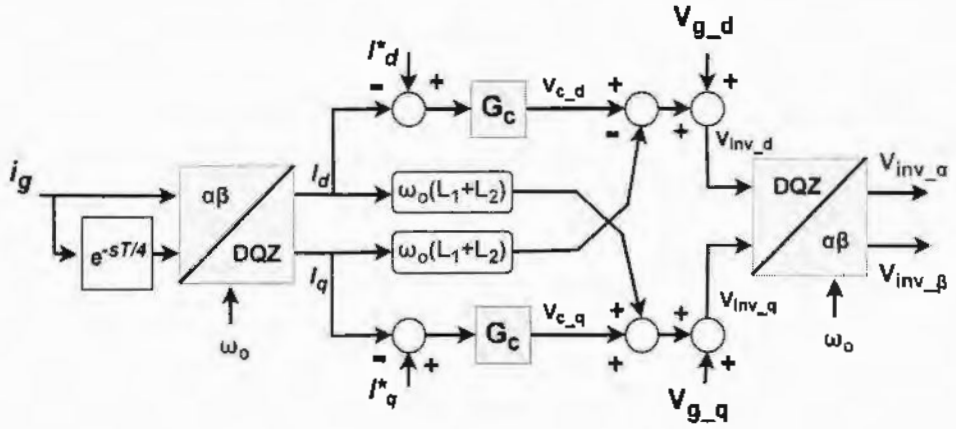

Figure 4.4: Block diagram of synchronous frame current controller along with DQZ and inverse DQZ transformation .

The values of k_p, T_i and T_L used in the PI controller are designed with the help of the MATLAB SISO tool, which are listed in Table 4.1.

4.4.3 Adaptive Harmonic Compensators

The harmonic compensators are used to minimize the harmonics contents within the current feeding into the grid. The reduction of harmonics in grid current enhances the performance and increases the stability of the GCIs. The Z_g variation changes the harmonics content in the grid current. Therefore, harmonic compensators are helpful to provide robustness against the variation of Z_g. Moreover, if there is Z_g variation then it is possible that there will be frequency variation due to the weak nature of the grid. Therefore, the harmonic compensator must also be able to handle the frequency variation.

The synchronous reference frame based harmonic compensators require two controllers for each harmonic suppression. Hence, for four harmonics eight controllers are required but if stationary reference frame controllers are used they will require only four controllers. Therefore, the resonant controllers are used here for harmonic compensation which are stationary reference frame-based compensators. These controllers, continuously estimate the harmonic frequencies present within the grid and mitigate the harmonics.

The realization of the controller in a digital domain is complex due to which its usage is limited. This limitation is overcome by adding a damping factor which not only makes it realizable but also increases its bandwidth. The advantage of the broad bandwidth is that controllers can estimate harmonics even if there exist small variations in fundamental and harmonic frequencies. The limitation of broader bandwidth is that some contents of fundamental frequency can also pass through the filters because the magnitude of the fundamental signal is very large as compared to the harmonics. To overcome this and stop the fundamental signal contents from entering the resonant filters a notch filter is used. The notch filter has a very narrow bandwidth and is difficult to realize therefore a damping factor is also added to the notch filter to increase its bandwidth for realization. Both filters with relatively larger bandwidths perform well under slight variations in the frequency of the grid. But in the case of larger frequency variations, the performance of these filters significantly degrades and sometimes produces adverse effects.

The notch filter transfer function G_{no} is given in (4.12) and the transfer function of resonant filters G_{ri} is given in (4.13). Both of these filters are cascaded with gain K_R to form a fixed value harmonic compensator G_R which is given in (4.14). The first four odd harmonic compensators are shown in area B of Figure 4.2.

$$G_{no} = \frac{s^2 + 0s + \omega_o^2}{s^2 + k_{on}s + \omega_o^2}. \tag{4.12}$$

$$G_{ri} = \frac{k_{or}\omega_o s}{s^2 + k_{or}\omega_o s + (n\omega_o)^2}. \tag{4.13}$$

$$G_R = K_R G_{no} \sum_{i=3}^{j} G_{ri}. \tag{4.14}$$

Where in (4.13), n is the number of odd harmonic and in (4.14), i is an odd integer starting from 3 and ending at j. Similarly, ω_o, k_{on} and k_{or} are grid frequency, the damping factor of the notch filter and damping factor of resonant filter respectively.

The equation (4.13) and (4.14) show that the notch filter and resonant filters are based on a fixed frequency. But sometimes, larger variations occur in grid frequency due to rapid

variations in load or generating stations. Under such conditions, the performance of the fixed value compensator degrades or produces some adverse effects. In this research, this limitation is overcome by designing adaptive filters. The bandwidths of the adaptive filters to estimate harmonics are the same as that of fixed value filters, but the adaptive filters tune themselves and shift their passband to the frequencies of the harmonics. Therefore, it is found that the variation in the fundamental frequency has a minor effect on the performance of compensators.

The designed adaptive filters adapt themselves according to the frequency estimated by PLL. The block diagrams of the adaptive compensators are given in Figure 4.5(a) and (b). The transfer functions of these filters are given in (4.15) and (4.16). These adaptive filters cascade with the gain K_R and work as adaptive harmonic compensators as given in (4.17).

$$G_{no_{ad}} = \frac{s^2 + \omega_{pll}^2}{s^2 + k_{on}s + \omega_{pll}^2}. \tag{4.15}$$

$$G_{ri_{ad}} = \frac{k_{or}\omega_{pll}s}{s^2 + k_{or}w_{pll}s + (n\omega_{pll})^2}. \tag{4.16}$$

$$G_{R_{ad}} = K_R G_{no_{ad}} \sum_{i=3}^{j} G_{ri_{ad}}. \tag{4.17}$$

Where in (4.16), n is the number of an odd harmonic and in (4.17), i is an odd integer starting from 3 and ending at j.

Figure 4.5(a) shows the block diagram of the adaptive notch filter which removes the grid frequency from the current signal i_g and passes the harmonics to the resonant filters. Figure 4.5(b) shows the block diagram of the resonant filter which extracts the desired harmonic to be compensated. Figure 4.5(c) depicts the Bode plot of the frequency response of adaptive resonance compensators and notch filter against the grid frequencies of 49Hz, 50Hz, or 51Hz which are plotted as blue, black and red respectively.

Thus, all adaptive harmonic compensators adapt themselves to the instantaneous estimated grid frequency extracted through PLL and set their cutoff values or passband of their filters such that low-order odd harmonics lie within the bandwidth of their corresponding com-

pensator. The Bode plot of Figure 4.5c shows the passing bands of filters depend on the instantaneous grid frequency that is if the grid frequency is 51Hz then the frequency of the 9^{th} odd harmonic becomes 459Hz.

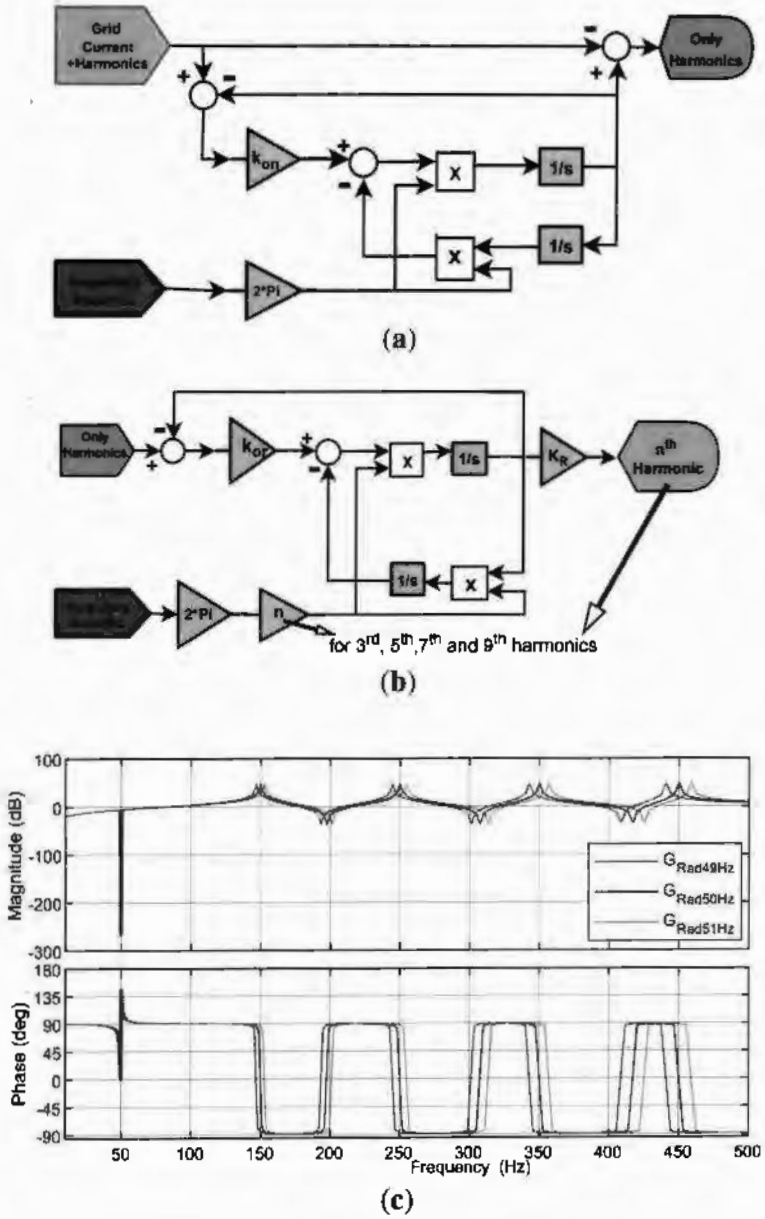

Figure 4.5: Adaptive resonance harmonic compensator (**a**) Adaptive notch filter (**b**) Adaptive resonance filter (**c**) Frequency response of adaptive harmonic compensator for 49Hz, 50Hz and 51Hz.

Thus, in the case of fixed values harmonic compensators the resonance filter will not pass the harmonic but in the case of adaptive, it will pass through the filter as the response of Figure 4.5 shows that the passband is also shifted around 459Hz. Thus in the case of frequency variation, fixed valued harmonic compensator devalues its performance, and a larger variation can make it unstable. The adaptive harmonic compensators take the estimated instantaneous frequency as the input from PLL continuously.

The notch filter in the proposed adaptive harmonic compensator has an important role in the process of harmonics compensation. The proposed notch filter is used to stop the fundamental content from entering the resonant filters and only harmonic contents are passed through the resonant filters.

The resonant filters have narrow bandwidth which can be increased by using a damping factor but when the damping factor is added to the resonant filters, a certain gain of each resonant filter is seen at grid frequency. The amplitude of fundamental frequency contents is much more than the harmonic contents of the grid current i_g therefore even a minimal gain of resonant filter at grid frequency can pass a significant amount of fundamental frequency content through resonant filters as shown in Figure 4.6(a) and it boosts up when it is multiplied with a gain of the harmonic compensator. These contents are subtracted from the current i_g as shown in Figure 4.1. Therefore, it increases the burden on the current controller because the current controller regulates the desired current that is injected into the grid. Therefore, the notch filter improves the performance of harmonic compensators by blocking the fundamental frequency contents from entering the resonant filters. The effect of the notch filter on 3^{rd} harmonic is given in Figure 4.6.

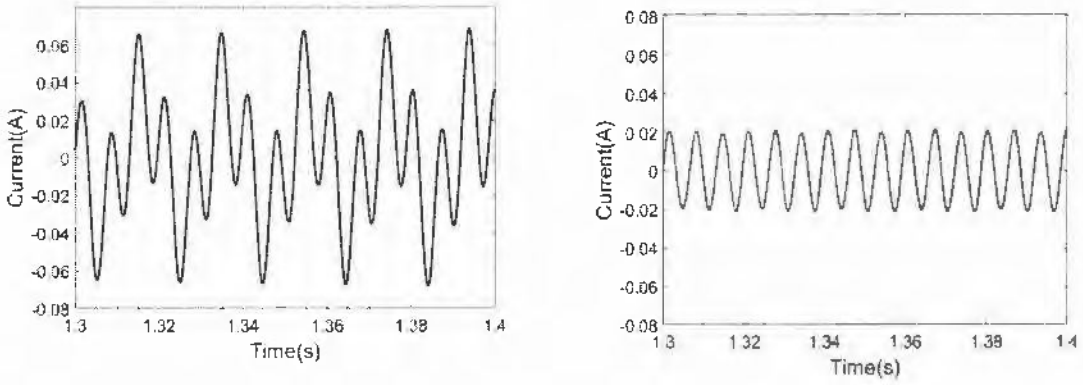

Figure 4.6: Effect of notch filter on the output of a harmonic compensator. (**a**) 3^{rd} harmonic without an adaptive notch filter. (**b**) 3^{rd} harmonic with an adaptive notch filter.

In Figure 4.6a, the result is presented for 3^{rd} harmonic that is extracted by the resonant filter when there is no notch filter. The result shows that grid frequency contents are not eliminated from the 3^{rd} harmonic. While Figure 4.6b shows the result when there is a notch filter used before the resonant filter which removes the content of grid frequency and leaves only 3^{rd} harmonic as an output. Therefore, the notch filter decreases the burden on the current controller to adjust the current because a pure harmonic is subtracted.

4.4.4 Controller Design Parameters

To find the appropriate parameters of the current controller and harmonic compensator for the desired stability margin (gain margin -3 to -5 dB and phase margin 30^o to 60^o), the open loop gain $G_4(s)$ is derived from the proposed system given in Figure 4.2 by using block reduction method and given in (4.18). The values of parameters of G_c that is k_p and T_i are extracted with the help of Bode plot and MATLAB SISO Tool and are listed in Table 4.1.

$$G_4(s) = \frac{G_c k_{pwm}}{[s^3 L_1 L_2 C_1 + s^2 L_1 Z_g C_1 + s^2 L_2 C_1 k_c k_{pwm} + s Z_g C_1 k_c k_{pwm} + sL_1 + sL_2 + Z_g - Z_g G_f G_h k_{pwm} + k_{pwm} K_R G_{R_{ad}}]}. \quad (4.18)$$

where,

$$G_h = \frac{k\omega_o s}{s^2 + k\omega_o s + \omega_o^2}. \tag{4.19}$$

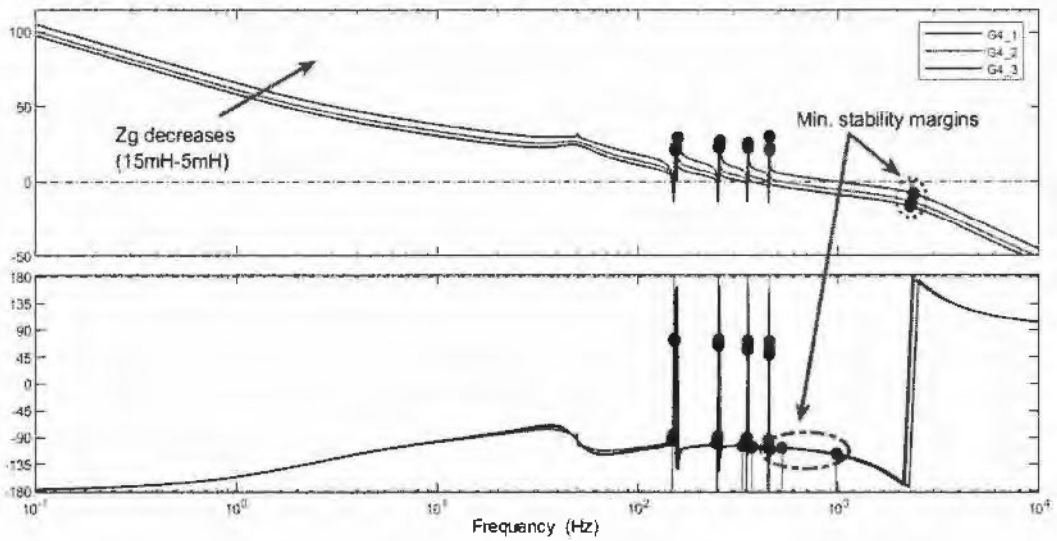

Figure 4.7: The open loop gain of the proposed system.

The Bode plots of the open loop gain are given in Figure 4.7 by using the parameters given in Table 4.1. The responses are for three different values of Z_gs 5mH, 10mH, and 15mH (these values of grid impedance are selected for ease of comparison with other contemporary techniques). The results show that the minimum gain and phase margins are $3dB$ and 50^o respectively. Hence, the system is stable.

4.5 Impedance-based Stability

The stability of the system is tested with the help of the impedance-based stability method. The proposed system shown in Figure 4.2 is divided into two equivalent subsystems the inverter side is represented in Norton equivalent form and the grid along with Z_g is represented in Thevenin equivalent form as given in Figure 4.8.

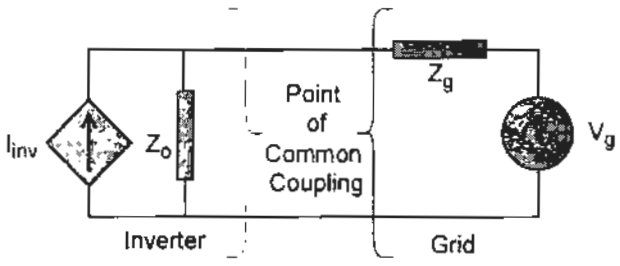

Figure 4.8: GCI presented in Norton form connected with grid represented in Thevenin form.

The network of Figure 4.8 can be solved with the help of the superposition theorem to find the grid current given in (4.20).

$$i_g = \frac{I_{inv}(s)Z_o(s)}{Z_o(s) + Z_g(s)} - \frac{V_s(s)}{Z_o(s) + Z_g(s)} \tag{4.20}$$

Where the Z_g is the grid impedance and Z_o is the inverter output. The equation can be further simplified in (4.21) to find the impedance ratio between grid impedance Z_g and Z_o.

$$i_g = \left[I_{inv}(s) - \frac{V_s(s)}{Z_o(s)}\right] \frac{1}{1 + Z_g(s)/Z_o(s)}. \tag{4.21}$$

By using the method of stability testing from [74], the impedance ratio Z_g/Z_o from (4.21) can be used for an impedance-based stability test.

Here, the system is evaluated for three values of Z_g that is 5mH, 10mH, and 15mH. The Z_g is derived from Figure 4.2 by ignoring the doted part of the Z_g. Furthermore, the relation between V_g and i_g is found by ignoring reference current i_{ref}. Thus, the derived output admittance is represented by $Y_{o4}(s)$ and impedance represented by $Z_{o4}(s)$ is given in (4.22) and (4.23) respectively.

$$Y_{o4}(s) = \frac{G_f G_h k_{pwm} - C_1 L_1 s^2 - C_1 k_c k_{pwm} s - 1}{L_1 L_2 C_1 s^3 + L_2 C_1 k_c k_{pwm} s^2 + (L_1 + L_2)\, s + G_c k_{pwm} + K_r k_{pwm} G_{PR}}. \tag{4.22}$$

$$Z_{o4}(s) = \frac{L_1 L_2 C_1 s^3 + L_2 C_1 k_c k_{pwm} s^2 + (L_1 + L_2)\, s + G_c k_{pwm} + K_r k_{pwm} G_{PR}}{G_f G_h k_{pwm} - C_1 L_1 s^2 - C_1 k_c k_{pwm} s - 1}. \tag{4.23}$$

The stability can be checked through the Bode plot or with the help of the Nyquist Plot.

The Bode plot of the Z_g ratio is given in Figure 4.9. Figure 4.9 shows that the system is stable where the inverter output impedance $Z_{o4}(s)$ is greater than the Z_g Zg. In other places, where the inverter impedance crosses Z_g the phase difference is between 90^o to 100^o which shows that the system is stable. The conditions are verified with the help of [74]. The pole-zero plot of the impedance ratio shows that all poles lie in the left half plane which further confirms that the roles of [74] are applicable.

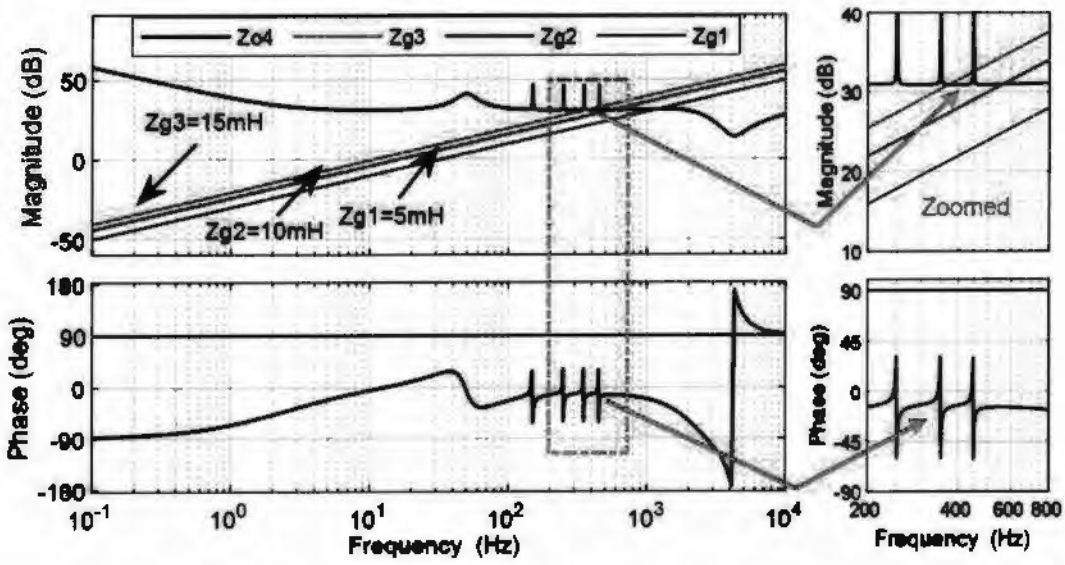

Figure 4.9: Impedance based stability using Bode Plot.

To further analyze the stability, the Nyquist plot of impedance ratio is plotted in Figure (4.10) which shows the stability of the inverter against three different impedances 5mH, 10mH, and 15mH respectively.

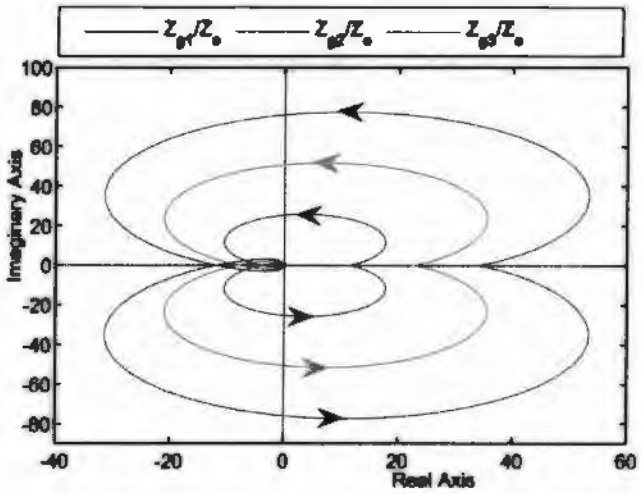

(a)

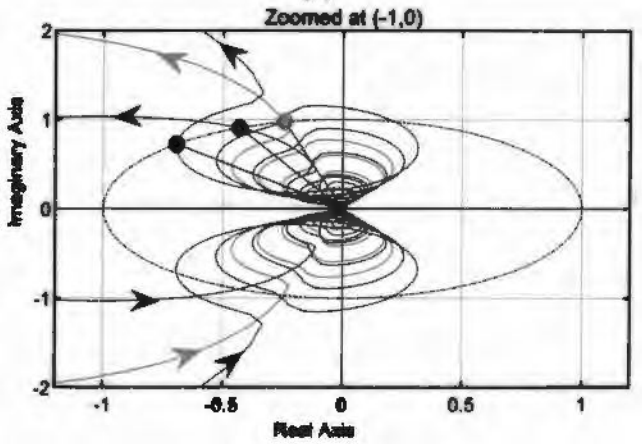

(b)

Figure 4.10: Impedance-based stability of proposed GTI by using Nyquist Plot (**a**) Nyquist plot of impedance ratio $Z_{g1}(s)/Z_o(s)$, $Z_{g2}(s)/Z_o(s)$ and $Z_{g3}(s)/Z_o(s)$. (**b**) Zoomed at (-1,0)

The Nyquist stability criteria state that a system is stable if there is no encirclement of point (-1,0) or the counterclockwise encirclements of point (-1,0) are equal or greater than the clockwise encirclement, vice versa the system is unstable if counterclockwise encirclement is less than the clockwise encirclement of point (-1,0). Thus, the Nyquist stability conditions are satisfied and the proposed system is a stable system. The Nyquist

plots of Figure 4.10 show that for all three values of Z_g, none of the loops encircle the point (-1,0) clockwise. Therefore, it is concluded that the closed system is stable.

4.6 Results and Analysis

The proposed design is analyzed for an arbitrary inverter of 5.5 kW which is also the minimum rating required by our utility. The rated current injected into the grid is assumed to be 25 A and the grid voltage to be 220V. The LCL filter is used to stop high-frequency harmonics. The filter and grid parameters are selected as given in [87] for comparison purposes. The reason for this selection is to make a comparison with existing techniques and to evaluate the performance of the proposed solution. The other parameters and values used in the simulation are also listed in Table 4.1. The proposed model is simulated in the MATLAB Simulink environment.

Figure 4.11 shows the polluted grid voltage used for the analysis of the proposed technique. Here all the results extracted are under the distorted grid voltage V_s with THD of 4.07%. This distorted grid voltage has a different THD from V_g, which is the grid voltage at the point of common coupling due to Z_g. The grid voltage given in Figure 4.11 is used for further analysis in this chapter.

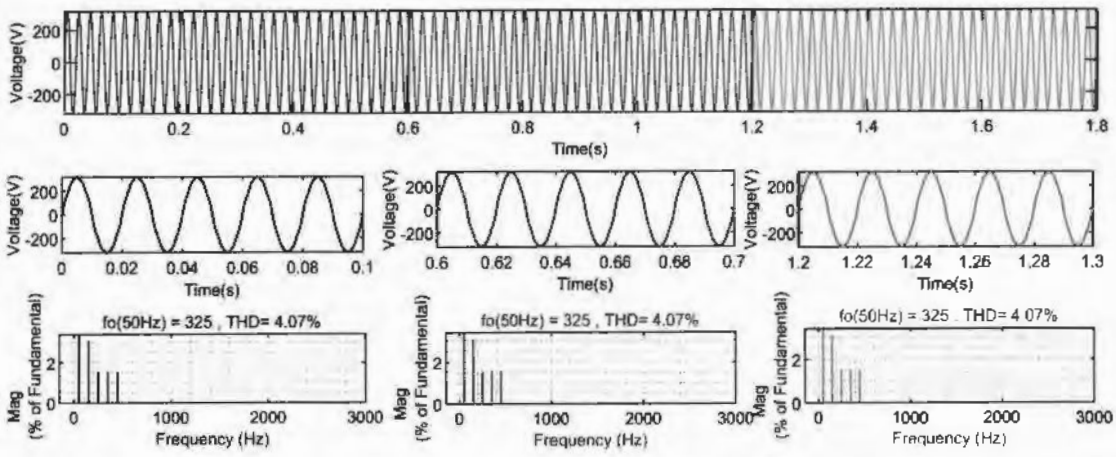

Figure 4.11: Distorted grid voltage V_s used for testing of proposed technique.

The proposed design is evaluated for two different cases having different conditions. In *Case 1* the proposed system is tested for variation in Z_g under fixed grid frequency and the results are compared with other relevant techniques. In *Case 2* the proposed system is tested under grid frequency variation with fixed Z_g and the results are compared with existing techniques. These two cases are discussed here in detail:

4.6.1 Case 1: Test for Grid Impedance Variation

In this case study the proposed GCI is tested for three different values of Z_g by keeping frequency and current fixed. Where, the three values of grid impedance Z_g are considered as 5mH, 10mH, and 15mH for simulation. The generated results are compared with the results of existing contemporary techniques.

In this research, SOGI-based voltage feedforward, active damping, and SOGI-based PLL is used along with a predefined fixed-value PI controller. Due to these factors, the results generated have shown a significant improvement. The results are given in Figure 4.12 where the system is tested for three values of Z_g under a fixed frequency of the grid.

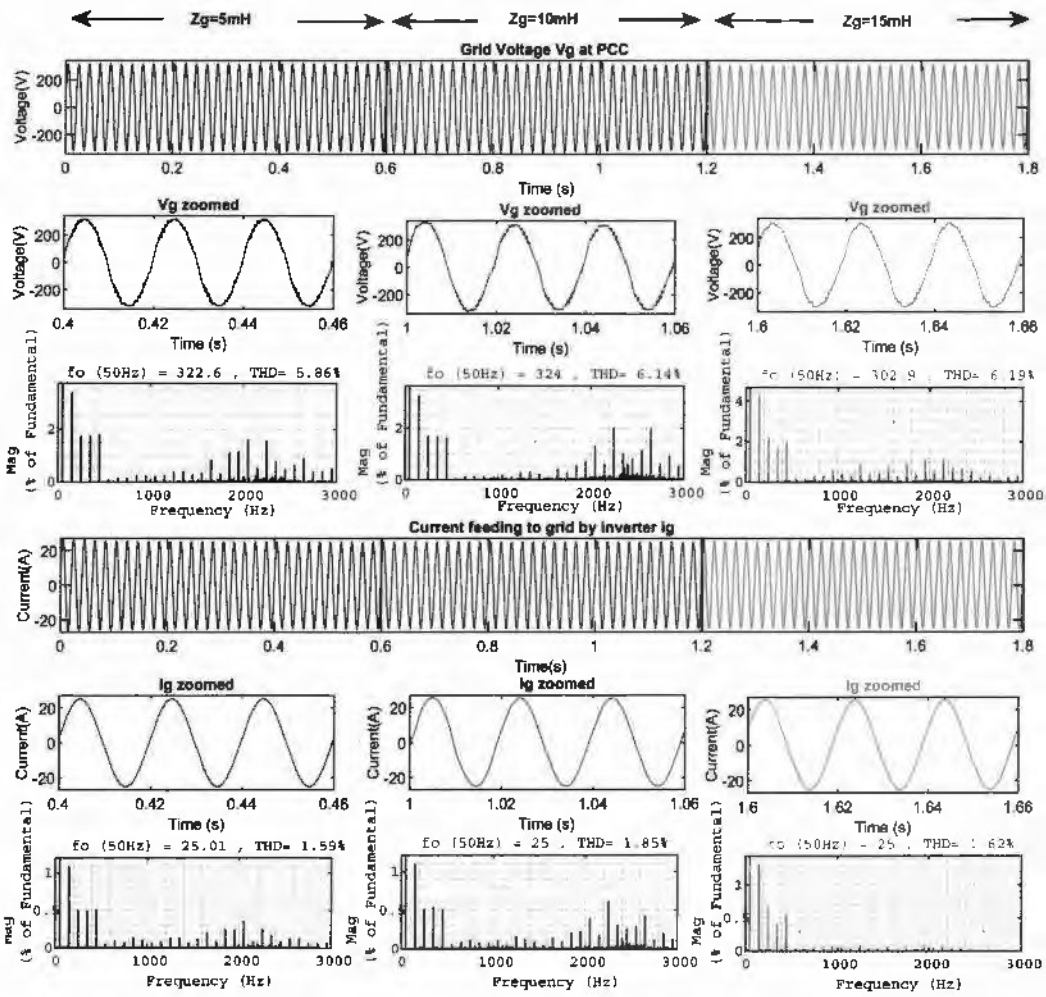

(a)

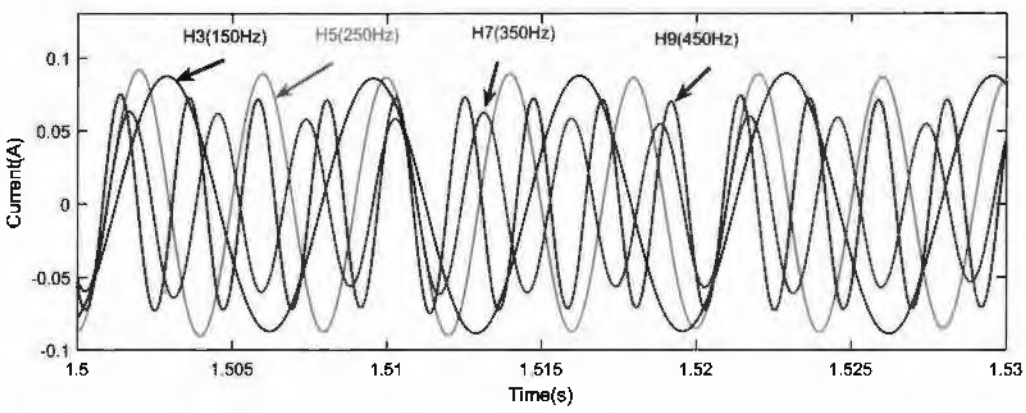

(b)

Figure 4.12: Results of GCI without harmonic compensator (**a**) PCC voltage V_g and grid current i_g with their FFT analysis (**b**) First four odd harmonics in i_g when $Z_g(s)$ is 15mH.

The results of Figure 4.12(a) show that there is a significant amount of THD in the current injecting into the grid. The first four odd harmonics of frequency 150Hz, 250Hz, 350Hz, and 450Hz are given in Figure 4.12(b). The THD can be reduced with the help of adaptive harmonic compensators. Figure 4.12 shows the results when there is no harmonic compensator.

When the proposed adaptive harmonic compensators are added to the current controller a significant improvement in the reduction of harmonic compensation is observed. The results generated of the proposed system where an adaptive harmonic controller is implemented for a GCI are given in Figure 4.13. Again, in Figure 4.13 the proposed system is tested for three different values of Z_g which are considered as 5mH, 10mH, and 15mH under the fixed grid frequency condition.

The first odd harmonics of the inverters with adaptive harmonic compensators are given in Figure 4.13(b). When these harmonics are compared with the harmonics in Figure 4.12(b) a clear improvement can be observed.

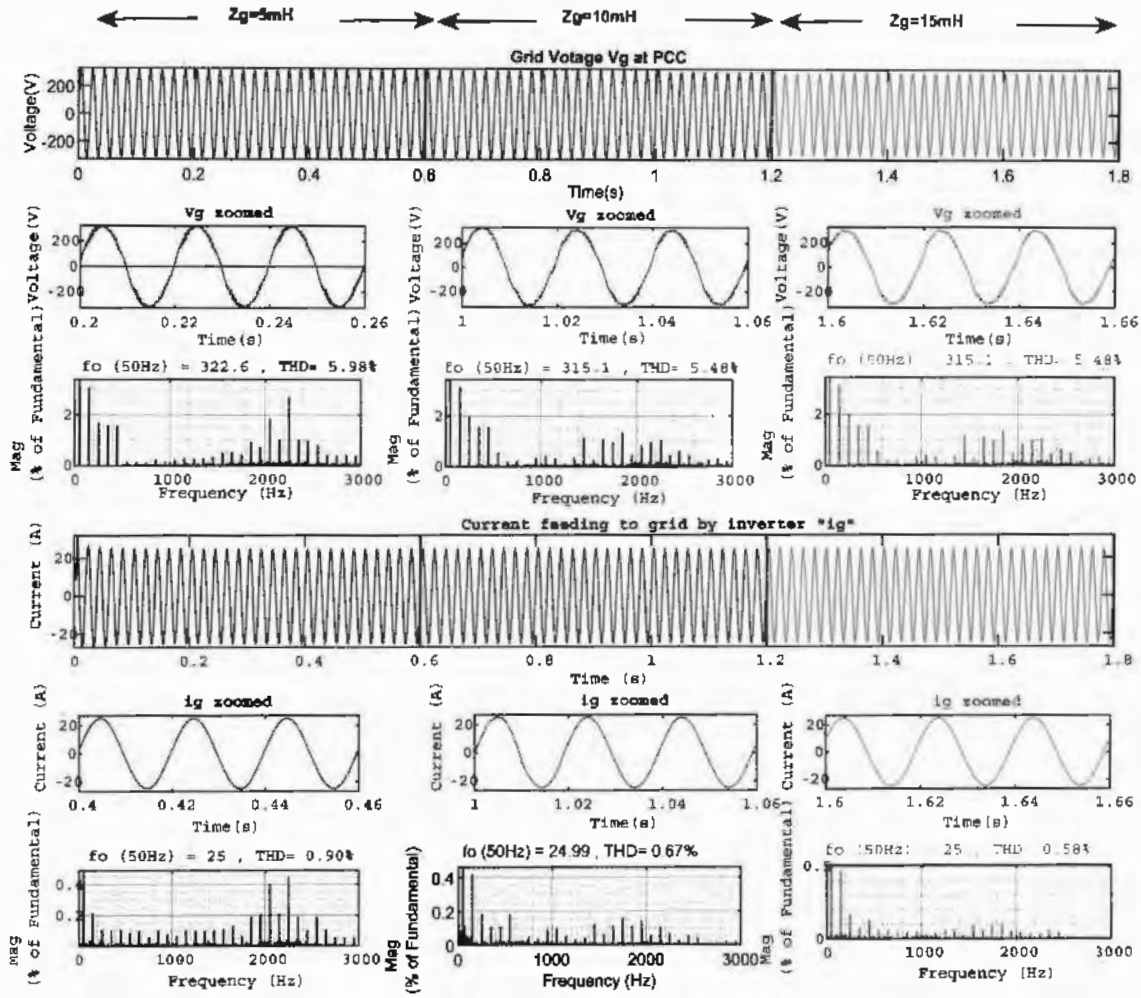

Figure 4.13: Results of GCI with proposed harmonic compensator. (**a**) PCC voltage V_g and grid current i_g with their FFT analysis. (**b**) First four odd harmonics in current i_g when grid impedance $Z_g(s)$ is 15 mH.

Table 4.2 shows the comparative analysis and cross-validation of the system without harmonic compensator and the system with proposed harmonic compensators. The results show that the proposed solution not only increases the robustness of the GCI but also minimizes the total harmonic distortion. Table 4.2 represents the first four odd harmonics H_3, H_5, H_7, and H_9 represent 3^{rd}, 5^{th}, 7^{th} and 9^{th} harmonics, respectively which are extracted from Figures 4.12 and 4.13 for grid impedance 5mH, 10mH and 15mH respectively. The table clearly shows that the proposed system reduces the total harmonics distortion by minimizing low-order odd harmonics and the effect of grid impedance on total harmonic distortion is also minimized which shows that the proposed system has more robustness against grid impedance variation.

Table 4.2: First four odd harmonics of *system 1* (without harmonic compensator) and *system 2* (with proposed harmonic compensator)s.

Systems	Z_g	H_3 (%)	H_5 (%)	H_7 (%)	H_9 (%)	THD (%)
System 1	5 mH	1.1	0.5	0.5	0.55	1.59
System 2	5 mH	0.2	0.1	0.1	0.15	0.9
Difference	5 mH	0.9	0.4	0.4	0.4	0.69
System 1	10 mH	1.1	0.5	0.5	0.5	1.89
System 2	10 mH	0.45	0.19	0.1	0.1	0.67
Difference	10 mH	0.65	0.31	0.4	0.4	1.22
System 1	15 mH	1.4	0.65	0.4	0.55	1.62
System 2	15 mH	0.4	0.2	0.1	0.15	0.58
Difference	15 mH	1	0.45	0.3	0.4	1.04

Figure 4.14 represents Table 4.2 in bar format, where *system 1* is a system without harmonic compensators and *system 2* is a system with a proposed harmonic compensator. The bar height represents the percentage of harmonic with reference to grid current i_g (keeping grid current 25 A as 100 percent).

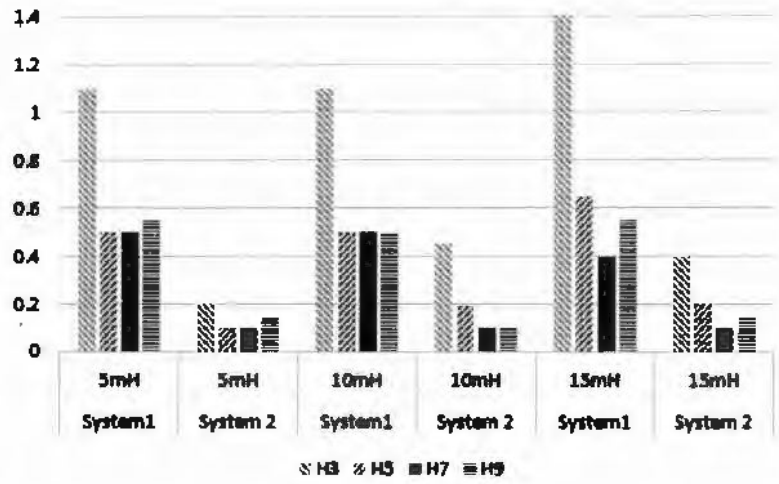

Figure 4.14: Bar representation of Table 4.3.

Hence, from Figure 4.12(b) and 4.13(b) the proposed harmonic compensators are working effectively and reduce the harmonics for which they are implemented. The effect is clearly observed that the first four odd harmonics of frequency are 150Hz, 250Hz, 350Hz, and 450Hz given in Figure 4.12(b) are reduced to the limit given in Figure 4.13(b). The other harmonics can also be compensated but they are small in quantity and can affect less the THD of the system therefore they are ignored to be compensated. Moreover, to validate the performance of the proposed harmonic compensators the comparison is made with the results of techniques used in reference [38], [89] and [90] is given in Table 4.3. The table shows that the proposed method has a better performance as compared to other existing techniques.

Table 4.3: THD of i_g (proposed system vs. [38]).

S.No.	Technique	Zg = 5 mH	Zg = 10 mH	Zg = 15 mH
1	Reference [38]	THD=3.5%	THD=3.20%	THD=2.9%
2	Technique used in [89]	THD=2.1%	THD=2.9%	THD=3.3%
3	Technique used in [90]	THD=1.9%	THD=2.4%	THD=2.8%
4	**Proposed (THD of V_s = 4.07%)**	**THD=0.9%**	**THD=0.67%**	**THD=0.58%**

4.6.2 Case 2: Test for Grid Frequency Variation

Figures 4.12 and 4.13 show the results of GCI without and with the proposed harmonic compensators tested for a grid frequency of 50 Hz respectively. The change in frequency can affect the performance of GCI specifically it has a greater effect on harmonic compensators. Sometimes due to change in frequency, the harmonic compensators produces adverse results and destabilizes the system. Therefore, testing of GCIs under grid frequency variation is very important. In this section, the testing of the proposed GCIs is conducted under fixed grid impedance and current to check the adaptive capability of the proposed harmonic compensators and overall GCI.

Figures 4.15 represent the results of the GCI without adaptive harmonic compensators, with fixed values harmonic compensators, and with proposed adaptive harmonic compensators under the condition of 50.5Hz grid frequency that is 1% increase in the grid frequency. The results show that the THD of GCI without harmonic compensators is 1.37%, with fixed valued harmonic compensator is 1.41% and with proposed adaptive harmonic compensators is 0.51%. Hence it is concluded that the proposed adaptive harmonic compensator has more promising results.

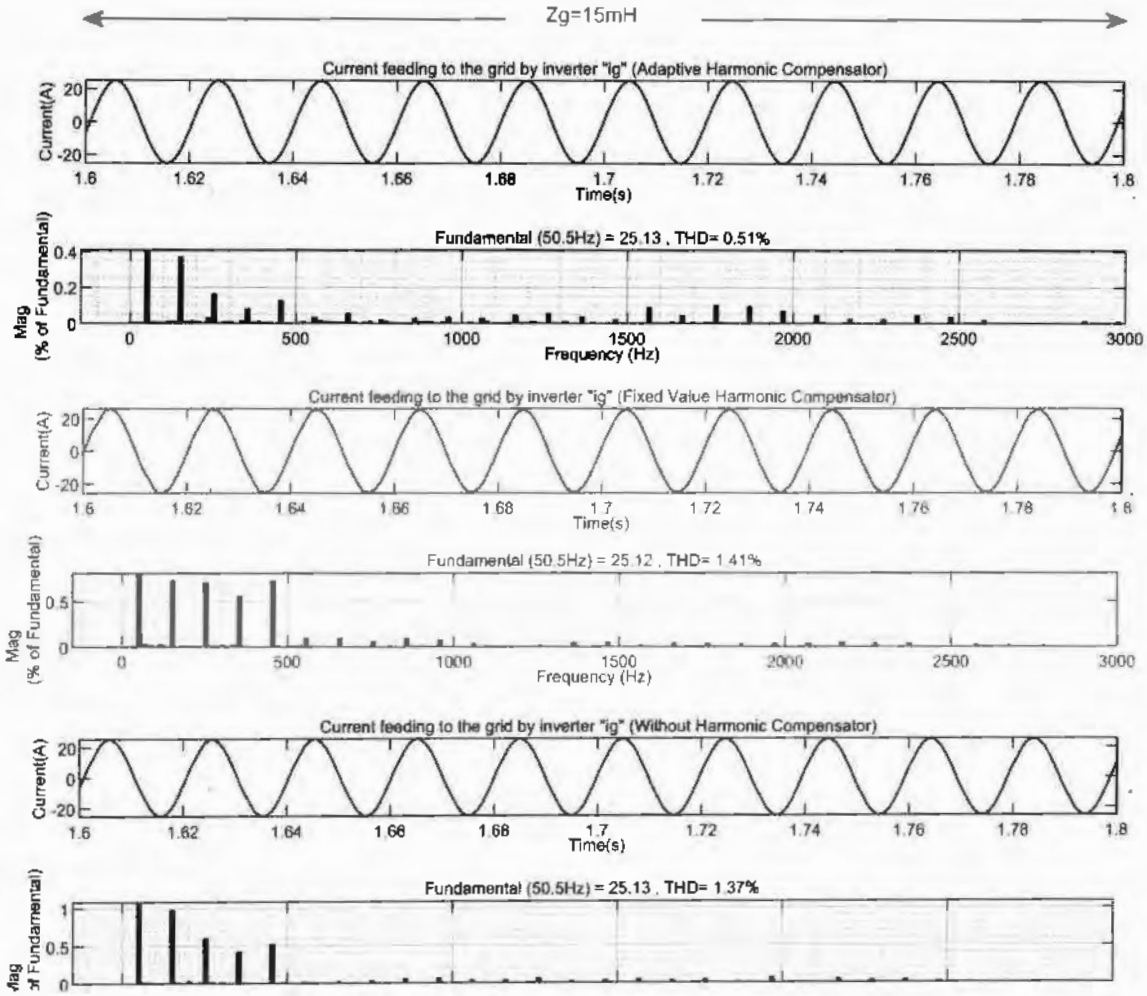

Figure 4.15: Results of the proposed adaptive harmonic compensator, fixed value harmonic compensator and without harmonic compensator when grid frequency is 50.5 Hz.

Figure 4.16 shows results of the GCI without adaptive harmonic compensators, with fixed values harmonic compensators, and with proposed adaptive harmonic compensators by considering a 1% decrease in grid frequency that is 49.5Hz. The results show that the THD of GCI without harmonic compensators is 1.89%, with fixed valued harmonic compensator is 1.15% and with proposed adaptive harmonic compensators is 0.66%. Hence it is concluded that again the proposed adaptive harmonic compensator has more promising results.

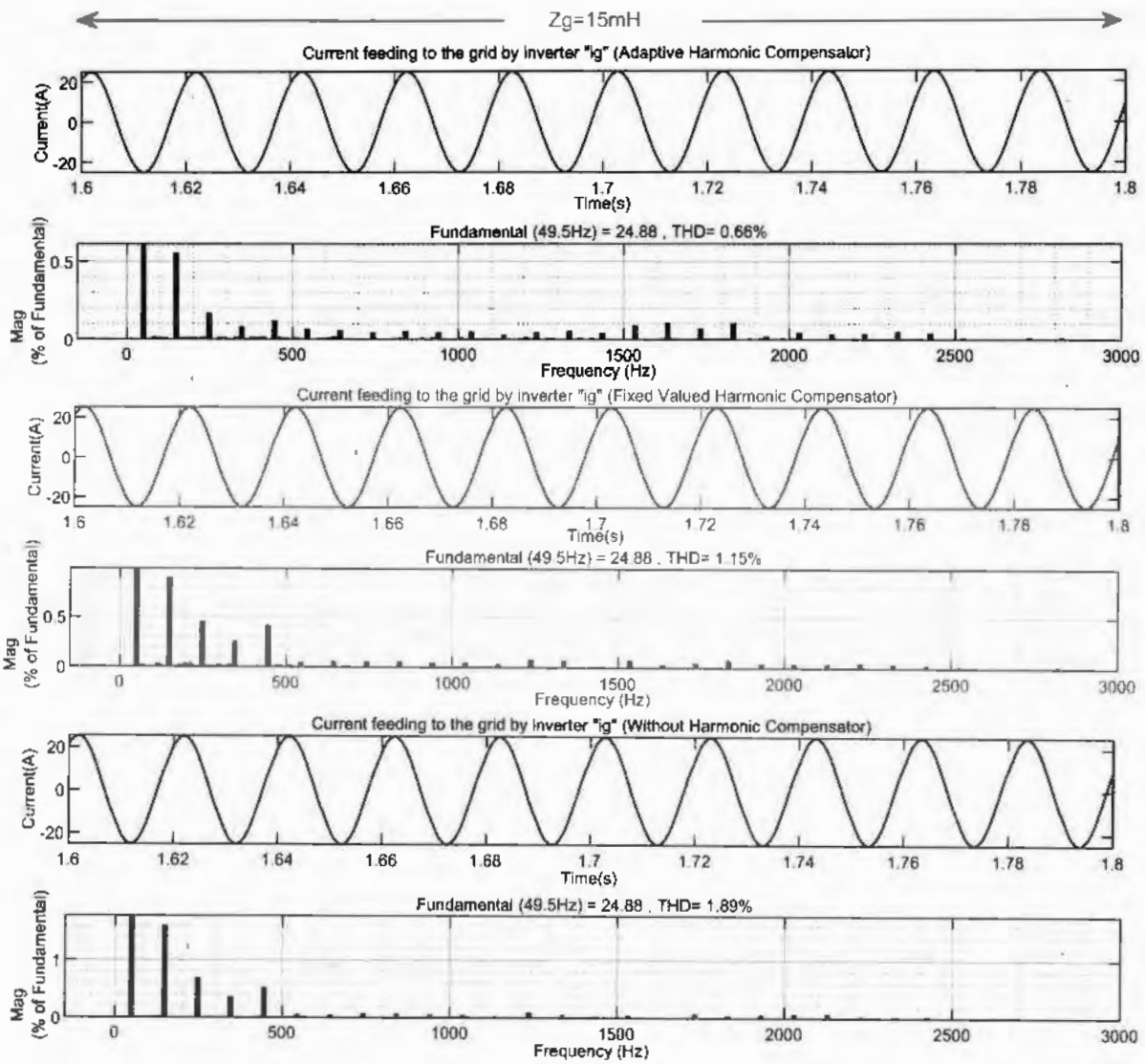

Figure 4.16: Results of the proposed adaptive harmonic compensator, fixed value harmonic compensator and without harmonic compensator when grid frequency is 49.5 Hz.

The observation from Figures 4.15 and 4.16 are tabulated in Table 4.4 which show that the proposed hybrid adaptive control of the GCI has better results than fixed value harmonic compensator and without harmonic compensator.

Table 4.4: Comparison of the GCI without harmonic, with fixed parameter harmonic and with adaptive harmonic compensator technique under 1% of grid frequency variation

Technique	**THD in %**	
Grid frequency	**49.5Hz**	**50.5Hz**
GCI without harmonic Compensators	1.89%	1.17%
GCI with fixed value harmonic Compensators	1.15%	1.41%
GCI with proposed adaptive harmonic Compensators	0.66%	0.51%

It is also observed from the results depicted in Figures 4.15 and 4.16 that due to wide bandwidth, the PI current controller is not affected by frequency variation. Therefore, the hybrid adaptive controller where the PI is a fixed value and the harmonics compensators are adaptive is working well and produces promising results.

Moreover, the proposed technique is also compared with other contemporary techniques in Table 4.5 and it is found that the proposed techniques generate better results.

Table 4.5: Comparison of the proposed technique for 1% of grid frequency variation

Technique	**THD in %**	
Grid frequency	**49.5Hz**	**50.5Hz**
Technique used in [91]	2.02%	2.13%
Technique used in [92]	2.9%	2.9%
Technique used in [93]	1.03%	0.95%
Proposed Technique	0.66%	0.51%

4.7 Summary

The adaptive hybrid control technique is proposed for inverters used in grid-tied applications which makes the system performance better by tracking the fundamental frequency

of the grid and tuning itself according to any variation. This adaptive nature of compensators has improved performance. It is found that the proposed adaptive system has greater immunity to grid-impedance variation and that the system has a better performance as compared to currently reported techniques. The system is tested using open loop gain and impedance-based stability using Bode plot and Nyquist plot. It is found that the system has shown significant improvement in performance as compared to existing techniques. The system is further tested for a highly distorted grid and the system performance is found to be more promising.

CHAPTER 5

DESIGN AND CONTROL OF MULTILEVEL GRID-CONNECTED INVERTER

Multilevel inverters (MLIs) are increasingly used in microgrid and distribution grid applications, as they provide a flexible and robust solution for integrating and controlling distributed energy resources (DERs). The main advantage of using a multilevel inverter in a grid-connected application is that it can produce a high-quality output waveform with reduced harmonic distortion, which improves the power quality of the electricity being fed into the grid. This can help to reduce power losses and improve the efficiency and stability of the overall system. In this chapter, a newly proposed cascaded symmetric MLI topology is presented along with the modulation technique for equal sharing of sources. Moreover, an adaptive hybrid control proposed in Chapter 4 is applied to the proposed MLI and its performance is analyzed. The proposed idea is validated by considering a case of the 9-level inverter. The stability of the proposed system is also analyzed in this chapter. In the end, the proposed system is verified through simulations and the results are compared with the existing techniques. Some of the work is published in [13] and the remaining is submitted for publication to IEEE Access which is under review.

5.1 Limitation of 3-Level Grid-connected Inverters

GCIs have a significant role in the integration of RE resources with utility grids. However, in recent studies, it is revealed that GCIs are vulnerable to instability when the nature of the grid changes from strong to weak, which produces uncertainty and performance degradation. An increase in Z_g decreases stability margins, tremendously increases total harmonic distortion after a certain limit, and amplifies the voltage harmonics in the grid. In a weak grid, the voltage harmonics of the grid affect the performance of the GCIs and therefore

an effective method to minimize the total harmonic distortion in the current injected into the grid is important. The proposed hybrid adaptive control technique in chapter 4 which is applied to a 3-level GCI, the results found are sound but 3-level inverters still have limitations: 1) it produces stress on its switching transistors, 2) it has lesser power handling capability, 3) the rate of change of voltage (dV/dt) is higher, and 4) produces more harmonic distortion in its output current. These limitations can be overcome by the proposed multilevel GCI presented in this chapter.

5.2 Proposed Solution for Improvement

A cascaded reduced switch symmetrical MLI along with an adaptive hybrid control technique is proposed for injecting power generated from distributed energy resources efficiently and stably to the utility grid. This research contributes twofold: an MLI topology and the other is its control method. The MLI mitigates four limitations of 3-level inverters by 1) decreasing stress on switching transistors, 2) improving power handling capability 3) decreasing the rate of change of voltage (dV/dt) and 4) producing lesser harmonic distortion in the output current. The control unit of the proposed system further consists of two parts: one is the synchronous frame current controller, and the other is stationary frame adaptive harmonic compensators. The grid current controller which is working in a synchronous reference frame ensures regulated current injection to the grid. It is not favorable to implement a harmonic compensator in a synchronous reference frame due to computation complexities. Therefore, the stationary reference frame controllers are used for harmonic compensations. But the resultant harmonic compensators have narrow bandwidth. Thus, these are not robust against variation in grid frequency. In this research, this problem is resolved by adding the adaptive features within the harmonic compensators which shift its passing band according to the frequency of the grid while remaining with the same bandwidth. The proposed design of the hybrid frame controller is validated by considering a nine-level inverter connected with a weak grid.

5.3 Multilevel Inverter and Grid-connected Application

The development of GCI occurs either in form of improvements in topology or in its controller. Both parts of GCI are of equal significance. Therefore, this research contributes to both domains by improving the power handling capability, stability and THD of the entire system.

An inverter is the core part of a GCI and it is critical to select an appropriate inverter topology. Therefore, the inverters can be classified on the basis of different parameters to find the appropriate topology. On the basis of power rating there are low, medium, and high-power inverters like fly back, push-pull and half-bridge inverters are used as low-cost and low-power inverters. The H-bridge inverters are used as medium power inverters and MLIs are suitable to use in medium to high power applications.

In a comparison of the H-bridge and MLIs, the H-bridge inverters have the advantage of the minimum number of power electronic switches, but it requires filter components with higher values which compromises the advantage of the minimum number of power electronic switches. The increase in the values of filter components increases the cost, size, weight, and losses. Moreover, the minimum number of switches increases stress on the switches, thus it requires switches with a higher rating. Therefore, considering these constraints the smaller number of switches does not look promising.

In contrast to a full bridge inverter, the MLI produces a sine wave in stair form where each stair is encoded with pulse width modulation (PWM). Hence, the voltages across the switches producing PWM vary by a smaller value as compared to the zero and peak values in the case of the full bridge inverter. Due to this, the stress on power switches and the rate of change of voltage (dV/dt) reduces while the transient response improves. A better dynamic response can also be observed in case of a voltage surge or sudden voltage drop. Another important advantage of MLI is its suitability for distributed RE resources integra-

tion. RE resources can be connected to the AC grid in four possible configurations as given in Figure 5.1. In Figure 5.1(a) solar panels are connected with a single DC-DC converter and the DC-DC converter is connected with a GCI which converts DC power into AC and hence transfers power from solar panels to the grid. In this structure, the solar panels have a centralized solution. Therefore, the separate use of a single panel or string of panels is not possible. In Figure 5.1(b) the solar panels or strings of solar panels are connected with their respective DC-DC converters and the DC-DC converters are connected together with each other in form of the microgrid which needs additional control. In Figure 5.1(c) solar panels are connected with their respective GCIs. These GCIs are close to each other and work like parallel inverters which decreases the output impedance of the inverter. For the case of the weak grid where the grid has a significant output impedance, the inverters with low output impedance can become unstable as discussed in Section 2.3. In Figure 5.1(d) DC sources are connected with a single inverter which is MLI that connects all the sources with the grid and remove the limitations of all the three topologies mentioned in Figure 5.1(a), (b) and (c). The merits and demerits of each configuration are summarized in Table 5.1. Table 5.1 shows that an MLI is a suitable solution. Because the DC sources can be used individually as well as they can be combined by using an MLI to connect it with the grid effectively.

Table 5.1: The advantages and disadvantages of topologies of GCI to connect PV panels to an AC grid

Figure	**Disadvantages**	**Advantages**
Figure 5.1a	Distributed system has centralized solution	Easy control
Figure 5.1b	Distributed sources can be used individually.	Integration of DC-DC converters needs a DC microgrid.
Figure 5.1c	Distributed system has distributed solution.	Parallel and nearer connection of GCI create stability issues
Figure 5.1d	Distributed system has distributed solution	Multiple DC-DC converters can be connected with a single grid-connected MLI.

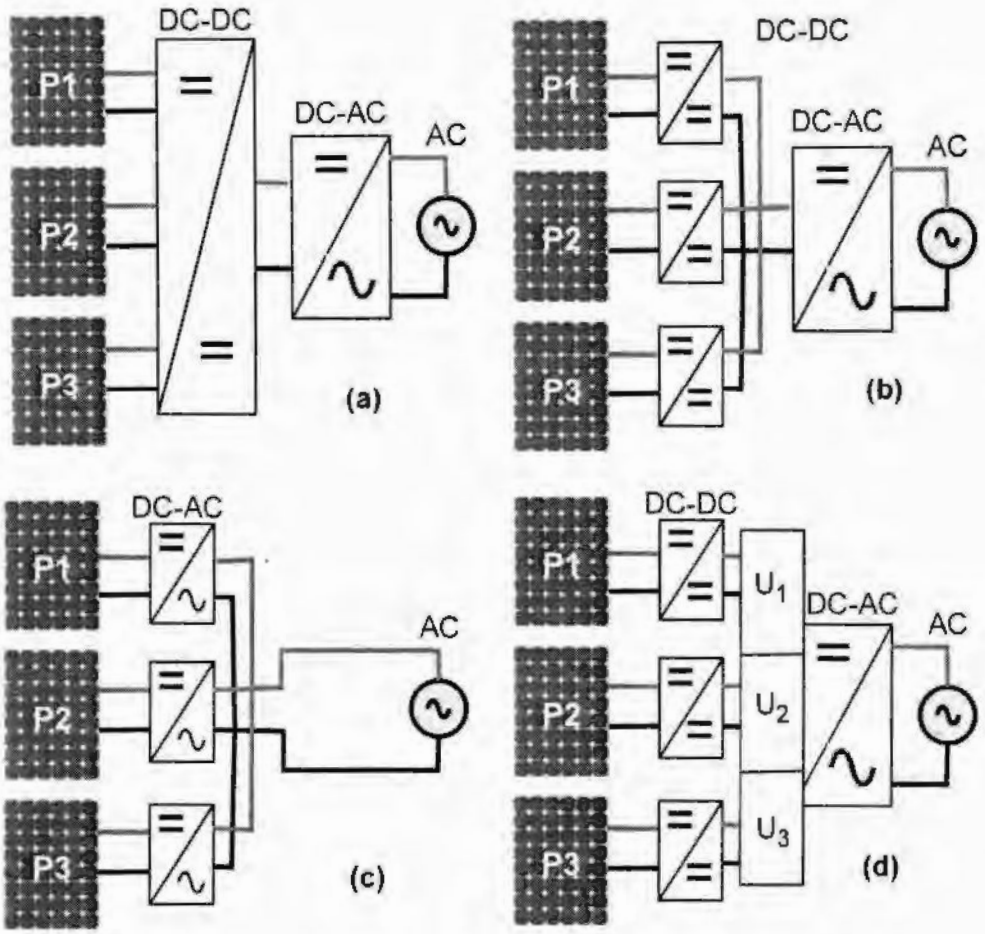

Figure 5.1: The topologies of GCI to connect PV panels to an AC grid.

There are many MLI topologies available in literature but clamped diodes, flying capacitors and cascaded MLIs are the classical topologies [12]. The other topologies are derived forms of these inverters. Each of these topologies has its own advantages and disadvantages. Based on better output waveform resolution, symmetry in the circuit, simple PWM technique, and reduced total harmonic distortion, the cascaded MLI is a good choice for GCI. Moreover, its structure is suitable for photovoltaic-based power plants, therefore the cascaded MLI is considered suitable for the way forward for this research.

The cascaded symmetrical MLI integrates multiple isolated sources to generate different levels in the output waveform. The requirement of isolated sources limits its usage. But in the case of PV panels as a source of energy, each panel or string of panels can be used

as an isolated source which makes it more feasible. Another limitation of MLI is the requirement for large numbers of power switches. To minimize this limitation, many variants have been proposed to reduce the number of switches. Similarly, in this research one such variant has been presented which uses a reduced number of switches.

In [13], the author has contributed by proposing a reduced switch topology with an additional feature of equal voltage source sharing to utilize all sources of energy equally. The topology is further enhanced here by proposing a hybrid adaptive control technique for it, in order to make it suitable for weak grid-connected applications.

5.4 Reduced Switch Cascaded Multilevel Inverter

The reduced switch cascaded MLI proposed for grid-connected applications is given in Figure 5.2. The inverter consists of two stages: stage 1 is a level synthesizing cell, while stage 2 consists of an H-bridge. The level synthesizing cells are used for generating different levels and the H-Bridge is used for polarity inversion. Each synthesizing cell can generate two levels a positive and a negative level. Moreover, a single synthesizing cell consists of a discrete diode and a power electronic transistor packed with an anti-parallel diode like MOSFET or IGBT. The required number of switches N_{sw}, diodes N_d and isolated DC sources N_{DC} can be calculated from (5.1), (5.2) and (5.3) respectively by using desired levels of the inverter N_L.

$$N_{sw} = \frac{N_L - 1}{2} + 4. \tag{5.1}$$

$$N_d = \frac{N_L - 1}{2}. \tag{5.2}$$

$$N_{DC} = \frac{N_L - 1}{2}. \tag{5.3}$$

Any number of levels can be generated by using this topology by keeping in view the size, switching losses, cost, modulation complexity and total harmonic distortion in considera-

tion. Next, a case study is presented to explain the working principle of the topology.

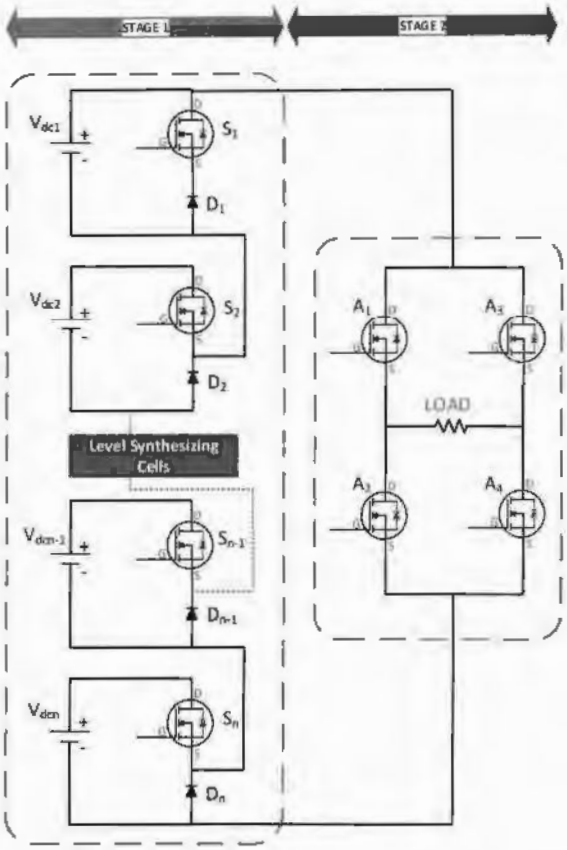

Figure 5.2: Reduced Switch Cascaded MLI topology with n-Levels.

5.5 Case Study: 9-Level Reduced Switch Cascaded Inverter

To demonstrate the working principle of the proposed design we have considered an arbitrary nine-level inverter ($N_L = 9$) as a case study as shown in Figure 5.3. The total control switches (power transistors) and discrete diodes required in the nine-level inverter are eight computed from (5.1) and (5.2). We have assumed that four DC sources of equal magnitude required are V_{dc1}, V_{dc2}, V_{dc3} and V_{dc4} and switches required in stage 1, are S_1, S_2, S_3 and S_4 along with four diodes D_1, D_2, D_3 and D_4, respectively while four switches in stage 2 are denoted by A_1, A_2, A_3 and A_4 coupled with their respective anti-parallel diodes.

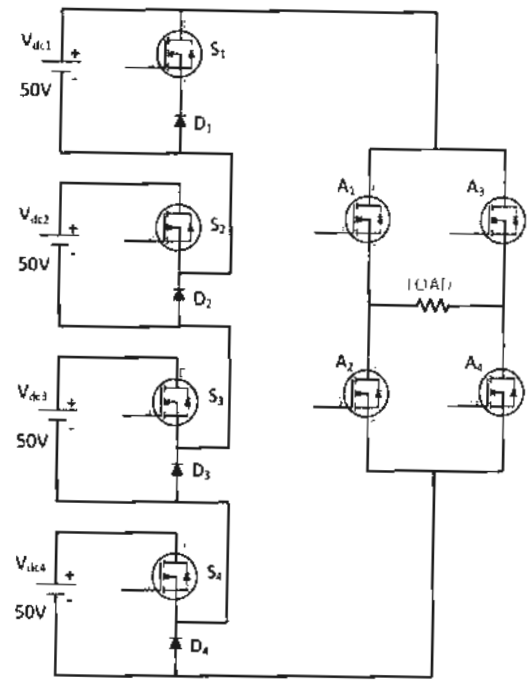

Figure 5.3: Reduced Switch Cascaded symmetric 9-level inverter.

5.5.1 Phase Disposition PWM with Equal Source Sharing and Working Principle

PWM plays an important role in the control of any power electronic converters. Some of these PWM techniques for MLIs are given in [94]. Here, the phase disposition (PD) PWM technique is used which consists of level-shifted carriers with the same amplitude and phase [95]. The carriers of the PDPWM are denoted here by C_i which has a frequency ω_c (the ω_c = 1kHz is assumed here in this section for the clarity in the demonstration while in the remaining sections, the ω_c is selected as 10kHz). The carriers can be defined as

$$C_i = E((-1)^{f(i)} y_c(w_c, \varphi) + i - \frac{N_L}{2}). \tag{5.4}$$

Where E is the amplitude of a single triangular carrier, N_L is the number of levels, i=1, 2,..., N_L-1 and y_c is a normalized symmetrical triangular carrier function defined as

$$y_c(w_c, \varphi) = (-1)^{|\alpha|}((\alpha mod 2) - 1) + \frac{1}{2}. \tag{5.5}$$

Where mod represents the modulus function and

$$\propto = \frac{w_c t + \varphi}{\pi}. \tag{5.6}$$

Here, φ is the phase angle of y_c and y_c is a periodic function having the time constant $T_c = 2\pi/\omega_c$. For the PDPWM technique $f(i) = 0$. Based on these assumptions and specifications the four carriers which are used here are summarized in Table 5.2.

Table 5.2: Specification of Phase Disposition Level Shifted Carriers.

Carrier Wave	Lower Peak Value	Upper Peak Value
Triangular1 lower peak	0V	0.25V
Triangular2 lower peak	0.25V	0.5V
Triangular3 lower peak	0.5V	0.75V
Triangular4 lower peak	0.75V	1V

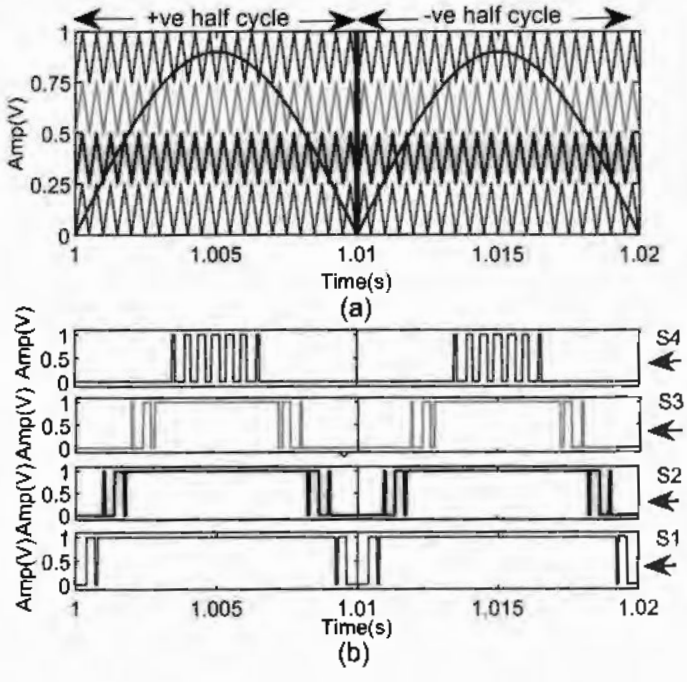

Figure 5.4: The PDPWM for a 9-Level GCI **(a)** Multi carriers and reference signal **(b)** Gate signal generated by conventional PDPWM

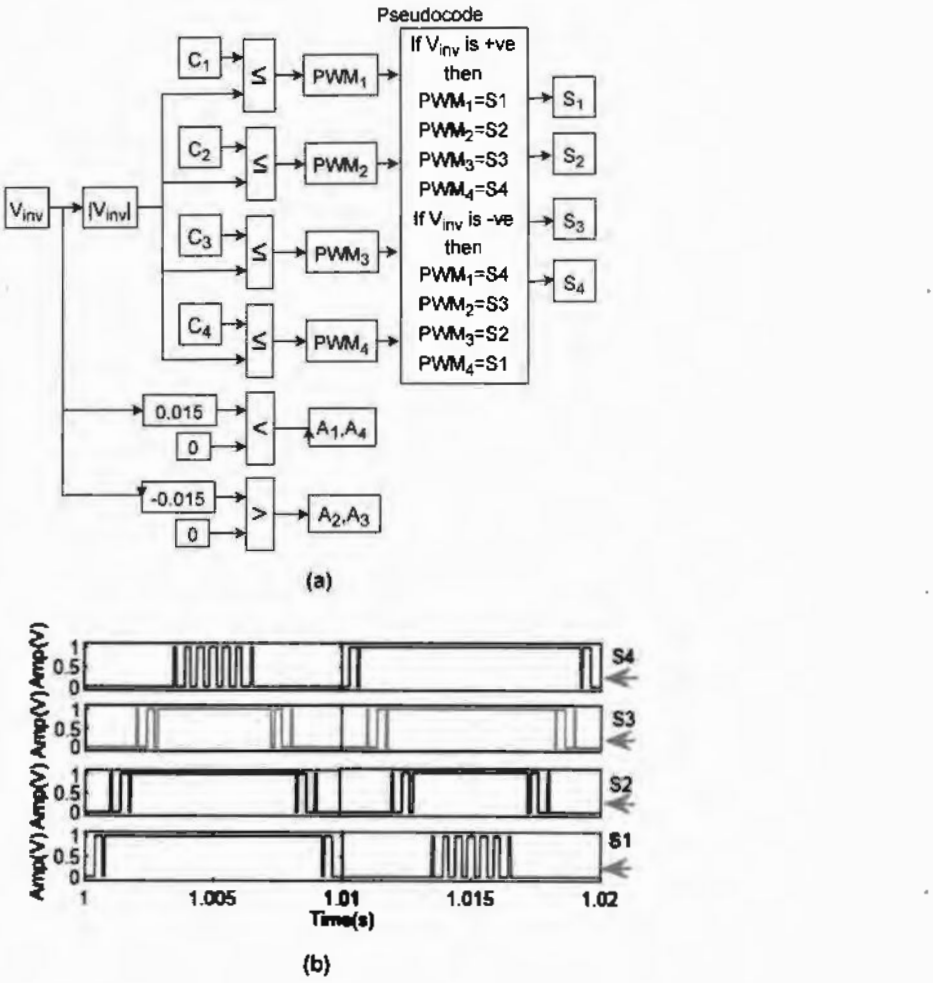

Figure 5.5: The PDPWM for 9-Level GCI for equal sources sharing **(a)** Modulation based on proposed pseudocode **(b)** gate signals generated for equal source sharing for one complete cycle

Figure 5.4 shows the classical PDPWM technique of MLI and the switching signals generated on the basis of classical PDPWM for the transistors of level enhancement cells. In Figure 5.5, the proposed modulation technique is presented along with pseudocode which utilizes all the sources on an equal basis. It is shown in Figure 5.5b that in the positive half cycle the utilization of source 1 to source 4 is decreasing while in the negative half cycle the utilization of source 4 to source 1 is decreasing. The switching signals for the corresponding switches of level enhancement cells are given in Figure 5.5b. In the first half cycle of Figure 5.5b which starts at time 1s and ends at time 1.01s, the source V_{dc1} remains

connected to the load for the maximum time, and the source V_{dc4} remains connected for the minimum time. Similarly, in the second half cycle of Figure 5.5b which is from starts at time 1.01s and ends at time 1.01s, the source V_{dc4} remains connected to the load for the maximum time, and the source V_{dc1} remains connected for the minimum time. Thus, the average time of connecting a source with the load is almost the same. Therefore, we are calling it equal source sharing.

To minimize the energy losses in the transistor switches, the PWM signal is applied to any one transistor in the track of the *ON* transistors at the same time and the remaining transistors of the same path will also remain *ON*. Similarly, zero is applied to the rest of the transistors to keep them *OFF*. This pattern of switching technique is explained with the help of Table 5.3.

Table 5.3: Patterns of PWM modulated signals for the switches of 9-level inverter.

Output Voltage	S_1	S_2	S_3	S_4	A_5, A_8	A_6, A_7
0	0	0	0	0	0	0
+(V_{dc1})	PWM	0	0	0	1	0
+(Vdc1+ V_{dc2})	1	PWM	0	0	1	0
+(Vdc1+ Vdc2+ V_{dc3})	1	1	PWM	0	1	0
+(Vdc1+ Vdc2+ Vdc3 +V_{dc4})	1	1	1	PWM	1	0
+ (Vdc1+ Vdc2+ V_{dc3})	1	1	PWM	0	1	0
+ (Vdc1+ V_{dc2})	1	PWM	0	0	1	0
+ (V_{dc1})	PWM	0	0	0	1	0
0	0	0	0	0	0	0
- (V_{dc4})	0	0	0	PWM	0	1
-(V_{dc3}+Vdc4)	0	0	PWM	1	0	1
-(V_{dc2}+ Vdc3+ Vdc4)	0	PWM	1	1	0	1
-(V_{dc1}+ Vdc2+ Vdc3 +Vdc4)	PWM	1	1	1	0	1
-(V_{dc2}+ Vdc3 +Vdc4)	0	PWM	1	1	0	1
-(V_{dc3}+ Vdc4)	0	0	PWM	1	0	1
-(V_{dc4})	0	0	0	PWM	0	1
0	0	0	0	0	0	0

On the basis of the modulation technique given in Figure 5.4, the generated output of the inverter is given in Figure 5.6a. Similarly, the switching patterns for S_1 to S_4 are generated on the basis of the modulation technique given in Figure 5.5 and the resulting output of the 9-level inverter is given in Figure 5.6b. The results show that there is no difference in the output wave of the inverter. The only difference is the total time for which a specific source is connected with the load. Figure 5.6a shows that the average time for which the

V_{dc1} is connected to the load is maximum, then it decreases to V_{dc2} and V_{dc3}. Thus, for the minimum time, V_{dc4} is connected to the load. In comparison to 5.6a and 5.6b shows that the average time of each source for which it is connected to the load is almost the same.

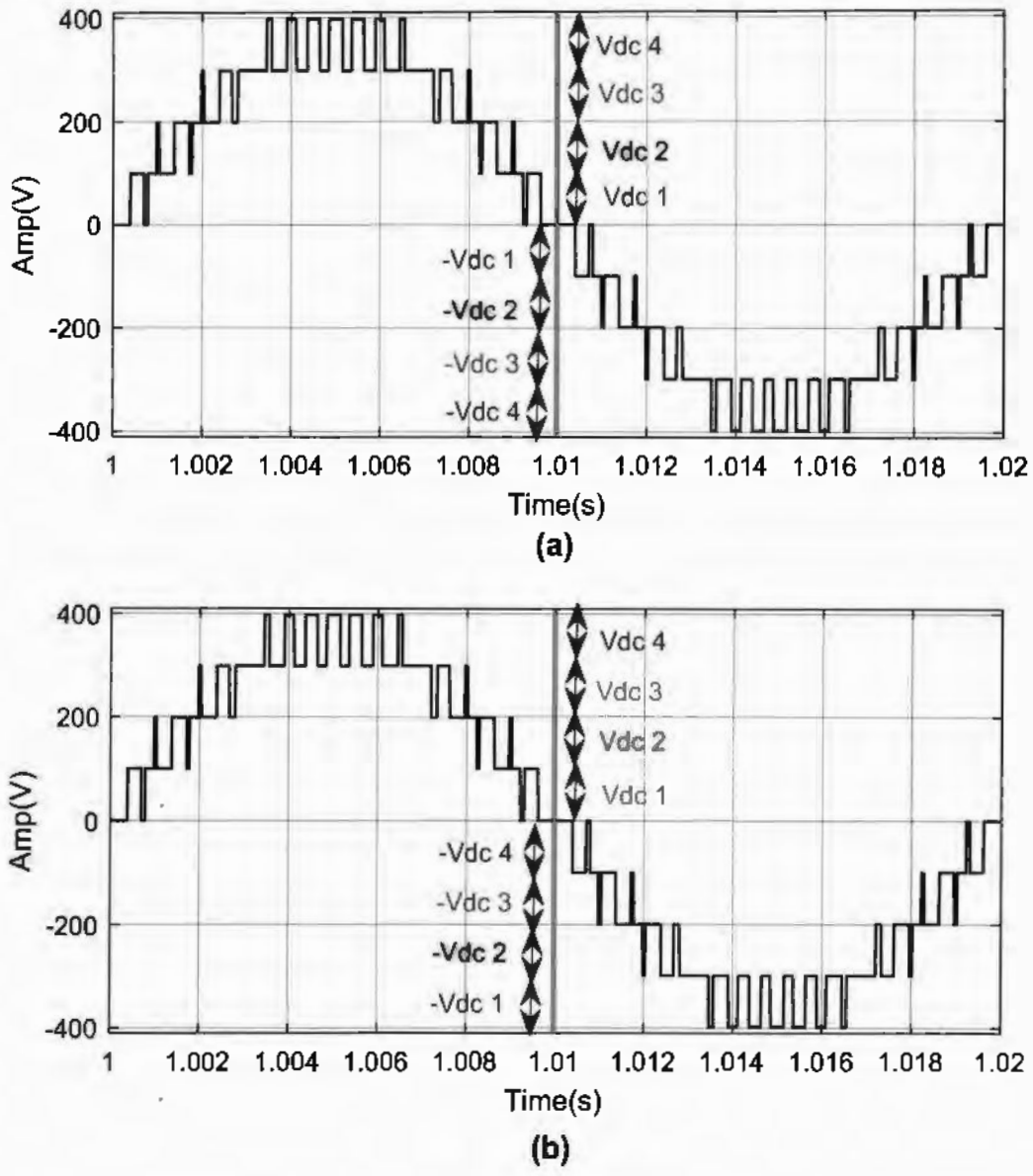

Figure 5.6: Output waveform of 9 level inverter **(a)** Conventional modulation technique **(b)** Proposed equal voltage source sharing modulation technique

5.6 Grid-connected Multilevel Inverter System Modeling

The proposed closed-loop model of the system is shown as a block diagram in Figure 5.7 including weak grid assumptions. Here the single-phase grid is considered because most of the residential consumers are connected to a single phase. The model can easily be extended to a 3-phase inverter with some minor modifications. The blocks of the proposed GCI system model consist of i) a 9-level inverter, ii) an LCL filter, iii) a control unit that further consists of a current regulator and harmonic compensator, iv) a pulse width modulator, v) A weak grid (represented by Thevenin circuit of an impedance along with a voltage source) at the point of common coupling(PCC), vi) A phase lock loop (PLL) used for the phase detection of grid voltage to generate reference current and frequency for the adaptive harmonic compensators and vii) an extra loop is used for active damping.

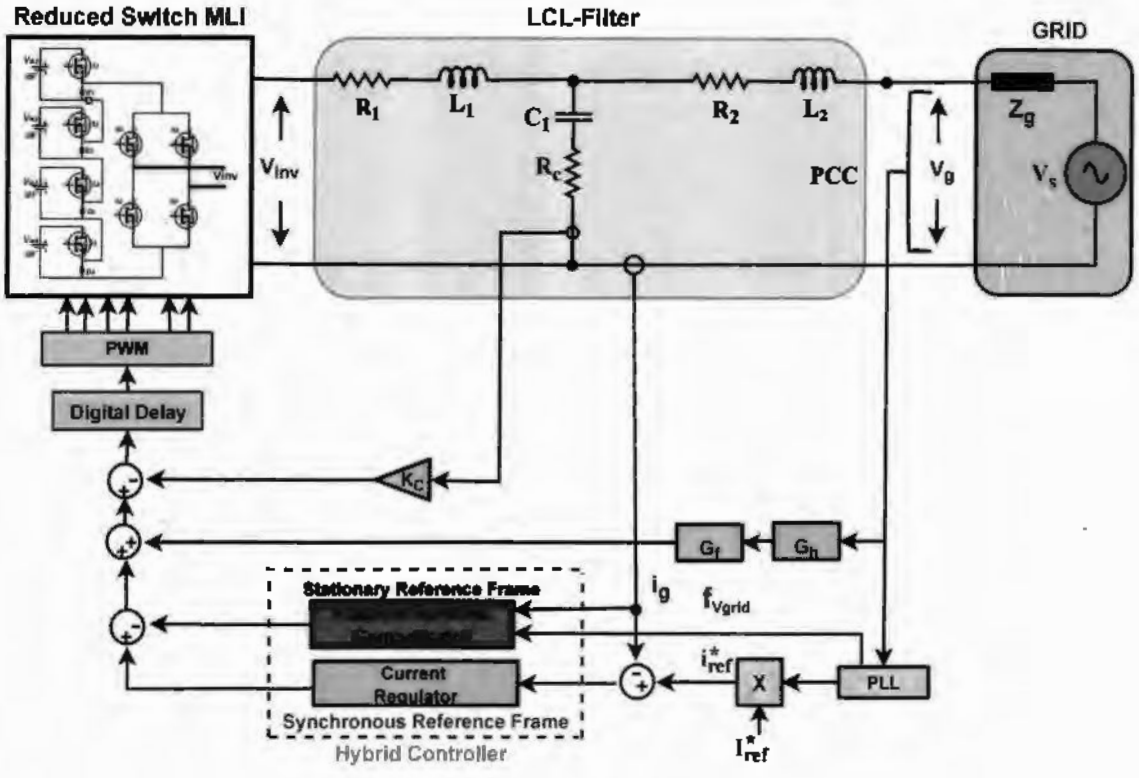

Figure 5.7: Closed loop system of 9-level GCI with weak grid assumption.

5.7 Proposed Hybrid Adaptive Control

The average switch control model of the proposed inverter in the frequency domain depicted in Figure 5.7 as a closed loop system is given in Figure 5.8. Based on the functionality of the systems, the system is organized into two Blocks:

Area A consisting of a grid, inverter, LCL filter, modulator, active damping loop, voltage feedforward loop and feedback current controller designed in a synchronous frame of reference.

Area B represents the adaptive harmonic compensator working in the stationary reference frame and an adaptive notch filter.

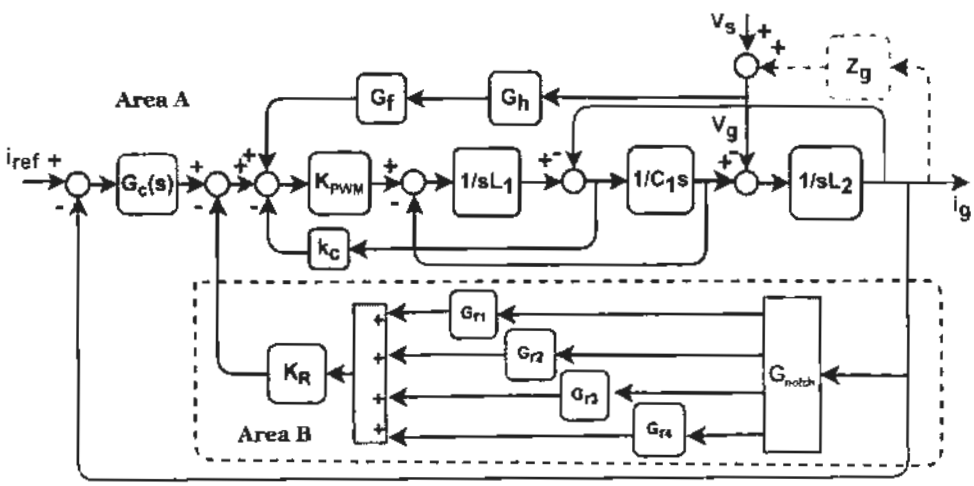

Figure 5.8: The proposed average switch controlled scheme of GCI.

The function of the controller is to ensure the injection of a pure sine wave and regulated current to the grid. In the presence of grid harmonics, the harmonics in the inverter's current also increase. In such cases, the inverter controller cannot minimize those harmonics and the inverter injects current which is polluted with low-order harmonics into the grid. Therefore, harmonic compensators are required in addition to the current controller to reduce these harmonics in the grid current.

The details of these controllers are covered in Section 4.4. Where, the synchronization

using PLL implemented by the DQ transformation method by using SOGI filters for orthogonal signal generation is discussed in Section 4.4.1. The current controller design is based on the PI controller, discussed in Section 4.4.2. The Clarke Transformation is done by two cascaded low pass first order filters for orthogonal signal generations and an adaptive harmonic compensator is designed and discussed in Section 4.4.3 by using adaptive notch and resonance filters.

The SOGI-based voltage feedforward technique is adopted here which was discussed in Section 3.2. Moreover, this section also covers the advantages of active damping, over passive damping, which is also used here. The main difference between the control of the 3-Level inverter discussed in Chapter 4 and MLI presented in this chapter is in the PWM technique. In Chapter 4, the conventional PWM technique is used but for this MLI the PDPWM technique along with an equal source sharing algorithm is used, which has been discussed earlier in this chapter.

5.7.1 Parameters of Current Controller and Harmonic Compensator

To find the appropriate parameters of the current controller and harmonic compensators for the desired stability margins (gain margin -3 to -5 dB and phase margin 30^o to 60^o), the open loop gain (5.7) is derived from the proposed system given in Figure 5.8 by using block reduction method. The values of parameters are extracted with the help of Bode Plot and MATLAB SISO Tool and are listed in Table 5.4.

$$G_{op}(s) = \frac{G_c k_{pwm}}{[s^3 L_1 L_2 C_1 + s^2 L_1 Z_g C_1 + s^2 L_2 C_1 k_c k_{pwm} + s Z_g C_1 k_c k_{pwm} + sL_1 + sL_2 + Z_g - Z_g G_f G_h k_{pwm} + k_{pwm} K r G_{PR}]}. \quad (5.7)$$

Where G_h is

$$G_h = \frac{k\omega_o s}{s^2 + k\omega_o s + \omega_o^2}. \quad (5.8)$$

Table 5.4: Symbols, description and values of designed system parameters

Symbols	Description	Values
P	Rated Power	5kW
V_{DC}	DC voltage sources V_{DC_1}, V_{DC_2}, V_{DC_3} and V_{DC_4}	100V each
V_s	Grid Source Voltage (RMS)	220V
f_g	Grid frequency	50Hz
	Grid frequency	49Hz¡ f_g ¡51Hz
L_1	Inverter side inductor	0.75mH
L_2	Grid side inductor	0.45mH
C_f	Fiter Capicitor	6.01uF
k_c	Active damping constant	10.6/400
$Z_{g(s)}$	Grid impedance	0–15 mH
k_o	SOGI filter damping factor	0.5
k_{or}	Compensator damping factor	0.001
k_{on}	Notch filter damping factor	7
K_r	Compensator gain	250
K_p	Proportional gain	50
K_i	Integral time constant	741
f_n	Low pass filter natural frequency	150 Hz
T_L	Low pass filter time constant	3.18 x 103
Kp_{pll}	Proportional gain PLL	10
Ti_{pll}	Integral time constant PLL	20 x 10
G_f	Proportional voltage feed-forward	1
K_{pwm}	Modulation index	0.7
k_c	Gain of active damping loop	$10.6/\lvert K_{PWM}\rvert$

The Bode plots of the open loop gain are given in Figure 5.9 by using the parameters given in Table 5.4. The responses are for three different values of Z_g 5mH, 10mH, and 15mH. The results show that the minimum phase margin and gain margins are $3dB$ and 50^o respectively. The stability margins of the proposed system show that the system will remain stable for the parameters given in Table 5.4 and 5.2 and the selected parameters are appropriate.

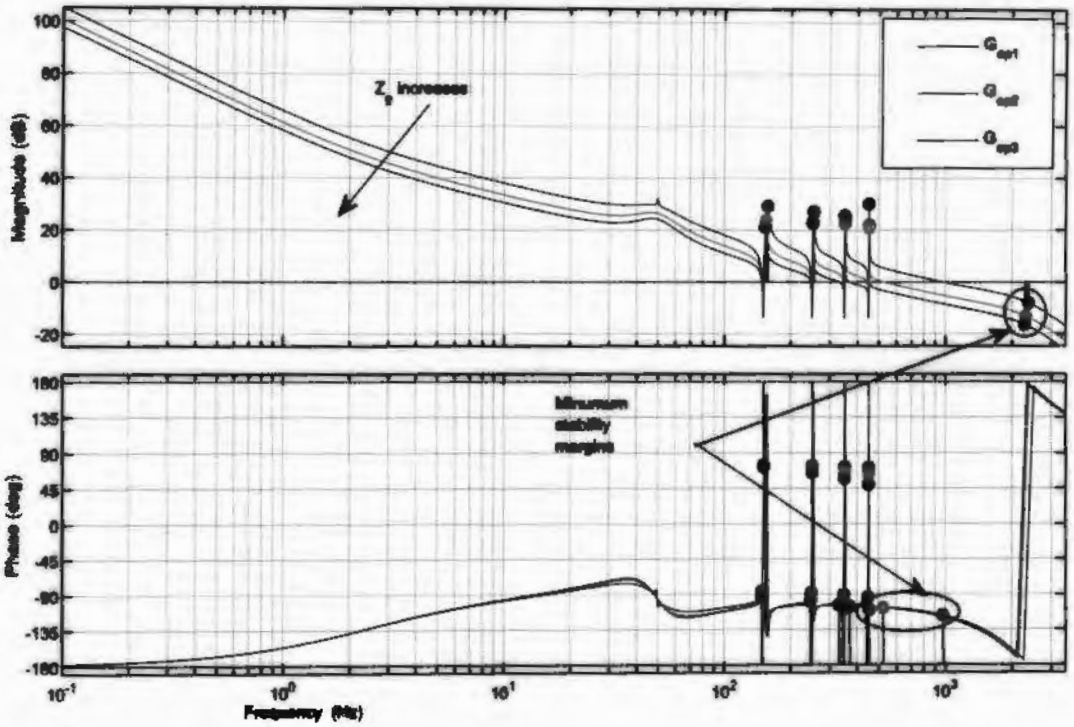

Figure 5.9: The open loop gain of the proposed system.

5.8 Impedance-based Stability Analysis

The stability of the system is tested with the help of the impedance-based stability method. The proposed system modeled in Figure 5.7 is divided into two equivalent subsystems the inverter side is represented in Norton form and the grid side is represented in Thevenin form as given in Figure 5.10.

The network of Figure 5.10 can be solved with the help of the superposition theorem to find the grid current given in (5.9) and further simplified in (5.10).

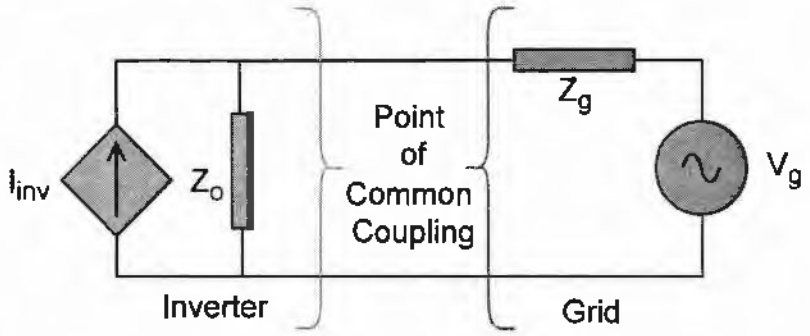

Figure 5.10: Equivalent circuit model of GCI.

$$i_g = \frac{I_{inv}(s)Z_o(s)}{Z_o(s) + Z_g(s)} - \frac{V_s(s)}{Z_o(s) + Z_g(s)} \tag{5.9}$$

$$i_g = \left[I_{inv}(s) - \frac{V_s(s)}{Z_o(s)}\right] \frac{1}{1 + Z_g(s)/Z_o(s)}. \tag{5.10}$$

Using the method of stability testing from [74], the impedance ratio Z_g/Z_o from (5.10) can be used for an impedance-based stability test.

Here, the system is evaluated by considering grid impedance Z_g=5mH, 10mH, and 15mH while the Z_g is derived from Figure 5.8 by ignoring the doted part of the Z_g. Furthermore, the relation between V_g and i_g is found by ignoring reference current i_{ref}. Thus, the derived output admittance (Y_o) and impedance (Z_o) are given in (5.11) and (5.12) respectively.

The stability is checked by using a Bode plot of the Z_g and Z_o in ratio with 1Ω. Then the stability is further verified with the help of the Nyquist Stability Theorem by checking the encirclement of the point (-1,0) using the impedance ratio. The Bode plot of the Z_g ratio is given in Figure 5.11. From Figure 5.11 the system is stable where the inverter output impedance is greater than the Z_g. In other places, where the Z_g intersects the inverter output impedance has phase differences of 100^o, 90^o 100^o and 100^o which shows enough

phase margin and therefore according to the role given in [74], the system is stable.

$$Y_o(s) = \frac{G_f G_h K pwm - C_1 L_1 s^2 - C_1 k_c k_{pwm} s - 1}{L_1 L_2 C_1 s^3 + L_2 C_1 k_c k_{pwm} s^2 + (L_1 + L_2)\, s + G_c k_{pwm} + K_r k_{pwm} G_{PR}}. \quad (5.11)$$

$$Z_o(s) = \frac{L_1 L_2 C_1 s^3 + L_2 C_1 k_c k_{pwm} s^2 + (L_1 + L_2)\, s + G_c k_{pwm} + K_r k_{pwm} G_{PR}}{G_f G_h K pwm - C_1 L_1 s^2 - C_1 k_c k_{pwm} s - 1}. \quad (5.12)$$

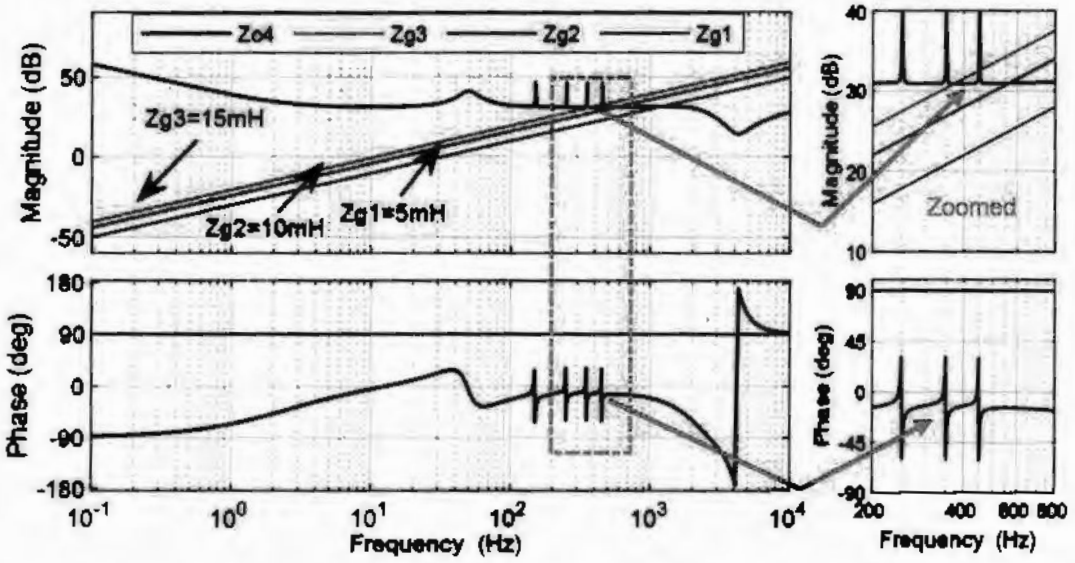

Figure 5.11: Impedance based stability analysis using Bode Plot.

To further confirm the stability, the Nyquist plot of impedance ratio is plotted in Figure 5.12 which shows the stability of the inverter against three different Z_g 5mH, 10mH, and 15mH respectively. The Nyquist stability criteria state that a system is stable if there is no encirclement of point (-1,0) or the counterclockwise encirclements of point (-1,0) are equal or greater than the clockwise encirclement, Vice versa the system is unstable if counter-clockwise encirclement is less than the clockwise encirclement of point (-1,0). Thus, the Nyquist stability conditions are satisfied and the proposed system is a stable system. The Nyquist plots of Figure 5.12 show that for all three graphs, none of the loops encircle the point (-1,0) clockwise. Therefore, it is concluded that the closed system is stable.

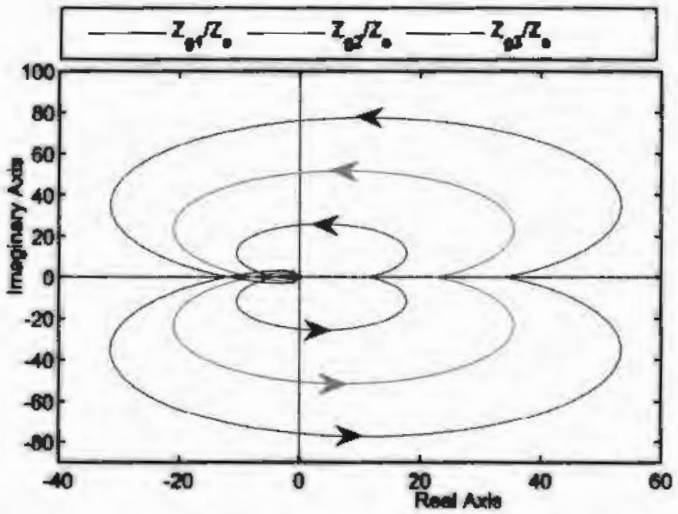

(a)

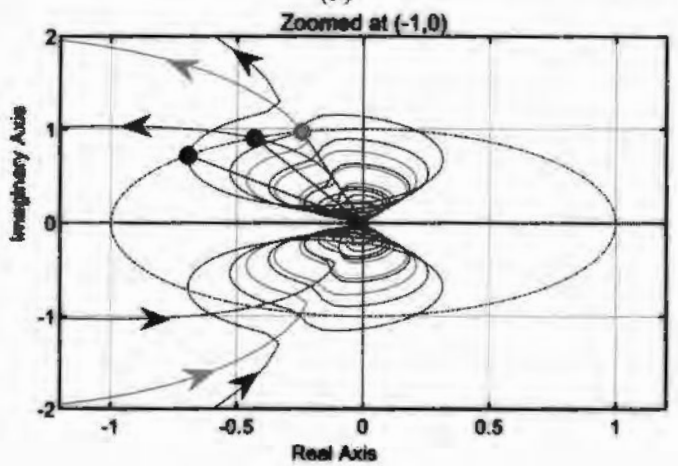

(b)

Figure 5.12: Impedance-based stability analysis using Nyquist Plot (**a**) Nyquist plot of impedance ratio $Z_{g1}(s)/Z_o(s)$, $Z_{g2}(s)/Z_o(s)$ and $Z_{g3}(s)/Z_o(s)$. (**b**) Zoomed at (-1,0)

5.9 Results and Analysis

Simulation of the proposed system is performed by using MATLAB Simulink environment. The study of a multilevel GCI is conducted by considering the peak current rating of the system as 50A and the peak voltage of the grid as 310V. The available grid is defined as

a voltage source in series with an impedance. Hence, it represents the weak grid. The real part of the impedance is ignored because it does not contribute to the instability of the system. Therefore, the impedance considered here is only inductive, which is represented in mili Henry (mH). The system is tested for three different values of grid impedances that is 5mH, 10mH, and 15mH.

The multilevel inverter uses a total of four DC voltage sources of 100V each and eight control switches with anti-parallel diodes. The inverter generates 9 levels of output and PWM is implemented with the help of the phase disposition level shift carrier method and the equal voltage source sharing technique described in Table 5.3.

The harmonic distortion within grid voltage affects the harmonic distortion of the current feeding to the grid. Therefore, low order first four odd harmonics are added in grid voltage for analysis in this work. The grid voltage along with the profile of the harmonics is given in Figure 5.13.

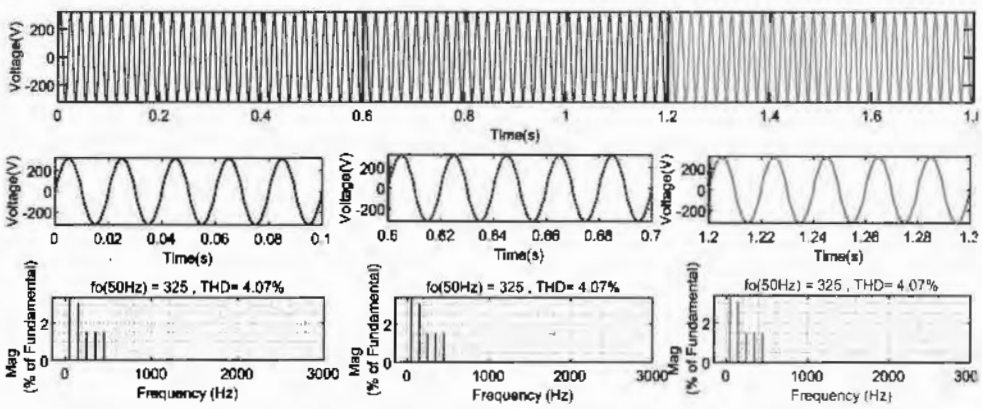

Figure 5.13: Grid source voltage along with its harmonic profile.

Here, the grid frequency is assumed to be 50Hz and the first four odd harmonics that is 150, 250, 350, and 450Hz are added to it in order to make it a harmonic polluted distorted voltage. The grid frequency has a peak amplitude of 310V and the 3^{rd}, 5^{th}, 7^{th} and 9^{th}

harmonics are assumed to have peak amplitude of 10V, 5V, 5V and 5V respectively. The grid frequency distortion is modeled by varying it between 49Hz to 51Hz is varied between 49Hz to 51Hz to check the adaptivity of harmonic compensators. The distorted grid voltage with harmonics (THD=4.07%) given in Figure 5.13 is used for analysis in this research.

Hence, the proposed design is evaluated for three different cases having different conditions. In *Case 1* the proposed system is tested for variation in Z_g under fixed grid frequency and the results are compared with other relevant techniques. In *Case 2* the proposed system is tested under grid frequency variation with fixed Z_g and the results are compared with existing techniques. Moreover, in *Case 3* the proposed system is tested for current or power change while keeping the grid frequency and Z_g fixed. The results of this case are also compared with recently published techniques. These three cases are discussed here in detail:

5.9.1 Case 1: Test for Grid Impedance Variation

In this case, the proposed system is tested to show its robustness against Z_g variations and its performance is evaluated based on THD. Here the proposed inverter is tested for three different values of grid impedance Zg=5mH, Zg=10mH, and Zg=15mH and results are given in Figure 5.14. The results reveal that the system is stable and the total harmonic distortion does not increase from the IEEE1547 Standard set for the GCIs and the performance in form of reduced total harmonic distortion is better than the existing techniques.

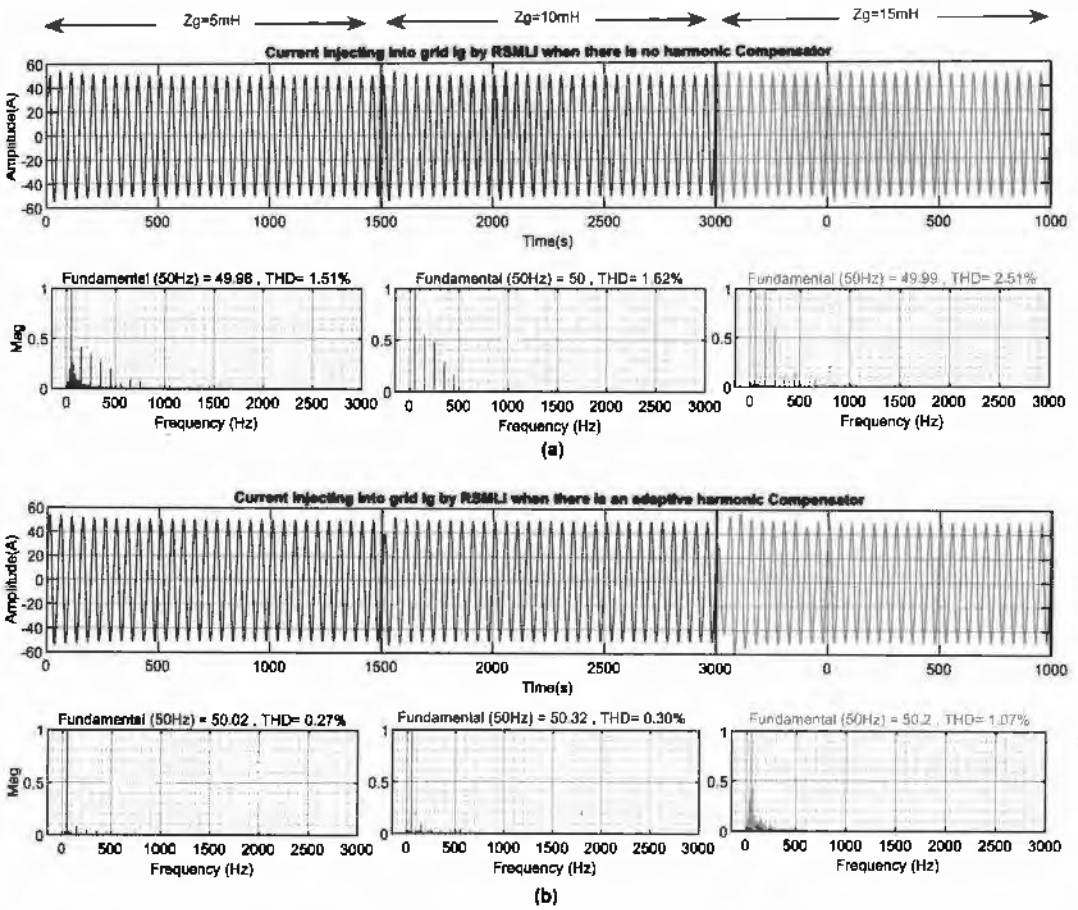

Figure 5.14: Performance of the inverter in form of THD (a) 9-MLI without adaptive harmonic compensator (b) 9-MLI with an adaptive harmonic compensator.

Moreover, the results of the proposed technique are compared with the existing techniques found in [38, 89], and [90] as given in Table 5.5

Table 5.5: Comparison of the proposed technique with the other contemporary technique on the bases of THD when there is variation in grid impedance.

Technique	**THD in %**		
Grid impedance	Z_g =5mH	Z_g= 10mH	Z_g=15mH
Technique used in [38]	3.5%	3.2%	2.9%
Technique used in [89]	2.1%	2.9%	3.3%
Technique used in [90]	1.9%	2.4%	2.8%
Proposed Technique	0.27%	0.3%	1.07%

5.9.2 Case 2: Test for Frequency Variation

The adaptive behavior of the proposed notch filter and harmonic compensators are described in this subsection. A variation of $\pm 2\%$ in the grid frequency is introduced here to check its robustness against the frequency variation. Hence, the proposed system is tested for grid frequencies 49Hz, 49.5Hz, 50Hz, 50.5Hz and 51Hz. The results are given in Figure 5.15. The results show that the system remained stable and the adaptive harmonic compensators work well if the frequency of the grid decreases or increases from its rated value by 1Hz.

Moreover, to evaluate the performance of the proposed system against frequency variations, the results are compared with the other techniques mentioned in [91] and [92]. Table 5.6 shows the comparison.

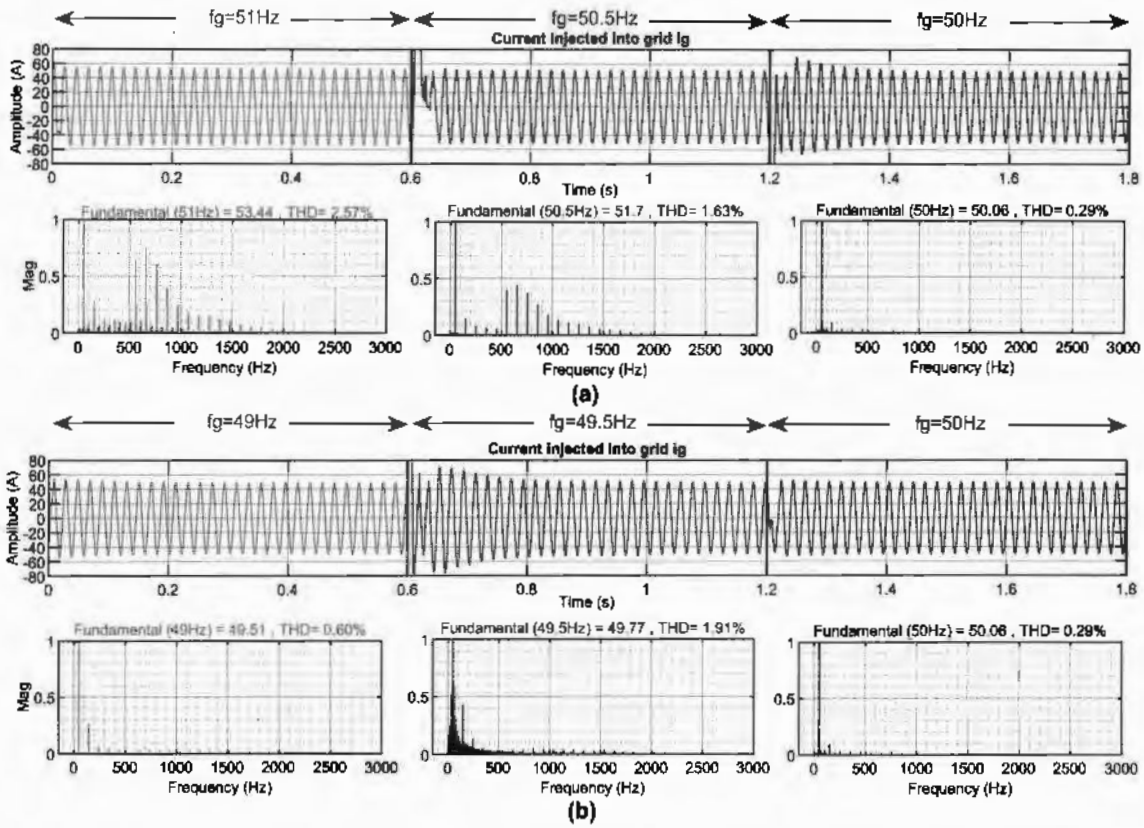

Figure 5.15: Adaptive analysis of proposed harmonic compensators (a) Results for 50Hz and above (b) Results for 50Hz and below.

Table 5.6: Comparison of the proposed technique on the basis of THD against grid frequency variation.

Technique	**THD in %**				
Grid Frequency	**49Hz**	**49.5Hz**	**50Hz**	**50.5Hz**	**51Hz**
Technique used in [91]	3.08%	2.02%	1.49%	2.13%	3.16%
Technique used in [92]	2.8%	2.9%	2.9%	2.9%	3.0%
Proposed Technique	2.57%	1.63%	0.29%	1.91%	0.6%

At a lower rating, when the grid current is 25A, the proposed system is tested and it is found that it has almost similar or better performance as compared to the 3-level inverter

given in [11] and [93]. The result for the 25A grid injected current at 50.5Hz and 49.5Hz generated from the proposed system are given in Figure5.16. The results are compared in Table 5.7.

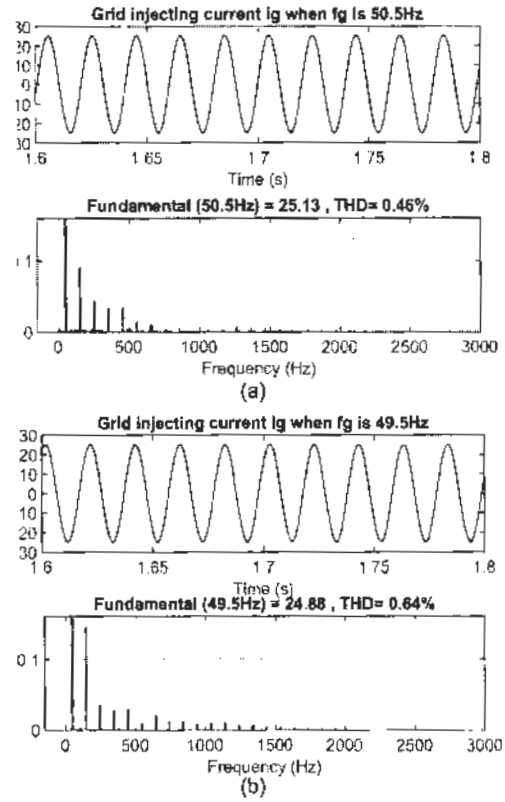

Figure 5.16: Results under frequency variation when i_g is 25A.(a) When the grid frequency is 50.5Hz (b) When the grid frequency is 49.5Hz

Table 5.7: Comparison of the proposed technique for 1% of grid frequency variation

Technique	**THD in %**	
Grid frequency	**49.5Hz**	**50.5Hz**
Technique used in [93]	1.03%	0.95%
Technique used in [11]	0.66%	0.51%
Proposed Technique	0.64%	0.46%

5.9.3 Case 3: Test for Power Handling

The power handling capability of the inverter increases when there is a change from three levels to nine levels. In MLI, the switches of low voltage rating are used in cascade to handle high voltage. Thus, the rating of the switches decreases as the level increases. There is another important aspect of a MLI that is the output of a MLI can be filtered by using smaller components of the filter. Hence, the weight, volume and losses of the LCL filter of the inverter decrease by using MLI. The MLI output has smoother output waveform voltages and current as compared to the 3 levels inverter. Therefore, an MLI shows much more stability than compared to a 3-level inverter.

In the proposed case of nine level inverter, the jump is almost four times smaller than the jump in 3 levels inverter. Here, both 3-levels and 9-level inverters are tested by using the same switching frequency and filter components and the results are given in Figure 5.17. The results show the three-level inverter becomes unstable when i_g exceeds 50A but the proposed MLI remains stable even after 70A. Even, in the case of i_g is 50A still the MLI has superior performance as compared to the 3-level inverter. From Figure 5.17 it is also concluded that the transient response of MLI is far better than a 3-level inverter and the settling time of MLI is much less than a 3-level inverter. Based on these conclusions, MLI has superior performance as compared to 3-level inverters.

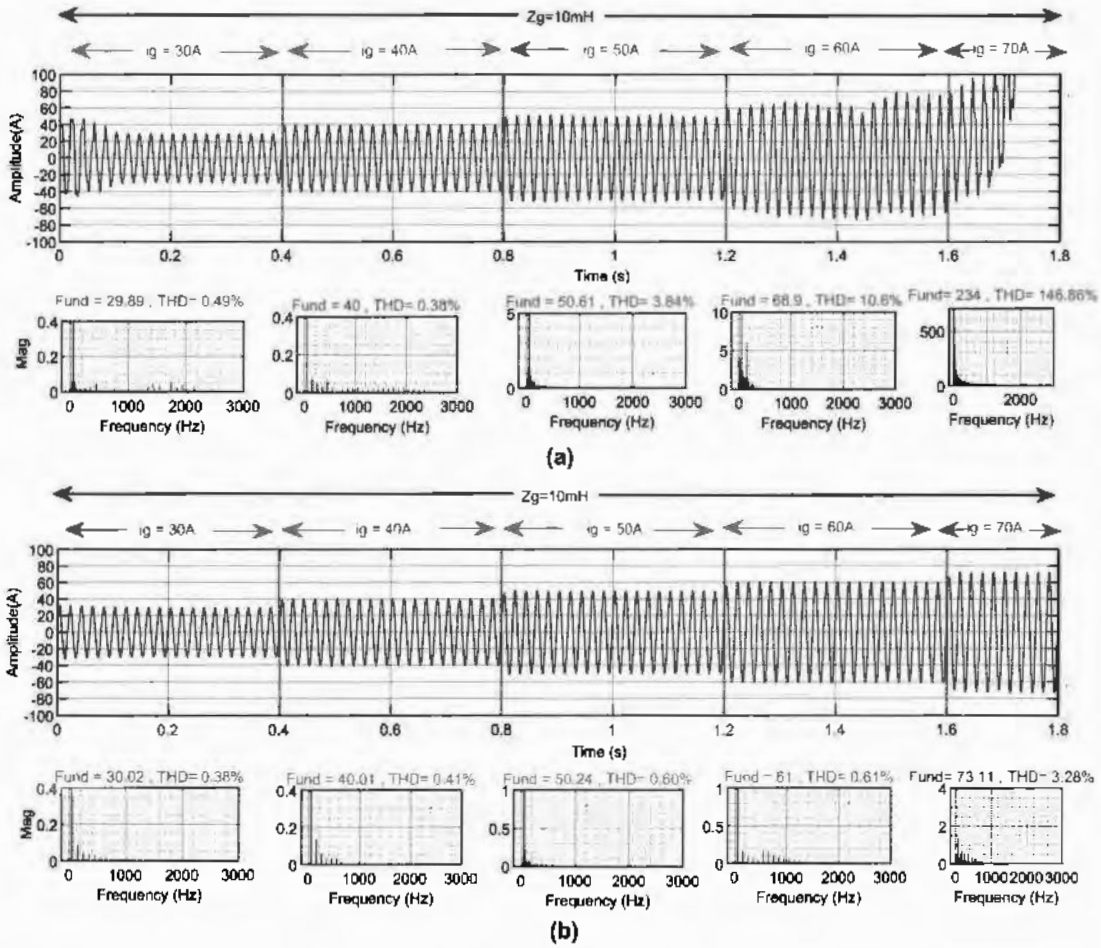

Figure 5.17: Power Handling capability testing (a) 3-Level Inverter (b) 9-level Inverter.

Figure 5.17 shows the comparison of 3-level inverter with hybrid adaptive control techniques given in [11] which is also discussed and analyzed in Chapter 4 and the proposed 9-level inverter with hybrid adaptive control technique given in this chapter. The results of Figure 5.17 are concluded in Table 5.8 which shows that the 9-level inverter is superior in performance as compared to the 3-level inverter when the output current or power of the inverter varies.

Table 5.8: Comparison of the proposed MLI-based GCI with 3-Level GCI in [11]

Technique	**THD in %**				
Current i_g	**30A**	**40A**	**50A**	**60A**	**70A**
3-level[11]	0.49% THD	0.38% THD	3.84% THD	unstable	unstable
9-Level MLI	0.38% THD	0.41% THD	0.60% THD	0.61% THD	3.28% THD

5.10 Summary

A hybrid adaptive controller of multilevel GCI is designed in this chapter, which consists of a fixed value current regulator and adaptive harmonic compensators. The MLI used is a cascaded symmetric MLI with a reduced switch and equal source-sharing techniques. The proposed MLI has low THD and increased power handling capability. The PLL used for synchronization of grid voltage and inverter current is SOGI-based PLL which removes unwanted signals from the sensing voltage signal and helps to increase robustness. Moreover, the same PLL is used for the estimation of frequencies of the first four odd harmonics which are used in adaptive harmonic compensators. The proposed control improved the performance of the inverter by decreasing the THD and increasing the robustness against the Z_g and frequency variation. The proposed solution is also compared with relevant research published in recent years and it is found the proposed solution is better in terms of THD reduction, power handling, the smaller value of (dV/dt), and lesser stress on the transistor switches.

CHAPTER 6

CONCLUSION AND FUTURE WORK

6.1 Conclusion

Grid-connected inverters are power electronic converters used in integrating RE resources, as they enable the integration of distributed energy sources such as solar panels and wind turbines into the power grid. The GCI generally includes a DC-DC converter, an inverter stage, and a filter to reduce harmonic distortion. Control strategies are implemented to ensure stability and optimal power transfer, and harmonic compensators can be used to reduce the impact of harmonic distortion on the power grid. Additionally, it is desired that GCIs must be able to work when there is a significant variation in the impedance and frequency of the grid. The inverter must be able to handle larger power so that the need for parallel inverters can be minimized. In this research, GCIs are designed and tested for weak grid applications where the Z_g can increase up to 15mH and the frequency variates up to 2Hz from its rated fundamental frequency.

Control strategies have also been an important research area for GCIs. The aim of control strategies is to ensure stability and optimal performance under varying operating conditions. The controller designed in this research consists of a synchronous framed fixed value PI current controller and adaptive harmonic compensators.

The current controller is used for the regulation of current and keeping the system stable. As LCL filter is required as a low pass filter which becomes a source for resonances. To suppress these resonances an active damping method is adopted in this research. Therefore, the current controller is accompanied by an additional feedback loop of capacitor current to suppress the resonance produced by the capacitor of the LCL filter. An additional grid voltage feed-forward loop based on the SOGI filter is also required with the current con-

troller to decrease the response time of the inverter and improve the steady-state error. It is found in this research that the PI controller can handle the frequency variation up to 2Hz from the fundamental frequency of 50Hz. Therefore, the author used a PI controller having fixed parameters for this purpose.

As the Z_g boosts the voltage harmonics of the grid which propagate through the control unit of the GCI, hence it increases the THD of its output current. Moreover, changes in Z_g variate the stability margins of GCI which change the THD of the current injected into the grid and it is possible that it will destabilize the GCI. Therefore the harmonic compensators are required to keep the THD as low as possible and thus inject good-quality current into the grid.

The harmonic compensators used here are stationary-framed adaptive harmonic compensators implemented with the help of adaptive resonant filters and an adaptive notch filter. The resonant filters designed in this research suppress the first four significant odd harmonics i.e. 150Hz, 250Hz, 350Hz, and 450Hz. If there is a variation of 2Hz in the fundamental frequency of the grid then it means a variation of 18Hz in 9^{th} harmonic will appear. Therefore, it is not possible to handle that large variation by the resonant filter of fixed characteristics and to separate it from others. Therefore, the frequency adaptive resonant filters are proposed that gets the information of grid fundamental frequency from PLL and adapts itself to the desired range. While the adaptive notch filter blocks the fundamental frequency which is considered to vary 2% within the grid from entering the resonant filters. Therefore, it helps the resonant filter to estimate only the desired harmonic and decreases the burden on the current regulator.

The proposed control technique is tested for a 3-level full bridge inverter to check its performance and stability under various conditions. The technique is tested for reducing the THD, robustness of THD against the Z_g variation, and adaptiveness to the grid frequency. The results found are promising and the proposed technique has demonstrated significant improvements.

The advancement of topology in GCIs has also been a significant research area, with the goal of optimizing power transfer and minimizing harmonic distortion. Researchers have proposed various topological solutions such as multilevel inverters, modular inverters, and cascaded inverters to achieve these goals. These topologies have proven to be effective in reducing harmonic distortion and improving power transfer efficiency.

Another contribution in this research is the new variant of MLI topology with reduced switches and supporting equal source sharing. The MLI topology has advantages in four ways: i) decreasing stress on switching transistors, ii) improving power handling capability iii) decreasing the rate of change of voltage (dV/dt), and iv) producing lesser harmonic distortion in the output current. The proposed hybrid adaptive control technique is applied to the new variant of MLI and it is demonstrated that the proposed controller can be applied to any MLI. Moreover, it is found that the results generated are more promising.

It is further concluded that GCIs are an essential technology in the field of RE, and research in this field is focused on improving the efficiency, reliability, and stability of these devices. Topological advancements have been made in order to optimize power transfer and minimize harmonic distortion. Control strategies have been proposed to ensure stability and optimal performance under varying operating conditions. Harmonic compensators have been proposed to reduce the impact of harmonic distortion on the power grid. Additionally, research has been conducted on how to handle variations in frequency and power levels, as well as provide total harmonic distortion reduction. Overall, the research on GCIs has been instrumental in the development of more efficient, reliable, and stable systems for integrating RE resources into the power grid. The integration of these technologies will play a crucial role in creating a sustainable energy future.

6.2 Future directions

One of the main benefits of using a GCI is that it allows for the excess energy generated by the RE source to be sent to the grid. This is known as "feed-in" and it allows for other

customers to use the excess energy, reducing the need for fossil fuels and reducing the overall carbon footprint. This also allows for a reduction in the cost of electricity for the end user.

Furthermore, as the use of RE continues to grow, the research in the GCI can help to ensure that the electrical grid is able to accommodate and utilize this increased amount of RE and make it accessible for many users connected to the grid. Thus, research in the area of GCIs is getting more importance. Additionally, research in this area can lead to the integration of advanced features such as energy storage and smart grid capabilities, further improving the reliability and stability of the electrical grid. Future work in the area of control and inverter topology for GCIs may include the following:

Control: Further research on control strategies for GCIs focusing on developing new and improved methods for ensuring stability and optimal performance under varying operating conditions. In this research a hybrid controller is implemented where the current controller is a fixed controller and while the harmonic compensators are adaptive. To upgrade the control system from hybrid to adaptive control, the fixed value current controller can also be replaced with an adaptive current controller. This conversion of a hybrid controller to an adaptive controller can further improve the performance and the robustness of the system can also be increased.

Inverter topology: Research on new and advanced inverter topologies could focus on increasing the efficiency and power density of GCIs. This could include the development of new multilevel inverter topologies such as symmetrical and asymmetric multilevel inverters, modular MLI, matrix inverters etc.

Power Quality: The integration of inverters in the grid is also causing a growing concern about power quality issues such as voltage and current harmonics, flicker, and power factor. The future work in this area could be oriented to improve the power quality by developing new and advanced harmonic compensation techniques, such as adaptive filtering, digital signal processing, and AI-based control algorithms.

Smart Grid integration: Future research could also focus on developing GCIs that can communicate with the smart grid and participate in demand response programs. This could include the development of new communication protocols and the integration of advanced control algorithms to enable the inverters to respond to grid conditions in real time.

Grid-Support Functions: Future work could also focus on developing GCIs that can provide grid-support functions such as voltage and frequency regulation, reactive power control, and islanding detection. This could include the development of new control algorithms and communication protocols to enable the inverters to provide these functions in real-time.

Impedance-based stability: Impedance-based stability analysis is a promising method for assessing the stability of GCIs. Impedance-based stability analysis of the proposed system shows that the stability depends on the ratio of Z_g (in the case of a weak grid) and the inverter output impedance. In this research, the Z_g is considered as a number but the Z_g can change from place to place and over time due to the connections of different equipment to the grid. To accommodate such variations, instead of considering a fixed value, the Z_g can be measured online and the inverter output impedance can be changed through the impudence reshaping method to reshape the output impedance of the inverter and keep the inverter stable. Future work in this area could also include developing more accurate models for the impedance of the grid and the inverter, as well as investigating new control strategies for maintaining stability.

Hardware Implementation: Experimenting with hardware implementation offers an invaluable opportunity to evaluate the proposed solution in practical scenarios. While hardware implementation may introduce challenges, such as processing delays, confronting these obstacles head-on can lead to critical insights and improvements. Identifying and addressing these challenges during the hardware implementation phase would be essential for establishing a reliable and efficient solution that stands up to real-world demands.

The future extension of this research for hardware implementation holds great promise.

A researcher or team of researchers can explore advanced control strategies and optimization techniques tailored for hardware platforms, seeking ways to minimize processing delays and enhance overall efficiency. Collaborating with industry experts and stakeholders in this endeavor could foster a seamless transition from theoretical concepts to real-world applications.

Furthermore, conducting comprehensive field tests and case studies on different weak grid scenarios would encourage the solution's practicality and generalizability. This practical testing would allow for a broader understanding of the solution's adaptability to various grid conditions and reveal any specific limitations or optimizations required for different settings.

In short, the research presented in this thesis marks a significant step forward in addressing the challenges faced by weak grid-connected inverters. By embracing real-time simulation, hardware-in-the-loop validation, and ultimately, hardware implementation, the proposed solution can be supported and refined to meet the needs of real-world applications. Embracing future advancements and interdisciplinary collaborations would unlock the full potential of this research, fostering a more stable and sustainable grid integration of renewable energy sources.

Overall, future work on GCIs could focus on developing more efficient, reliable, and stable systems for integrating RE sources into the power grid. The integration of advanced control and inverter topology, power quality improvement, smart grid integration, and grid-support functions will play a crucial role in creating a sustainable energy future.

REFERENCES

[1] I. Colak, "Introduction to smart grid," in *2016 International Smart Grid Workshop and Certificate Program (ISGWCP)*, IEEE, 2016, pp. 1–5.

[2] Z. Chen, A. M. Amani, X. Yu, and M. Jalili, "Control and optimisation of power grids using smart meter data: A review," *Sensors*, vol. 23, no. 4, p. 2118, 2023.

[3] K. Boora and J. Kumar, "General topology for asymmetrical multilevel inverter with reduced number of switches," *IET power electronics*, vol. 10, no. 15, pp. 2034–2041, 2017.

[4] S. Kouro, J. I. Leon, D. Vinnikov, and L. G. Franquelo, "Grid-connected photovoltaic systems: An overview of recent research and emerging pv converter technology," *IEEE Industrial Electronics Magazine*, vol. 9, no. 1, pp. 47–61, 2015.

[5] J. I. Leon, S. Kouro, L. G. Franquelo, J. Rodriguez, and B. Wu, "The essential role and the continuous evolution of modulation techniques for voltage-source inverters in the past, present, and future power electronics," *IEEE Transactions on Industrial Electronics*, vol. 63, no. 5, pp. 2688–2701, 2016.

[6] S.-Y. Park, C.-L. Chen, J.-S. Lai, and S.-R. Moon, "Admittance compensation in current loop control for a grid-tie lcl fuel cell inverter," *IEEE Transactions on Power Electronics*, vol. 23, no. 4, pp. 1716–1723, 2008.

[7] C. Bao, X. Ruan, X. Wang, W. Li, D. Pan, and K. Weng, "Step-by-step controller design for lcl-type grid-connected inverter with capacitor–current-feedback active-damping," *IEEE Transactions on Power Electronics*, vol. 29, no. 3, pp. 1239–1253, 2013.

[8] Y. Han *et al.*, "Modeling and stability analysis of LCL-type grid-connected inverters: A comprehensive overview," *IEEE Access*, vol. 7, pp. 114 975–115 001, 2019.

[9] B Kavya Santhoshi, K Mohana Sundaram, S. Padmanaban, J. B. Holm-Nielsen, and P. KK, "Critical review of pv grid-tied inverters," *Energies*, vol. 12, no. 10, p. 1921, 2019.

[10] M. Y. Ali Khan, H. Liu, Z. Yang, and X. Yuan, "A comprehensive review on grid connected photovoltaic inverters, their modulation techniques, and control strategies," *Energies*, vol. 13, no. 16, p. 4185, 2020.

[11] T. Muhammad *et al.*, "An adaptive hybrid control of grid tied inverter for the reduction of total harmonic distortion and improvement of robustness against grid impedance variation," *Energies*, vol. 15, no. 13, p. 4724, 2022.

[12] T. Muhammad, A. U. Khan, J. Hanif, M. Y. Usman, J. Javed, and A. Aslam, "Cascaded symmetric multilevel inverter with reduced number of controlled switches," *International Journal of Power Electronics and Drive Systems*, vol. 8, no. 2, p. 795, 2017.

[13] D. Batool, Q. Malik, T. Muhammad, A. U. Khan, and J. Kim, "Comparative study on minimization of conduction and switching losses in cascaded multilevel inverter via reduced switches and equal voltage source-sharing," *Circuit World*, 2022.

[14] S. Jayalath and M. Hanif, "Generalized lcl-filter design algorithm for grid-connected voltage-source inverter," *IEEE Transactions on Industrial Electronics*, vol. 64, no. 3, pp. 1905–1915, 2016.

[15] A. Singh and B. Mirafzal, "An efficient grid-connected three-phase single-stage boost current source inverter," *IEEE Power and Energy Technology Systems Journal*, vol. 6, no. 3, pp. 142–151, 2019.

[16] S. Azmi, K. Ahmed, S. Finney, and B. Williams, "Comparative analysis between voltage and current source inverters in grid-connected application," 2011.

[17] Y. Li, S. Jiang, J. G. Cintron-Rivera, and F. Z. Peng, "Modeling and control of quasi-z-source inverter for distributed generation applications," *IEEE Transactions on Industrial Electronics*, vol. 60, no. 4, pp. 1532–1541, 2012.

[18] L. Chen, A. Amirahmadi, Q. Zhang, N. Kutkut, and I. Batarseh, "Design and implementation of three-phase two-stage grid-connected module integrated converter," *IEEE Transactions on Power Electronics*, vol. 29, no. 8, pp. 3881–3892, 2013.

[19] T.-F. Wu, C.-H. Chang, L.-C. Lin, and C.-L. Kuo, "Power loss comparison of single- and two-stage grid-connected photovoltaic systems," *IEEE Transactions on Energy Conversion*, vol. 26, no. 2, pp. 707–715, 2011.

[20] R. Bisht, S. Subramaniam, R. Bhattarai, and S. Kamalasadan, "Active and reactive power control of single phase inverter with seamless transfer between grid-connected and islanded mode," in *2018 IEEE Power and Energy Conference at Illinois (PECI)*, IEEE, 2018, pp. 1–8.

[21] S. Paghdar, U. Sipai, K. Ambasana, and P. J. Chauhan, "Active and reactive power control of grid connected distributed generation system," in *2017 Second International Conference on Electrical, Computer and Communication Technologies (ICECCT)*, IEEE, 2017, pp. 1–7.

[22] D. I. Brandao, F. E. Mendes, R. V. Ferreira, S. M. Silva, and I. A. Pires, "Active and reactive power injection strategies for three-phase four-wire inverters during symmetrical/asymmetrical voltage sags," *IEEE transactions on industry applications*, vol. 55, no. 3, pp. 2347–2355, 2019.

[23] W. Wu, Y. He, T. Tang, and F. Blaabjerg, "A new design method for the passive damped lcl and llcl filter-based single-phase grid-tied inverter," *IEEE transactions on industrial electronics*, vol. 60, no. 10, pp. 4339–4350, 2012.

[24] A. K. Balasubramanian and V. John, "Analysis and design of split-capacitor resistive-inductive passive damping for lcl filters in grid-connected inverters," *IET Power Electronics*, vol. 6, no. 9, pp. 1822–1832, 2013.

[25] J. C. Giacomini, L. Michels, H. Pinheiro, and C. Rech, "Design methodology of a passive damped modified lcl filter for leakage current reduction in grid-connected transformerless three-phase pv inverters," *IET Renewable Power Generation*, vol. 11, no. 14, pp. 1769–1777, 2017.

[26] D. Pan, X. Ruan, C. Bao, W. Li, and X. Wang, "Capacitor-current-feedback active damping with reduced computation delay for improving robustness of lcl-type grid-connected inverter," *IEEE Transactions on Power Electronics*, vol. 29, no. 7, pp. 3414–3427, 2013.

[27] J. Xu, S. Xie, and T. Tang, "Active damping-based control for grid-connected LCL-filtered inverter with injected grid current feedback only," *IEEE Transactions on Industrial Electronics*, vol. 61, no. 9, pp. 4746–4758, 2013.

[28] L. Jia, X. Ruan, W. Zhao, Z. Lin, and X. Wang, "An adaptive active damper for improving the stability of grid-connected inverters under weak grid," *IEEE Transactions on Power Electronics*, vol. 33, no. 11, pp. 9561–9574, 2018.

[29] J. Rodriguez, J.-S. Lai, and F. Z. Peng, "Multilevel inverters: A survey of topologies, controls, and applications," *IEEE Transactions on industrial electronics*, vol. 49, no. 4, pp. 724–738, 2002.

[30] S. Kouro *et al.*, "Recent advances and industrial applications of multilevel converters," *IEEE Transactions on industrial electronics*, vol. 57, no. 8, pp. 2553–2580, 2010.

[31] I. E. Tashiwa, G. D. Dung, and B. S. Adole, "Review of multilevel inverters and their control techniques," *European Journal of Engineering and Technology Research*, vol. 5, no. 6, pp. 659–664, 2020.

[32] X. Zhang, T. Zhao, W. Mao, D. Tan, and L. Chang, "Multilevel inverters for grid-connected photovoltaic applications: Examining emerging trends," *IEEE Power Electronics Magazine*, vol. 5, no. 4, pp. 32–41, 2018.

[33] M. Malinowski, K Gopakumar, J. Rodriguez, and M. A. Perez, "A survey on cascaded multilevel inverters," *IEEE Transactions on industrial electronics*, vol. 57, no. 7, pp. 2197–2206, 2009.

[34] E. Babaei, S. Laali, and S. Alilu, "Cascaded multilevel inverter with series connection of novel h-bridge basic units," *IEEE transactions on industrial electronics*, vol. 61, no. 12, pp. 6664–6671, 2014.

[35] M. F. Kangarlu and E. Babaei, "A generalized cascaded multilevel inverter using series connection of submultilevel inverters," *IEEE transactions on power electronics*, vol. 28, no. 2, pp. 625–636, 2012.

[36] R Seyezhai, "A comparative study of asymmetric and symmetric cascaded multilevel inverter employing variable frequency carrier based pwm," *International Journal of Emerging Technology and Advanced Engineering*, vol. 2, no. 3, pp. 230–237, 2012.

[37] X. Zhang, D. Xia, Z. Fu, G. Wang, and D. Xu, "An improved feedforward control method considering pll dynamics to improve weak grid stability of grid-connected inverters," *IEEE Transactions on Industry Applications*, vol. 54, no. 5, pp. 5143–5151, 2018.

[38] J. Xu, Q. Qian, B. Zhang, and S. Xie, "Harmonics and stability analysis of single-phase grid-connected inverters in distributed power generation systems considering phase-locked loop impact," *IEEE Transactions on Sustainable Energy*, vol. 10, no. 3, pp. 1470–1480, 2019.

[39] H. Athari, M. Niroomand, and M. Ataei, "Review and classification of control systems in grid-tied inverters," *Renewable and Sustainable Energy Reviews*, vol. 72, pp. 1167–1176, 2017.

[40] Q. Liu, T. Caldognetto, and S. Buso, "Review and comparison of grid-tied inverter controllers in microgrids," *IEEE Transactions on Power Electronics*, vol. 35, no. 7, pp. 7624–7639, 2019.

[41] R. A. Khan and W. Choi, "An improved harmonic compensation method for a single-phase grid connected inverter," *The Transactions of the Korean Institute of Power Electronics*, vol. 24, no. 3, pp. 215–227, 2019.

[42] G. Shen, X. Zhu, J. Zhang, and D. Xu, "A new feedback method for pr current control of lcl-filter-based grid-connected inverter," *IEEE Transactions on Industrial Electronics*, vol. 57, no. 6, pp. 2033–2041, 2010.

[43] A. M. Mnider, D. J. Atkinson, M. Dahidah, and M. Armstrong, "A simplified dq controller for single-phase grid-connected pv inverters," in *2016 7th international renewable energy congress (IREC)*, IEEE, 2016, pp. 1–6.

[44] M. E. Meral and D. Çelik, "Comparison of srf/pi-and strf/pr-based power controllers for grid-tied distributed generation systems," *Electrical Engineering*, vol. 100, no. 2, pp. 633–643, 2018.

[45] J. Hu, J. Zhu, and D. G. Dorrell, "Model predictive control of grid-connected inverters for pv systems with flexible power regulation and switching frequency reduction," *IEEE Transactions on Industry Applications*, vol. 51, no. 1, pp. 587–594, 2014.

[46] E. Z. Bighash, S. M. Sadeghzadeh, E. Ebrahimzadeh, and F. Blaabjerg, "Improving performance of lvrt capability in single-phase grid-tied pv inverters by a model-predictive controller," *International Journal of Electrical Power & Energy Systems*, vol. 98, pp. 176–188, 2018.

[47] J. Rodriguez *et al.*, "State of the art of finite control set model predictive control in power electronics," *IEEE Transactions on Industrial Informatics*, vol. 9, no. 2, pp. 1003–1016, 2012.

[48] A. Merabet, L. Labib, and A. M. Ghias, "Robust model predictive control for photovoltaic inverter system with grid fault ride-through capability," *IEEE Transactions on Smart Grid*, vol. 9, no. 6, pp. 5699–5709, 2017.

[49] D. Chen, J. Zhang, and Z. Qian, "An improved repetitive control scheme for grid-connected inverter with frequency-adaptive capability," *IEEE Transactions on Industrial Electronics*, vol. 60, no. 2, pp. 814–823, 2012.

[50] M. Shadoul, H. Yousef, R. Al Abri, and A. Al-Hinai, "Adaptive interval type-2 fuzzy tracking control of pv grid-connected inverters," *IEEE Access*, vol. 9, pp. 130 853–130 861, 2021.

[51] M. Omar, A. El-Deib, A. El Shafei, M. Abdallah, *et al.*, "Comparative study between pi and fuzzy-logic controllers for three-phase grid-connected photovoltaic systems," in *2016 Eighteenth International Middle East Power Systems Conference (MEPCON)*, IEEE, 2016, pp. 380–386.

[52] K. Zeb *et al.*, "A comprehensive review on inverter topologies and control strategies for grid connected photovoltaic system," *Renewable and Sustainable Energy Reviews*, vol. 94, pp. 1120–1141, 2018.

[53] S. Ramaiah, N Lakshminarasamma, and M. K. Mishra, "Loss modulated deadbeat control for grid connected inverter system," *IEEE Journal of Emerging and Selected Topics in Power Electronics*, 2022.

[54] G. Elhassan *et al.*, "Deadbeat current control in grid-connected inverters: A comprehensive discussion," *IEEE Access*, vol. 10, pp. 3990–4014, 2021.

[55] F. R. Badal *et al.*, "Robust controller design for tracking enhancement of a grid-tied pv-battery microgrid under industrial loads," *IEEE Transactions on Applied Superconductivity*, vol. 31, no. 8, pp. 1–5, 2021.

[56] R. Errouissi and A. Al-Durra, "Design of pi controller together with active damping for grid-tied lcl-filter systems using disturbance-observer-based control approach," *IEEE Transactions on Industry Applications*, vol. 54, no. 4, pp. 3820–3831, 2018.

[57] A. Al-Durra and R. Errouissi, "Robust feedback-linearization technique for grid-tied lcl filter systems using disturbance estimation," *IEEE Transactions on Industry Applications*, vol. 55, no. 3, pp. 3185–3197, 2019.

[58] N. Yıldıran and E. Tacer, "A new approach to h-infinity control for grid-connected inverters in photovoltaic generation systems," *Electric Power Components and Systems*, vol. 47, no. 14-15, pp. 1413–1422, 2019.

[59] B. E. Sedhom, M. M. El-Saadawi, A. Y. Hatata, and E.-H. E. Abd-Raboh, "H-infinity versus model predictive control methods for seamless transition between islanded-and grid-connected modes of microgrids," *IET Renewable Power Generation*, vol. 14, no. 5, pp. 856–870, 2020.

[60] S. Xiao, Z. Ou, J. Peng, Y. Zhang, and X. Zhang, "Single-phase photovoltaic grid-connected inverter based on fuzzy neural network," *Journal of Advanced Computational Intelligence and Intelligent Informatics*, vol. 25, no. 3, pp. 310–316, 2021.

[61] S. R. Das, P. K. Ray, A. K. Sahoo, K. K. Singh, G. Dhiman, and A. Singh, "Artificial intelligence based grid connected inverters for power quality improvement in smart grid applications," *Computers & Electrical Engineering*, vol. 93, p. 107 208, 2021.

[62] J. K. Singh and R. K. Behera, "An improved hysteresis current controller for grid-connected inverter system to address power quality issues at reduced switching frequency," *IEEE Transactions on Industry Applications*, vol. 57, no. 2, pp. 1892–1901, 2021.

[63] B. Guo *et al.*, "A robust second-order sliding mode control for single-phase photovoltaic grid-connected voltage source inverter," *IEEE Access*, vol. 7, pp. 53 202–53 212, 2019.